A System-Level Analysis of Migratory Shorebird Habitat Use, Diet, and the Influence of Climate-Driven Ecosystem Change in the Virginia Barrier Islands

Kristy Lapenta

Thesis submitted to the faculty of the Virginia Polytechnic Institute and State University in partial fulfillment of the requirements for the degree of

Master of Science
In
Fish and Wildlife Conservation

Sarah M. Karpanty, Chair
Elizabeth A. Hunter
Ruth Boettcher

August 22, 2025
Blacksburg, Virginia

Keywords: migratory shorebirds, foraging ecology, diet, climate change, habitat use, red knot

A System-Level Analysis of Migratory Shorebird Habitat Use, Diet, and the Influence of Climate-Driven Ecosystem Change in the Virginia Barrier Islands

Kristy Lapenta

ABSTRACT

Migratory shorebirds rely on high-quality coastal staging habitats to refuel during migration, but these sites are threatened by climate change. The Virginia barrier island system supports over 100,000 shorebirds annually, including federally threatened red knots (*Calidris canutus rufa*) and other state and regional species of conservation concern such as dunlin (*Calidris alpina*) and semipalmated sandpipers (*Calidris pusilla*). The goals of my thesis were: 1) to advance understanding of the foraging ecology of these imperiled shorebird species in the understudied mudflat habitats of the coastal lagoon behind the barrier islands, and 2) to examine how a changing climate may impact red knots by altering barrier island habitats and the invertebrate prey that sustain them during migration. I compared habitat use and prey availability across sand, peat, and mudflat substrates during spring migration (May 14 – June 2, 2023 – 2024) and used fecal DNA metabarcoding to examine diet and prey selection on mudflats. Mudflats supported comparable shorebird numbers and invertebrate densities to barrier island sand substrate. The composition of shorebird and invertebrate communities differed across substrates. Dunlin and semipalmated sandpipers primarily used mudflats and consumed mostly crustaceans while red knots primarily foraged on barrier islands, feeding mainly on bivalves. Red knots foraging on mudflats preferred bivalves. Dunlin similarly showed a preference for bivalves but to a lesser extent than red knots. Semipalmated sandpipers exhibited a generalist diet strategy. All species consumed diatoms, providing the first evidence of biofilm grazing in this system. These findings highlight the ecological importance of mudflats in supporting diverse shorebird foraging strategies. To assess how climate-driven ecosystem change influences red

knots and their prey, I used piecewise structural equation modeling integrating long-term data from peak spring migration when red knots are most abundant in Virginia (May 21 – 28, 2009 – 2023). I found that red knots were indirectly influenced by climate change via bottom-up effects on invertebrate prey mediated by barrier island morphology. Prey responses were taxon-specific, suggesting future change may alter invertebrate community structure. I then examined how barrier island morphology has changed since long-term red knot monitoring began in 2007. Half of the barrier islands in our study area significantly narrowed in island width or beach width between 2007 and 2023, though a lack of system-level trends in either indicated relative stability for the barrier island system as a whole. However, accelerated geomorphic change and increasing climate variability may alter foraging conditions, with broader implications for red knot population resilience. My research highlights the importance of preserving habitat heterogeneity at coastal staging sites and incorporating climate-driven landscape-scale processes into conservation planning for migratory shorebirds along the U.S. Atlantic flyway.

A System-Level Analysis of Migratory Shorebird Habitat Use, Diet, and the Influence of Climate-Driven Ecosystem Change in the Virginia Barrier Islands

Kristy Lapenta

GENERAL AUDIENCE ABSTRACT

Migratory shorebirds travel great distances and rely on coastal areas to rest and feed during migration, but these habitats are under increasing pressure from rising sea levels, warming oceans, and stronger storms. The Virginia barrier island system, located along the Eastern Shore of Virginia, is a chain of mostly undeveloped barrier islands that support over 100,000 shorebirds each year. This includes the federally threatened red knot and other declining species such as dunlin and semipalmated sandpipers. I compared shorebird habitat use and food availability on mudflats and barrier islands during spring migration (May 14 – June 2, 2023 – 2024) to understand how important mudflats are for shorebirds. I then collected droppings from red knots, dunlin, and semipalmated sandpipers on mudflats and used DNA analysis to identify their diets. I then studied diet preferences by comparing what they ate to what was available. Mudflats and sandy barrier island habitats had similar numbers of shorebirds and invertebrates, but each shorebird species used each habitat differently. Dunlin and semipalmated sandpipers mostly fed on mudflats, mainly eating crustaceans. Red knots mainly used barrier island habitats, but when they fed on mudflats, they mainly ate bivalves. All species ate biofilm, a paste-like mixture of diatoms and other unicellular algae that grows on mudflats, which is the first evidence of this in Virginia. Red knots and dunlin preferred to eat bivalves, while semipalmated sandpipers showed no preferences. To explore how climate change affects red knots, I analyzed 10 years of spring migration data (May 20 – 28, 2009 – 2023), along with information on prey, barrier island features, sea-level rise, and storms to test how they are connected. I found that sea-level rise and storms affected beach and island width, which altered prey availability and

indirectly affected red knots. I also examined how beach and island width have changed from the beginning of long-term red knot monitoring in 2007 to 2023. While half the islands in our study area narrowed over time, the system as a whole did not change in a major way for this measure. However, other research predicts that faster sea-level rise and stronger storms will greatly change barrier islands in the future. Based on our findings, these changes could alter prey communities and indirectly harm red knots. This work shows that protecting many types of coastal habitats is important in Virginia and all along the Atlantic coast, and that the effects of climate change need to be a part of future conservation planning to protect migratory shorebirds.

ACKNOWLEDGEMENTS

I am deeply grateful to my advisor, Sarah Karpanty, for seeing something in me that day on the beach and for providing guidance and encouragement throughout this process. Her mentorship has shaped not only this thesis but also my growth as a coastal scientist. I would also like to thank my committee members, Elizabeth Hunter and Ruth Boettcher, for their valuable feedback. Having the guidance of strong female mentors has been an honor and has profoundly shaped my professional identity and career goals. This work also would not have been possible without the help of colleagues, collaborators, and friends in the Karpanty Lab and in FIWGSA, who provided invaluable assistance with fieldwork, data analysis, discussions, editing, and overall camaraderie. I probably would have finished my thesis three months earlier without office shenanigans and had a way worse time.

I gratefully acknowledge the National Science Foundation's Virginia Coast Reserve Long-Term Ecological Research Program (DEB-1832221 and DEB-2425178), the Virginia Tech Department of Fish and Wildlife Conservation, and the Virginia Society of Ornithology for supporting this research. I also thank partners at The Nature Conservancy, the Virginia Department of Wildlife Resources, U.S. Fish and Wildlife Service, the Virginia Department of Conservation and Recreation, the Commonwealth of Virginia Marine Resource Commission, the National Oceanic and Atmospheric Administration, the National Aeronautics and Space Administration, the Virginia Institute of Marine Science, and Seaside Ecotours, LLC for logistical, intellectual, and permitting support throughout this project.

I am deeply appreciative to my family and friends for their unwavering support and patience as I tried to make this degree happen. To my mom, Cathy Lapenta, thank you for showing me that women can thrive in STEM and inspiring me to become a scientist. To my dad,

Bill Lapenta, thank you for your constant encouragement through years of underpaid internships, for always taking an interest in my work, and for giving me career advice that I now share with aspiring scientists. I know you would be proud of who I have become. Finally, to my husband, Michael Holden, I can't thank you enough for your unwavering support and unconditional love throughout the challenges of graduate school and beyond. You are my everything.

TABLE OF CONTENTS

Acknowledgements vi

List of Figures x

List of Tables xiii

Attribution xiv

Chapter 1: Introduction

Background 1

Thesis Objectives 5

Literature Cited 6

Chapter 2: Diet and Prey Selection of Migratory Shorebirds on Mudflats in the Virginia Barrier Island System using Fecal DNA Metabarcoding

Abstract 11

Introduction 12

Methods 15

Results 23

Discussion 28

Data Archiving Statement 32

Acknowledgements 32

Literature Cited 34

Figures 43

Chapter 3: Geomorphic and Climate Drivers Shape Bottom-Up Controls on Spring Staging Red Knots (*Calidris canutus rufa*) in the Virginia Barrier Island System

Abstract 49

Introduction 50

Methods 53

Results 63

Discussion 67

Acknowledgements 72

Literature Cited 74

Tables 84

Figures 93

Chapter 4: Conclusions

Novel Findings 99

Management Implications 100

Future Research Directions 102
Literature Cited 103
Appendices 106
Chapter 2: Diet and Prey Selection of Migratory Shorebirds on Mudflats in the Virginia Barrier Island System using Fecal DNA Metabarcoding
Appendix S.1 106
Supplementary Tables 108
List of External Supplementary Tables 128
Supplementary Figures 130
Chapter 3: Geomorphic and Climate Drivers Shape Bottom-Up Controls on Spring Staging Red Knots (*Calidris canutus rufa*) in the Virginia Barrier Island System
Appendix S.2 136
Supplementary Tables 136
List of External Supplementary Tables 144
Literature Cited 145

LIST OF FIGURES

Chapter 2: Diet and Prey Selection of Migratory Shorebirds on Mudflats in the Virginia Barrier Island System using Fecal DNA Metabarcoding

Figure 1. Study area within the Virginia barrier island system during spring migration (May 14 – June 2) 2023 – 2024, including 13 barrier islands (Wallops to Fisherman Island) and 58 mudflats distributed throughout the lagoon system. Inset maps provide examples of 2024 sampling points on mudflats (top) and barrier islands (bottom). Yellow indicates barrier island sampling points collected during the early migration period (May 14 – 20) and red during the peak migration period (May 21 – 28). Mudflats were sampled throughout the spring migration window (May 14 – June 2). 43

Figure 2. Shorebird habitat use across sand, peat, and mudflat substrates during spring migration May 14 – June 2, 2023 – 2024 in the Virginia barrier island system including (A) mean abundance (birds/point) of all shorebirds (B) mean species richness (species/point), and (C) mean abundances (birds/point) of Calidris alpina (dunlin), Calidris canutus rufa (red knot), and Calidris pusilla (semipalmated sandpiper). Error bars represent standard error (SE). Asterisks indicate significant differences based on pairwise Wilcoxon rank sum tests with Bonferroni correction: $P < 0.05$ (*), $P < 0.01$ (**), $P < 0.001$ (***), $P < 0.0001$ (****). Note: y-axis scales differ between graphs. 44

Figure 3. Mean density (organisms/m^2) of (A) all invertebrates, (B) crustaceans, (C) insects, (D) bivalves, (E) snails, (F) worms, and (G) other organisms captured in core samples collected on sand, peat, and mudflat substrates during spring migration (May 14 – June 2) 2023 – 2024 in the Virginia barrier island system. Error bars represent standard error (SE). Asterisks indicate significant differences based on pairwise Wilcoxon rank sum tests with Bonferroni correction: $P < 0.05$ (*), $P < 0.01$ (**), $P < 0.001$ (***), $P < 0.0001$ (****). Note: y-axis scales differ between graphs. 45

Figure 4. Diet composition of (A, B) Calidris alpina (dunlin), (C, D) Calidris canutus rufa (red knot), and (E, F) Calidris pusilla (semipalmated sandpiper) determined using 18S rDNA markers on fecal samples collected on mudflats during spring migration (May 14 – June 2) 2023 – 2024 in the Virginia barrier island system. We summarized 80 taxonomic categories from 157 ESVs and grouped into coarse diet bins. Weighted percent occurrence (wPOO; left panel) and relative read abundance (RRA; right panel) of diet bins are indicated by color blocks. Biofilm includes diatoms, microalgae, and dinoflagellates. Only diet bins with wPOO or RRA > 1% are shown (see Table S6a-c for details). 46

Figure 5. Diet composition of (A, B) Calidris alpina (dunlin), (C, D) Calidris canutus rufa (red knot), and (E, F) Calidris pusilla (semipalmated sandpiper) determined using 23S rDNA markers on fecal samples collected on mudflats during spring migration (May 14 – June 2) 2023 – 2024 in the Virginia barrier island system. We summarized 29 taxonomic categories from 194 ESVs and grouped into coarse diet bins. Weighted percent occurrence (wPOO; left panel) and relative read abundance (RRA; right panel) of diet bins are indicated by color blocks. Only diet bins with wPOO or RRA > 1% are shown (see Table S8a-c for details). 47

Figure 6. Preference plots illustrating selection of invertebrate prey by (A) Calidris alpina (dunlin), (B) Calidris canutus rufa (red knot), and (C) Calidris pusilla (semipalmated sandpiper) during spring migration (May 14 – June 2) 2023 – 2024 in the Virginia barrier island system. Plots compare observed consumption frequencies (dots) to 95% confidence intervals (bars) illustrating expected consumption frequencies based on the null model. Orange dots denote consumption frequencies stronger than expected (preference), blue dots weaker than expected (avoidance), and white dots consistent with the null model (no selection). 48

Chapter 3: Geomorphic and Climate Drivers Shape Bottom-Up Controls on Spring Staging Red Knots (*Calidris canutus rufa*) in the Virginia Barrier Island System

Figure 1. Conceptual diagram of hypothesized relationships influencing (a) red knot (Calidris canutus rufa) presence and abundance and (b) densities of crustaceans, coquina clams (Donax variabilis), blue mussels (Mytilus edulis), and miscellaneous prey, tested using piecewise structural equation modeling (SEM). Networks were informed by prior research on shorebird foraging ecology, geomorphology, and climate divers in the Virginia barrier island system. Units of measurement for continuous variables are shown in parentheses. Dashed lines indicate variable groupings. Blue boxes indicate response variables in component models within the piecewise SEMs. 93

Figure 2. Study area within the Virginia barrier island system on the Eastern Shore of Virginia. Data on red knots (Calidris canutus rufa) and invertebrate prey were collected on 12 barrier islands during spring migration (May 21 – 28) from 2009–2023. the inset map (right) shows examples of random survey points (black dots) and island measurements (island width = yellow lines, beach width = blue lines, and island length = black line) used to assess morphometric change over time, based on 2023 aerial imagery from the U.S. Department of Agriculture's National Agriculture Imagery Program (NAIP). 94

Figure 3. Final causal network for the red knot (Calidris canutus rufa) piecewise structural equation model showing significant paths ($p < 0.05$) influencing red knot presence and abundance during spring migration (May 21–28, 2009–2023) in the Virginia barrier island system. Black and red arrows denote positive and negative relationships, with widths scaled by standard coefficients in text boxes. Missing coefficients for the invertebrate richness component model are marked with * and dashed arrows. Blue boxes show response variables with conditional R^2 values. Correlated errors are omitted for clarity. The model includes an interaction between storminess and North Atlantic Oscillation (NAO). 95

Figure 4. Interactive effects of storminess and the North Atlantic Oscillation (NAO) from final component models in piecewise structural equation models (SEM). Plots show the effects of storminess on (a) beach width and (b) island width across different NAO phases. Lines represent predicted marginal effects of storminess and NAO while holding other variables constant, with shaded areas showing 95% confidence intervals. 96

Figure 5. Final causal network for invertebrate piecewise structural equation model showing all significant paths ($p < 0.05$) influencing densities of crustaceans, coquina clams (Donax

variabilis), blue mussels (Mytilus edulis), and miscellaneous (misc.) prey during spring migration (May 21 – 28, 2009 – 2023) in the Virginia barrier island system. Black and red arrows denote positive and negative relationships, with widths scaled by standard coefficients in text boxes. Blue boxes show response variables with conditional R^2 values. Correlated errors are omitted for clarity. The model includes an interaction between storminess and North Atlantic Oscillation (NAO)..... 97

Figure 6. Trends in barrier island morphometrics from 2007–2023 for (a) mean island width (km) and (b) mean beach width (km) on barrier islands with significant morphometric change in the Virginia barrier island system. Shaded ribbons represent 95% confidence intervals from loess-smoothing lines. Red lines denote statistically significant trends based on Kendall's tau correlation analyses. Note the difference in scales between panels..... 98

LIST OF TABLES

Chapter 3: Geomorphic and Climate Drivers Shape Bottom-Up Controls on Spring Staging Red Knots (*Calidris canutus rufa*) in the Virginia Barrier Island System

Table 1. Distributions used to fit component models in piecewise structural equation models (SEMs) investigating direct and indirect drivers of red knot (Calridris canutus rufa) and invertebrate prey dynamics in the Virginia barrier island system during spring migration (May 21 – 28, 2009 – 2023). Continuous response variables were modeled with Gaussian distribution (identity-link), while count data were modeled with negative binomial distributions (log link). Zero-inflated negative binomial models accounted for excess zeros in invertebrate density components of the red knot SEM and in crustacean, coquina clam (Donax variabilis), and miscellaneous prey density responses (see Table S2). Invertebrate richness, exhibiting underdispersed, was modeled with a Generalized Poisson distribution (log link). Red knot presence was modeled with a binomial distribution (logit link). 84

Table 2. Unstandardized estimates (B), standardized coefficients (β), standard error (SE), and p-values (p) from piecewise structural equation models (SEM; Figure 3) investigating the direct and indirect effects of habitat, climate, and geomorphic drivers on red knot (Calidris canutus rufa) presence, abundance, and invertebrate prey densities, in the Virginia barrier island system during spring migration (May 21 – 28, 2009–2023). R^2_M = marginal (fixed effects); R^2_C = conditional (fixed + random efftects). 87

Table 3. Mean (± SD) island and beach width for individual barrier islands and the overall study system from Assawoman to Fisherman Island for 2007 and 2023. Kendall's tau (τ) and p-values indicate the direction and significance of temporal trends. Percent change represents the relative difference between 2007 and 2023, and total change provides a relative index of morphometric change across all measured features. Statistical significance was set at $p < 0.05$. 91

ATTRIBUTION

Chapter 2:

Diet and Prey Selection of Migratory Shorebirds on Mudflats in the Virginia Barrier Island System using Fecal DNA Metabarcoding

Kristy C. Lapenta[1], Mikayla N. Call[1], Camille R. Alvino[1], Sarah M. Karpanty[1]

[1]Department of Fish and Wildlife Conservation, Virginia Tech, 310 W Campus Drive, Blacksburg, VA 24061, USA

Target journal: *Environmental DNA*

Author Contributions:

Concept and design: K. Lapenta and S. Karpanty

Data acquisition: K. Lapenta, M. Call, C. Alvino, and S. Karpanty

Analysis/interpretation: K. Lapenta

Manuscript drafting/revisions: K. Lapenta, M. Call, C. Alvino, and S. Karpanty

Chapter 3:

Geomorphic and Climate Drivers Shape Bottom-Up Controls on Spring Staging Red Knots (*Calidris canutus rufa*) in the Virginia Barrier Island System.

Kristy C. Lapenta[1], Christy N. Wails[1,2], Mikayla N. Call[1], Camille R. Alvino[1], Sarah M. Karpanty[1], Elizabeth A. Hunter[3], Ruth Boettcher[4], James D. Fraser[1], Jonathan Cohen[5]

[1]Department of Fish and Wildlife Conservation, Virginia Tech, 310 W Campus Drive, Blacksburg, VA 24061, USA

[2]Department of Natural Resource Management, South Dakota State University, 1155 North Campus Drive, Brookings, SD 57007, USA

[3]U.S. Geological Survey, Virginia Cooperative Fish and Wildlife Research Unit, Department of Fish and Wildlife Conservation, Virginia Polytechnic Institute and State University, Blacksburg, VA, USA

[4]Virginia Department of Wildlife Resources, 12610 Jacobus Creek Road, Machipongo, VA 23405, USA

[5]Department of Environmental and Forest Biology, The State University of New York, Syracuse, NY 13210, USA

Target journal: *Estuaries and Coasts*

Author Contributions:

Concept and design: K. Lapenta, S. Karpanty, E. Hunter, R. Boettcher, J. Fraser, and J. Cohen

Data acquisition: K. Lapenta, M. Call, C. Alvino, S. Karpanty, and J. Fraser

Analysis/interpretation: K. Lapenta, C. Wails, and E. Hunter

Manuscript drafting/revisions: K. Lapenta, C. Wails, M. Call, C. Alvino, S. Karpanty, E. Hunter, and R. Boettcher.

CHAPTER 1

Introduction

BACKGROUND

Migratory shorebirds undertake some of the longest migrations in the animal kingdom, spanning continents, hemispheres, and a multitude of ecosystems (Robinson et al. 2009). This annual feat poses unique conservation challenges as birds are exposed to threats across diverse ecological and geopolitical boundaries. Despite much diversity across species with respect to migration distance and habitat needs, migratory shorebird populations are declining globally (Koleček et al. 2021). In North America, most species are continuing to decline despite decades of conservation efforts (Rosenberg et al. 2019, Smith et al. 2023). Shorebirds have low reproductive rates and relatively long life spans, and thus populations are particularly sensitive to factors that influence adult survival (Sæther and Bakke 2000). Weiser et al. (2018) argued that few environmental or ecological factors at breeding sites significantly affected adult survival rates, suggesting that conditions during the non-breeding season were key drivers of ongoing declines.

During migration, some shorebird populations congregate at staging sites, large areas of high-quality foraging habitat that can support significant numbers of shorebirds for weeks at a time (Warnock 2010). Staging sites function as critical habitats where birds must replenish fat and muscle reserves to successfully complete migration (Piersma 1998) and inadequate refueling can lead to decreased survival rates and reproductive success (Baker et al. 2004). Major staging sites, such as geographically isolated coastal areas, often support substantial proportions of entire breeding populations (Warnock 2010), forming an ecological bottleneck (Iwamura et al. 2013) where changes in foraging quality can have far-reaching demographic consequences. Human

land-use changes have degraded coastal staging areas, contributing to global population declines (Studds et al. 2017, Murray et al. 2018). Accelerating sea-level rise and intensifying climate variability are exacerbating pressure on migratory shorebird populations by further reducing the extent of suitable foraging habitat and altering resource availability (Galbraith et al. 2002). Given the critical importance of abundant, high-quality food resources at staging sites, and the increasing threat posed by climate change, understanding shorebird foraging ecology is essential for assessing risk and informing adaptive conservation strategies.

The Virginia barrier island system, recognized as an internationally significant staging site by the Western Hemisphere Shorebird Reserve Network (WHSRN), supports over 100,000 staging migratory shorebirds annually (Wilke et al. 2005). This includes an estimated 30% of the federally threatened red knot (*Calidris canutus rufa*; Cohen et al. 2009, Watts and Truitt 2015), as well as 10 other shorebird Species of Greatest Conservation Need (VDWR 2015). This coastal system is almost entirely undeveloped and is permanently protected from future development by multiple non-governmental, state, and federal conservation organizations (Watts and Truitt 2015). As a result, it serves as a vital refuge for migratory shorebirds along the U.S. Atlantic flyway. Additionally, the undeveloped condition of the Virginia barrier island system provides a unique opportunity to study climate-driven ecosystem changes. This region hosts the Virginia Coast Reserve (VCR), part of the National Science Foundation's Long-Term Ecological Research program (NSF LTER). The VCR LTER aims to understand the mechanisms driving ecosystem state changes, or shifts from one stable ecological condition to another, and how long-term climate change influences these transitions in coastal barrier systems (UVA 2022).

As part of the interdisciplinary VCR LTER research team, Virginia Tech has conducted long-term monitoring of migratory shorebirds since 2007, focusing on the threatened red knot.

The research from this project has demonstrated that the Virginia barrier island system serves as a distinct and valuable spring staging site, separate from the intensively studied Delaware Bay, with minimal movement of individuals between the two regions in a given year (Cohen et al. 2009). In Virginia, red knots primarily forage along the ocean-facing intertidal zone of the barrier islands, where site selection is strongly influenced by invertebrate prey abundance (Cohen et al. 2010). Prey abundance varies with intertidal substrates, tidal phase, and daily water temperature (Heller et al. 2022). Red knot presence at foraging sites is closely associated with coquina clams (*Donax variabilis*) and blue mussels (*Mytilus edulis*), as the subpopulation staging in Virginia specialize on bivalves (Heller 2020, Lapenta et al., *in prep*), consistent with their behavior throughout much of their non-breeding range (Dekinga and Piersma 1993). Though food availability does not appear to be a limiting factor in Virginia, red knots must forage at night in order to meet energetic requirements on a digestively constrained diet of hard-shelled prey (Cohen et al. 2011). While this body of research has advanced understanding of red knot foraging ecology in Virginia, far less is known about other migratory shorebird species or the role of other critically important foraging habitats, such as intertidal mudflats.

Recent work on mudflats in the Virginia barrier island system suggests that shorebird responses to changing foraging conditions, such as biological invasions, vary by foraging mode. On mudflats throughout the lagoon system, flexible foraging species appear to prefer microhabitats where prey availability is modified by invasive macroalgae, while specialized foragers prefer uninvaded microhabitats (Besterman et al. 2020, Besterman and Pace 2021). Macroalgae presence does not drive prey abundance at mudflat foraging sites, rather mudflat topography determined prey accessibility and indirectly shorebird habitat use. Besterman and Pace (2021) found on smooth mudflats, shorebird abundance increased with prey abundance

while on hummocky mudflats, shorebird abundance increased with macroalgae abundance. These findings suggested that flexible foraging species such as dunlin (*Calidris alpina*) and semipalmated sandpipers (*Calidris pusilla*), the most abundant species found foraging on mudflats in the Virginia barrier island system during spring migration (Besterman and Pace 2021), can adapt to spatial and structural variation in a highly dynamic environment. However, despite these insights, major knowledge gaps remain regarding prey availability, selection and preferences among various species utilizing mudflats in this system.

Another pressing research priority is understanding how climate change may impact the long-term viability of the Virginia barrier island system as a staging site for red knots and other migratory shorebirds. Because the system is undeveloped, climate-related factors such as sea-level rise, storm events, and warming ocean temperatures, are the dominant drivers of ecosystem state change (UVA 2022). Virginia experiences one of the highest rates of sea-level rise on the U.S. Atlantic coast due land subsidence (Sweet et al. 2022), and tropical and extra-tropical storms impacting the region are increasing in intensity (Dominguez et al. 2024). Additionally, average daily water temperature and frequency of marine heat waves have risen (UVA 2022). These changing climate drivers are projected to increase the likelihood of rapid shifts in barrier island morphology, with uncertain consequences for shorebird populations. Previous studies indicate that barrier island features such as beach width and vegetation proximity can influence migratory shorebird habitat use (Dekker and Ydenberg 2004, Murchison et al. 2016), highlighting the importance of understanding how geomorphic changes affect shorebird foraging ecology. Dramatic declines in red knot populations have been linked to significant changes in prey availability (Baker et al. 2004, Morrison et al. 2004). Therefore, identifying how red knots

respond to both local and system-wide ecosystem changes is critical for developing adaptive management strategies in these increasingly vulnerable coastal systems.

THESIS OBJECTIVES

My thesis aims to advance understanding of migratory shorebird foraging ecology in the Virginia barrier island system during spring migration to better inform management of these shorebirds and their broader ecosystem. In **Chapter 2**, I evaluated the importance of intertidal mudflats as foraging habitat by comparing shorebird use and invertebrate prey density across barrier island sand and peat substrates and intertidal lagoonal mudflats. I also used fecal DNA metabarcoding to characterize the diets of red knots, dunlin, and semipalmated sandpipers on mudflats, including both invertebrate and biofilm components, and assessed invertebrate prey selection using a use-versus-availability framework. In **Chapter 3**, I examined how red knot presence and abundance, along with the density of their invertebrate prey, were influenced by broader barrier island features and long-term geomorphic and climate-driven changes. Using piecewise structural equation modeling, I tested a hypothesized causal network integrating 10 years of red knot foraging data (2009 – 2023), remotely sensed morphometric characteristics, mesoscale island behavior, and measures of storm frequency and intensity, water temperature, and global climate oscillations such as the North Atlantic Oscillation (NAO). I also assessed changes in barrier island morphology between 2007, the start of Virginia Tech's long-term monitoring program, 2023, the most recent year of available aerial imagery. Together, these results provide an integrated perspective on the climate and environmental factors shaping staging habitat quality and offer insights to guide management of coastal foraging areas in Virginia and along the broader U.S. Atlantic flyway.

LITERATURE CITED

Baker, A. J., P. M. González, T. Piersma, L. J. Niles, I. de Lima Serrano do Nascimento, P. W. Atkinson, N. A. Clark, C. D. T. Minton, M. K. Peck, and G. Aarts. 2004. Rapid population decline in red knots: fitness consequences of decreased refuelling rates and late arrival in Delaware Bay. Proceedings of the Royal Society of London. Series B: Biological Sciences 271:875–882.

Besterman, A. F., S. M. Karpanty, and M. L. Pace. 2020. Impact of exotic macroalga on shorebirds varies with foraging specialization and spatial scale. PLOS ONE 15:e0231337.

Besterman, A. F., and M. L. Pace. 2021. Mudflat geomorphology determines invasive macroalgal effect on invertebrate prey and shorebird predators. Ecology 102.

Cohen, J. B., B. D. Gerber, S. M. Karpanty, J. D. Fraser, and B. R. Truitt. 2011. Day and Night Foraging of Red Knots (*Calidris canutus*) during Spring Stopover in Virginia, USA. Waterbirds 34:352–356.

Cohen, J. B., S. M. Karpanty, J. D. Fraser, and B. R. Truitt. 2010. The effect of benthic prey abundance and size on red knot (Calidris canutus) distribution at an alternative migratory stopover site on the US Atlantic Coast. Journal of Ornithology 151:355–364.

Cohen, J. B., S. M. Karpanty, J. D. Fraser, B. D. Watts, and B. R. Truitt. 2009. Residence Probability and Population Size of Red Knots During Spring Stopover in the Mid-Atlantic Region of the United States. Journal of Wildlife Management 73:939–945.

Dekinga, A., and T. Piersma. 1993. Reconstructing diet composition on the basis of faeces in a mollusc-eating wader, the knot Calidris canutus. Bird study 40:144–156.

Dekker, D., and R. Ydenberg. 2004. Raptor predation on wintering Dunlins in relation to the tidal cycle. The Condor 106:415–419.

Dominguez, R., M. Fenster, and J. McManus. 2024. Storm surge frequency, magnitude, and cumulative storm beach impact along the US east coast. EGUsphere 2024:1–31.

Galbraith, H., R. Jones, R. Park, J. Clough, S. Herrod-Julius, B. Harrington, and G. Page. 2002. Global Climate Change and Sea Level Rise: Potential Losses of Intertidal Habitat for Shorebirds. Waterbirds 25:173.

Heller, E. L. 2020. Factors affecting Western Atlantic red knots (Calidris canutus rufa) and their prey during spring migration on Virginia's barrier islands. doctoral, Virginia Polytechnic Institute and State University, Blacksburg, VA, USA.

Heller, E. L., S. M. Karpanty, J. B. Cohen, D. H. Catlin, S. J. Ritter, B. R. Truitt, and J. D. Fraser. 2022. Factors that affect migratory Western Atlantic red knots (Calidris canutus rufa) and their prey during spring staging on Virginia's barrier islands. V. H. R. Paiva, editor. PLOS ONE 17:e0270224.

Iwamura, T., H. P. Possingham, I. Chadès, C. Minton, N. J. Murray, D. I. Rogers, E. A. Treml, and R. A. Fuller. 2013. Migratory connectivity magnifies the consequences of habitat loss from sea-level rise for shorebird populations. Proceedings of the Royal Society B: Biological Sciences 280:20130325.

Koleček, J., J. Reif, M. Šálek, J. Hanzelka, C. Sottas, and V. Kubelka. 2021. Global population trends in shorebirds: migratory behaviour makes species at risk. The Science of Nature 108:9.

Morrison, R. I. G., R. K. Ross, and L. J. Niles. 2004. Declines in Wintering Populations of Red Knots in Southern South America. The Condor 106:60–70.

Murchison, C. R., Y. Zharikov, and E. Nol. 2016. Human Activity and Habitat Characteristics Influence Shorebird Habitat Use and Behavior at a Vancouver Island Migratory Stopover Site. Environmental Management 58:386–398.

Murray, N. J., P. P. Marra, R. A. Fuller, R. S. Clemens, K. Dhanjal-Adams, K. B. Gosbell, C. J. Hassell, T. Iwamura, D. Melville, C. D. T. Minton, A. C. Riegen, D. I. Rogers, E. J. Woehler, and C. E. Studds. 2018. The large-scale drivers of population declines in a long-distance migratory shorebird. Ecography 41:867–876.

Piersma, T. 1998. Phenotypic Flexibility during Migration: Optimization of Organ Size Contingent on the Risks and Rewards of Fueling and Flight? Journal of Avian Biology 29:511.

Robinson, R. A., H. Q. Crick, J. A. Learmonth, I. M. Maclean, C. D. Thomas, F. Bairlein, M. C. Forchhammer, C. M. Francis, J. A. Gill, and B. J. Godley. 2009. Travelling through a warming world: climate change and migratory species. Endangered species research 7:87–99.

Rosenberg, K. V., A. M. Dokter, P. J. Blancher, J. R. Sauer, A. C. Smith, P. A. Smith, J. C. Stanton, A. Panjabi, L. Helft, M. Parr, and P. P. Marra. 2019. Decline of the North American avifauna. Science 366:120–124.

Sæther, B.-E., and Ø. Bakke. 2000. Avian life history variation and contribution of demographic traits to the population growth rate. Ecology 81:642–653.

Smith, P. A., A. C. Smith, B. Andres, C. M. Francis, B. Harrington, C. Friis, R. I. G. Morrison, J. Paquet, B. Winn, and S. Brown. 2023. Accelerating declines of North America's shorebirds signal the need for urgent conservation action. Ornithological Applications 125:duad003.

Studds, C. E., B. E. Kendall, N. J. Murray, H. B. Wilson, D. I. Rogers, R. S. Clemens, K. Gosbell, C. J. Hassell, R. Jessop, and D. S. Melville. 2017. Rapid population decline in migratory shorebirds relying on Yellow Sea tidal mudflats as stopover sites. Nature communications 8:14895.

Sweet, W. V., B. D. Hamlington, R. E. Kopp, C. P. Weaver, P. L. Barnard, D. Bekaert, W. Brooks, M. Craghan, G. Dusek, T. Frederikse, G. Garner, A. S. Genz, J. P. Krasting, E. Larour, D. Marcy, J. J. Marra, J. Obeysekera, M. Osler, M. Pendleton, D. Roman, L. Schmied, W. Veatch, K. D. White, and C. Zuzak. 2022. Global and Regional Sea Level Rise Scenarios for the United States: Updated Mean Projections and Extreme Water Level Probabilities Along U.S. Coastlines. Technical Report, National Oceanic and Atmospheric Administration.

UVA. 2022. Virginia Coast Reserve LTER Annual Report. University of Virginia, Charlottesville, VA, USA.

Virginia Department of Game and Inland Fisheries. 2015. Virginia's 2015 Wildlife Action Plan. Virginia Department of Game and Inland Fisheries, Henrico, VA, USA.

Warnock, N. 2010. Stopping vs. staging: the difference between a hop and a jump. Journal of Avian Biology 41:621–626.

Watts, B. D., and B. R. Truitt. 2015. Spring migration of red knots along the Virginia barrier island system: Virginia Red Knots. The Journal of Wildlife Management 79:288–295.

Weiser, E. L., R. B. Lanctot, S. C. Brown, H. R. Gates, R. L. Bentzen, J. Bêty, M. L. Boldenow, W. B. English, S. E. Franks, and L. Koloski. 2018. Environmental and ecological conditions at Arctic breeding sites have limited effects on true survival rates of adult shorebirds. The Auk: Ornithological Advances 135:29–43.

Wilke, A. L., B. D. Watts, B. R. Truitt, and R. Boettcher. 2005. Breeding Season Status of the American Oystercatcher in Virginia, USA. Waterbirds 28:308–315.

CHAPTER 2

Diet and Prey Selection of Migratory Shorebirds on Mudflats in the Virginia Barrier Island System using Fecal DNA Metabarcoding

ABSTRACT

Intertidal mudflats are important foraging areas for migratory shorebirds at coastal staging sites, but these habitats are rapidly being degraded by land use changes and rising sea levels. Our objective was to provide data on the foraging ecology of migratory shorebirds using mudflats in the Virginia barrier island system, and to contextualize these findings within the broader coastal system. We compared shorebird habitat use and invertebrate prey availability between sand and peat substrates on barrier islands and intertidal lagoon mudflats during spring migration (May 14 – June 2) 2023–2024. We collected fecal samples on mudflats from *Calidris alpina* (dunlin), *Calidris canutus rufa* (red knot), and *Calidris pusilla* (semipalmated sandpiper) and analyzed diet composition using fecal DNA metabarcoding. We then combined diet composition data with invertebrate prey availability to investigate dietary selectivity on mudflats. Mudflats supported similar total shorebird abundances, species richness, and invertebrate abundances as barrier island sand substrate, but the invertebrate community structure on mudflats differed significantly from barrier island substrates. *C. alpina* and *C. pusilla* were most abundant on peat and mudflats while *C. c. rufa* mainly used sand and peat. *C. alpina* and *C. pusilla* fed primarily on crustaceans and exhibited wider diet breadth whereas *C. c. rufa* mainly fed on bivalves. All species consumed biofilm, a microbial mixture primarily comprised of diatoms, especially *C. pusilla*. *C. alpina* and *C. c. rufa* preferentially consumed bivalves while *C. pusilla* exhibited no prey selection. Our results support that mudflats are key foraging areas for migratory shorebirds in the Virginia barrier island system. We provide new evidence that biofilm is consumed by migrating shorebirds at staging sites in the mid-Atlantic region. Conservation

efforts must consider habitat connectivity and landscape dynamics across coastal staging sites to support the diverse foraging needs of migratory shorebirds.

KEYWORDS

Migratory shorebirds, staging, mudflats, foraging, fecal DNA metabarcoding, diet, conservation

INTRODUCTION

Shorebirds (order Charadriiformes) are experiencing rapid population declines despite ongoing conservation efforts (Smith et al. 2023). Migratory shorebirds are declining more rapidly than resident populations (Koleček et al. 2021), perhaps driven by widespread habitat degradation across migratory flyways. A large percentage of the world's migratory shorebirds rely on coastal staging sites while migrating (Butler et al. 2001) and rapid degradation of intertidal foraging habitats has been linked to regional population declines (Studds et al. 2017). Collectively, increasing pressure from human development and sea-level rise threaten coastal ecosystems (Murray et al. 2019), placing shorebird populations at an increased risk and emphasizing the need for science-based management.

Shorebirds distribute across coastal areas based on food abundance and quality (Cohen et al. 2009, Heller et al. 2022), though species-specific foraging strategies further shape these patterns (Burger et al. 1997). Shorebirds primarily feed on intertidal invertebrates and most species exhibit some degree of dietary flexibility (MacDonald et al. 2012). Generalist and specialist foraging strategies developed as a method to optimize the exploitation of resources, either with a range of flexibility to exploit the most abundant resources or with high efficiency for exploiting few, specific resources (Durell 2000). Specialist strategies are thought to evolve

under stable environments, making dietary specialists vulnerable to rapid environmental change (Clavel et al. 2011). Establishing baseline data on habitat use, diet, and prey preferences at critical staging sites provides a foundation for effective site-and flyway-wide conservation efforts.

The Virginia barrier island system is an internationally significant staging site along the U.S. Atlantic flyway, supporting over 100,000 shorebirds annually (Wilke et al. 2005), including a significant portion of the U.S. federally threatened *Calidris canutus rufa* (red knot) population during spring migration (Cohen et al. 2009, Watts and Truitt 2015). *C. c. rufa* staging in Virginia are bivalve specialists (Heller 2020), consistent with patterns observed across other parts of their non-breeding range (Dekinga and Piersma 1993). However, knowledge gaps exist regarding how *C. c. rufa* and other migratory shorebirds use different foraging habitats across the coastal landscape. Intertidal mudflats, in particular, are critical foraging areas at many coastal staging sites (Studds et al. 2017), yet their role in the Virginia barrier island system is not as well-studied compared to barrier island habitats (Cohen et al. 2010, Heller et al. 2022).

Calidris alpina (dunlin) and *Calidris pusilla* (semipalmated sandpiper) are among the most abundant species that forage on mudflats in the Virginia barrier island system (Besterman and Pace 2021). Both species are recognized dietary generalists in other parts of their North American range, where their non-breeding diet have been well studied (Gerwing et al. 2016, Hobson et al. 2022). Although aspects of their foraging behavior have been examined in the mid-Atlantic region (Novcic 2016, Novcic et al. 2016), comprehensive dietary data for *C. alpina* and *C. pusilla* remain limited. A growing body of research highlights the importance of biofilm, a microbial mixture comprised of cyanobacteria and unicellular eukaryotes such as diatoms, dinoflagellates, and other unicellular algae (Schnurr et al. 2020), as a food resource for these

species during spring migration (Gerwing et al. 2016, Hobson et al. 2022). However, it is unknown whether *C. alpina* and *C. pusilla* consume biofilm in on mudflats in Virginia. Identifying the diets of migratory shorebirds on mudflats at this internationally significant staging site, including potential biofilm consumption, is essential for understanding the ecological value of these foraging habitats.

The objective of this study was to examine the importance of mudflats to migratory shorebirds during spring migration in the Virginia barrier island system. We compared shorebird habitat use and prey abundance between mudflats and ocean-facing barrier island intertidal zones, which are comprised of sand and peat substrates, to contextualize the role of mudflats in the foraging landscape. We used fecal DNA metabarcoding to describe diet composition, including invertebrates and biofilm, and to assess the preferential selection of invertebrate prey by *C. c. rufa*, *C. alpina*, and *C. pusilla* foraging on mudflats. Fecal DNA metabarcoding provides a non-invasive and effective method for identifying a broad range of taxa at a fine taxonomic resolution (Correia et al. 2023), making it well suited for studies involving sensitive species. Fecal DNA metabarcoding has been successfully applied to describe *C. c. rufa* diet on barrier island substrates in Virginia (Heller 2020), offering a valuable opportunity to characterize the diet of this critically imperiled species across the coastal landscape at a major staging site.

We hypothesized that shorebird habitat use would be comparable between barrier island and mudflat substrates, but that *C. alpina* and *C. pusilla* would be more abundant on mudflats. Based on prior research (Heller et al. 2022), we further hypothesized that peat substrate would support the highest density of invertebrates, and that invertebrate community structure would differ across and between substrate types. We predicted that 1) all three species would consume biofilm, with higher consumption expected in *C. pusilla* and *C. alpina,* and 2) *C. c. rufa* foraging

on mudflats would preferentially consume bivalves, while *C. alpina* and *C. pusilla* would exhibit more generalist selection patterns. The results of this research can be used to inform management practices of coastal foraging areas in Virginia and the broader U.S. Atlantic flyway by highlighting the ecological value of mudflat habitats and dietary needs of diverse shorebird species during spring migration.

METHODS

Study area

The Virginia barrier island system is characterized by open water, tidal creeks, mudflats, and saltmarshes (Wilke et al. 2005). It includes 14 barrier islands that extend ~100km from Assateague Island to Fisherman Island, as well as shallow lagoons that formed between the islands and the Delmarva Peninsula. Our study focused on 13 barrier islands (from Wallops Island in the north to Fisherman Island in the south) and 58 mudflats (Figure 1). The barrier islands are primarily owned and managed by The Nature Conservancy, U.S. Fish and Wildlife Service, and the Commonwealth of Virginia, comprising the Volgenau Virginia Coast Reserve. Our research was additionally carried out within the Virginia Coast Reserve Long-Term Ecological Research Site (VCR LTER) as part of the larger National Science Foundation's LTER Network. The barrier islands in the system are largely undeveloped and access is limited, protecting them from development and minimizing human disturbance to shorebirds (Cohen et al. 2009). Wallops Island, owned by the National Aeronautics and Space Administration (NASA), is the only developed island in the chain.

During spring migration, shorebirds foraged along ocean-facing intertidal zones of the barrier islands and on intertidal mudflats located within the saltmarshes and lagoons (Besterman

et al. 2020, Heller et al. 2022). Barrier island intertidal zones are primarily sandy, with peat banks that are patchy and comprise < 10% of the shoreline (Watts and Truitt 2015). Peat banks form as the barrier islands migrate landward over backbarrier marsh platforms, exposing buried marsh when overwash events redistribute sediment and erode the shoreface (Walters et al. 2014). Peat banks support dense populations of invertebrates and attract high numbers of shorebirds when exposed (Heller et al. 2022). Crustaceans (i.e., amphipods and calanoid copepods) are the most abundant prey across barrier island beaches, followed by bivalves, including spat of *Mytilus edulis* (blue mussel) and *Cyrtopleura costata* (angel wing clam) in peat and *Donax variabilis* (coquina clam) in sand (Heller et al. 2022). Mudflats are primarily muddy but range from mud to sand, and occur patchily along the lagoon's east-west gradient (Besterman et al. 2021). Macroalgae mats cover 10-40% of the exposed mudflat surfaces and dominant species include invasive *Agarophyton vermiculophyllum* and native *Ulva spp*. (Besterman et al. 2021). Polychaetes and small crustaceans (i.e., amphipods and isopods) are the most abundant invertebrate taxa on mudflats (Besterman and Pace 2021).

Field surveys and sample collection

We collected data on migratory shorebirds and their invertebrate prey from 14 May– 2 June 2023–2024, along the ocean-facing intertidal zone of barrier islands and the water's edge of intertidal mudflats (Figure 1). This period corresponds with the peak of *C. c. rufa* migration in Virginia (Cohen et al. 2009). To overcome tide-related logistical constraints, we divided barrier island sampling into two distinct periods: early (14–20 May) and peak (21–28 May) migration (Heller et al. 2022). During early migration, we exclusively sampled exposed peat banks within 2 hours of low tide to obtain an adequate sample size. During peak migration, we sampled all

barrier island substrates regardless of tide, with the vast majority of samples falling on sandy substrates. We sampled mudflats throughout early and peak migration and extended the mudflat sampling through 2 June to accommodate weather and tide-related access challenges.

We identified potential mudflat sampling locations using expert knowledge of region (Alex Wilke, The Nature Conservancy, personal communication) and publicly available data including mudflat sampling sites from previous studies (Besterman 2018). We generated random sampling points in ArcGIS Pro 3.0 (ESRI, Redlands, California, USA) using the most recently available (2021) orthoimagery of our study area obtained from the United States Department of Agriculture Farm Service Agency's National Agriculture Imagery Program. Given the dynamic nature of coastal systems, we generated 100 random mudflat points in 2023 and 50 in 2024, adjusting for changes in mudflat distribution and accessibility. For each year of barrier island sampling, we generated 60 early migration points constrained to known peat bank locations and 115 peak migration points along the intertidal zone, spaced to fall at least 200 m apart (Figure S1; Heller et al. 2022).

We counted all non-flying shorebirds on the shoreline at each point within a 100 m radius semicircle, with the water's edge serving as the diameter of the semicircle. We then collected a core sample at the waterline using a section of PVC pipe (10 cm diameter x 3.5 cm depth; volume = 275 cm^3) consistent with the bill length of *C. c. rufa* (Tomkovich 1992), to ensure comparability with prior studies (Cohen et al. 2010, Heller et al. 2022). While *C. alpina* and *C. pusilla* have different bill lengths (3.8 cm and 2.1 cm, respectively; MacLean and Holmes 1971, Hicklin and Gratto-Trevor 2020), we assume this core depth captures a representative sample of prey accessible to all focal species. Core samples were extracted using a trowel, sealed into resealable plastic bags, and later frozen until analysis. To extract shorebird prey items from the

core samples, we washed cores through a series of sieves (4–0.25 mm) and sorted invertebrates under a dissecting microscope into coarse prey bins (i.e., crustaceans, insects, bivalves, snails, worms, and all other organisms), as we could not visually identify most invertebrates to lower taxonomic orders. We report invertebrate prey results on the organisms/m^2 scale following Heller et al. (2022).

We opportunistically collected fecal samples from *C. alpina*, *C. c. rufa*, and *C. pusilla* on mudflats during both field seasons. To ensure accurate species identification, we collected fecal samples when birds were observed defecating or when flocks were ≥ 90% a single species (Heller 2020). To minimize environmental contamination and DNA degradation, common risks due to contact with sediment and exposure to sunlight and saltwater (Oehm et al. 2011), we used sterilized tweezers to isolate the brown digested matter, avoiding uric acid and contact with substrates (Gerwing et al. 2016) and avoided collecting samples in contact with water. When defecation was not directly observed, we used appearance as an indicator of freshness (McInnes et al. 2017), collecting only wet-looking samples likely to have been deposited recently. Although time since feeding can affect dietary detection (Oehm et al. 2011), shorebirds have fast digestive turnover times with average defecation rates of 0.42 droppings/min in medium-bodied shorebirds (e.g., *C. c. rufa;* González et al. 1996) and 0.50 droppings/minute in small-bodied shorebirds (Kuwae et al. 2008), ensuring relative freshness of samples. We placed each fecal sample into separate 14.8 mL vials and froze them immediately upon returning from the field. Frozen samples were stored at -20°C.

DNA metabarcoding

We packed frozen fecal samples in dry ice and shipped them overnight to Jonah Ventures, LLC (Boulder, CO) for laboratory analysis. DNA from shorebird droppings was extracted using the Omega Biotek Mag-Bind® Universal Pathogen Core Kit (4x96 Preps; Cat. No. / ID: M4030-01) according to the manufacturer's protocol. Samples were manually processed through all cell lysis steps and transferred to a Hamilton Microlab Starlet for automated extraction. Approximately 300µl of lysate was used for genomic DNA extraction. Genomic DNA was eluted into 100µl and frozen at -20°C. To identify invertebrate components of diet, we used a universal genetic marker, 18S (primers set F1391 and REukBr: forward GTACACACCGCCCGTC and reverse TGATCCTTCTGCAGGTTCACCTAC), designed to amplify the V9 hypervariable region (Ramirez et al. 2014). To identify biofilm components of diet, we used 23S (p23SrV_f1 and Diam23Sr1 23S primers; forward GGACAGAAAGACCCTATGAA and reverse TGAGTGACGGCCTTTCCACT) designed to amplify a portion of the chloroplast trnL intron (Sherwood and Presting 2007, Hamsher et al. 2011, Cannon et al. 2016). In both cases, forward and reverse primers contained a 5' adaptor sequence to allow for subsequent indexing and Illumina sequencing. All fecal DNA samples were used for library preparation using 18S and 23S rDNA markers through two rounds of PCR amplification (Appendix S1). Pooled sample libraries were sent for sequencing on an Illumina MiSeq (San Diego, CA) at the Texas A&M Agrilife Genomics and Bioinformatics Sequencing Core facility using the v2 500-cycle kit (cat# MS-102-2003). Necessary quality control measures were performed at the sequencing center prior to sequencing.

Bioinformatic analysis

All bioinformatics were conducted by Jonah Ventures LLC. Raw sequence data were demultiplexed using pheniqs v2.1.0 (Galanti et al. 2021), enforcing strict matching of sample barcode indices (i.e, no errors). Cutadapt v3.4 (Martin 2011) was then used to remove gene primers from the forward and reverse reads, discarding any read pairs where one or both primers were not found at the expected location (5') with an error rate < 0.15. Read pairs were then merged using vsearch v2.15.2 (Rognes et al. 2016), discarding resulting sequences with a length of < 50 bp, > 200 bp for the invertebrate primers, and of < 300 bp, > 380 bp for the biofilm primers, or with a maximum expected error rate (Edgar and Flyvbjerg 2015) > 0.5 bp. For each sample, reads were then clustered using the unoise3 denoising algorithm (Edgar 2016) as implemented in vsearch, using an alpha value of 5 and discarding unique raw sequences observed less than 8 times. Counts of the resulting exact sequence variants (ESV) were then compiled and putative chimeras were removed using the uchime3 algorithm, as implemented in vsearch. For each final ESV, a consensus taxonomy was assigned using a custom best-hits algorithm and either the SILVA v138.1 reference database (Pruesse et al. 2007) for invertebrates, or GenBank reference database (Benson et al. 2005) consisting of publicly available sequences as well as Jonah Ventures voucher sequences records for biofilm. Reference database searching used an exhaustive semi-global pairwise alignment with vsearch, and match quality was quantified using a custom, query-centric approach, where the % match ignores terminal gaps in the target sequence, but not the query sequence. The consensus taxonomy was then generated using either all 100% matching reference sequences or all reference sequences within 1% of the top match, accepting the reference taxonomy for any taxonomic level with > 90% agreement across the top hits.

Post-bioinformatics filtering

We filtered both 18S and 23S datasets to remove non-diet items (e.g. Bacteria, Fungi, Cyanobacteria, and Magnoliopsida), low resolution taxa (e.g., Eukaryota), and sequences lacking key taxonomic information (e.g., missing class). We excluded samples with fewer than 100 reads, as likely amplification failures. Within the remaining samples, we removed sequence reads comprising < 1% of total sample reads to eliminate low-level contaminants, and reads comprising < 0.5% of each ESV's total reads to reduce false positives (Drake et al. 2022). We assigned the remaining ESVs to the lowest reliable taxonomic level based on percent thresholds of base pairs in the sequence matched to a specific taxon: ≥ 99% for species, ≥ 98% for genus, ≥ 95% for family, and ≥95% without lower resolution to order or class (Stenhouse et al. 2023). We cross-referenced species, genus, and family level assignments with the Ocean Biodiversity Information System (OBIS) to confirm geographic relevance (Grassle 2000). Finally, we grouped ESVs into diet bins to align with field-based core sampling resolution. We grouped items in the 18S dataset as: crustaceans, insects, bivalves, snails, worms, other organisms, diatoms, dinoflagellates, microalgae (e.g., unicellular algae), and macroalgae (e.g., multicellular algae) and in the 23S dataset as: diatoms, microalgae, and macroalgae.

Statistical analyses

To assess differences in shorebird habitat use and prey availability across substrate types, we combined data collected from peat banks during early and peak migration periods. Shapiro-Wilk normality tests indicated that metrics of shorebird habitat use (i.e., shorebird abundance and species richness) and invertebrate densities were not normally distributed (Table S1). We then used Kruskal-Wallis tests to compare shorebird and prey metrics across sand, peat, and mudflat

substrates, followed by pairwise Wilcoxon rank sum tests with Bonferroni correction to assess differences among substrate types.

We summarized diet data obtained from each DNA marker separately due to differences in resolution between primer sets using three standard metrics: frequency of occurrence (FOO), the proportion of samples containing a diet item; weighted percent of occurrence (wPOO), which adjusts FOO based on the total number of items in a sample; and relative read abundance (RRA), the proportion of sequence reads attributed to each diet item. Occurrence-based diet summaries produce are typically more consistent but provide a less accurate representation of overall diet as this method can artificially inflate the importance of rare food taxa (Deagle et al. 2019) which may be an issue in the case of environmental contamination or secondary consumption (McInnes et al. 2017). In contrast, RRA estimates are less affected by this and are considered more accurate if more variable but are more sensitive to sequence recovery biases (Deagle et al. 2013). We used recommended minimum sequence thresholds shown to effectively eliminate a high proportion of potential biases introduced by environmental contamination, secondary consumption, and sequencing errors (Drake et al. 2022). We present results from both summaries as recommended by Deagle et al. (2019) when there is uncertainty surrounding which method will be most accurate. We express all values as percentages and only present results of taxa representing ≥ 1% of the diet. For each species, we averaged wPOO and RRA values across all samples, giving each sample equal weight.

To test for prey selectivity, we used a network-based null-modeling approach implemented in the R package *econullnetr* (Vaughan et al. 2018). This method compares observed consumption frequencies obtained from diet data to expected frequencies based on the relative abundance of prey in core samples under the null hypothesis that individual consumers

(shorebirds) are using resources (invertebrate prey) relative to their availability on the landscape (Agusti et al. 2003). Observed consumption frequencies higher or lower than expected indicate preference or avoidance, while frequencies consistent with the null model indicate no selection. We excluded insects from this analysis due to limitations in core sampling methodology capturing flying insects. We generated a null model, incorporating the presence/absence of prey bins in fecal samples (FOO) and ran it for 9,999 iterations. All statistical analyses were conducted in R version 4.4.1 (R Core Team 2024).

RESULTS

Shorebird and invertebrate composition across substrates

We surveyed 333 points across sand (n = 176), peat (n = 89), and mudflat (n = 68) substrates in the Virginia barrier island system during spring migration 2023 and 2024, recording 13,254 shorebirds ($\bar{x}$ = 39.8 ± 3.8 SE birds/point) over the sampling period (Table S2). Most shorebirds were observed on sand (45%; n = 5895) and peat (42%; n = 5,623), with fewer on mudflats (13%; n = 1,736). We documented 17 shorebird species ($\bar{x}$ = 3.7 ± 0.1 SE species/point) across all points, 53% (n = 9) of which are listed as species of critical to moderate conservation concern in the Virginia Wildlife Action Plan (VDWR 2015; Table S2). Total species richness was highest on mudflats (n = 15), followed by peat (n = 13) and sand (n = 12). Out of all shorebirds recorded during our study, *C. alpina* was the most abundant species observed on peat (n = 3,416, $\bar{x}$ = 38.4 ± 6.2 SE birds/point) and mudflats (n = 608, $\bar{x}$ = 8.9 ± 1.9 SE birds/point), while *C. c. rufa* was the most abundant species observed on sand (n = 2,585, $\bar{x}$ = 14.7 ± 4 SE birds/point; Table S2).

Shorebird abundance ($\chi^2 = 19.9$, $p < 0.0001$), species richness ($\chi^2 = 36.9$, $p < 0.0001$) and the abundances of *C. alpina* ($\chi^2 = 98.5$, $p < 0.0001$), *C. c. rufa* ($\chi^2 = 11.6$, $p = 0.003$), and *C. pusilla* ($\chi^2 = 15.6$, $p = 0.0004$) differed across substrates. Total shorebird abundance and species richness were higher on peat than on sand and mudflats (Figures 2A – 2B). *C. alpina* was more abundant on peat than sand and mudflats and more abundant on mudflats compared to sand (Figure 2C). *C. c. rufa* was more abundant on sand and peat compared to mudflats, while *C. pusilla* was more abundant on mudflats compared to sand (Figure 2C).

We analyzed 333 core samples collected on sand ($n = 176$), peat ($n = 89$), and mudflat ($n = 68$) substrates. Crustaceans were the most abundant invertebrates across all substrates (sand: $\bar{x}$ = 3,330.9 ± 654.6 SE organisms/m^2; peat: $\bar{x}$ = 28,194.3 ± 7,132.7 SE organisms/m^2; mudflats: $\bar{x}$ = 1,157.7 ± 776.2 SE organisms/m^2), and the most frequently occurring in sand (80%) and peat (85%) samples. Worms were most common on mudflats, occurring in 79% of samples. Of our core samples, 8% ($n = 27$) contained no prey. The invertebrate community varied by substrate type, with the sand and peat substrates dominated by crustaceans (77% and 66%, respectively) and bivalves (20% and 33%, respectively), and mudflats composed primarily of crustaceans (46%) and worms (43%; Figure S2).

Total invertebrate density ($\chi^2 = 72.6$, $p < 0.0001$) and the densities of crustaceans ($\chi^2 = 58.3$, $p < 0.0001$), bivalves ($\chi^2 = 95.9$, $p < 0.0001$), snails ($\chi^2 = 48.1$, $p < 0.0001$), worms ($\chi^2 = 106.6$, $p < 0.0001$), and other organisms ($\chi^2 = 9.3$, $p = 0.01$) differed across substrates. While insect density also differed across substrates ($\chi^2 = 6.9$, $p = 0.03$), there were no significant pairwise differences detected for insects (Figure 3C). Total invertebrate density was higher in peat than in sand and mudflats (Figure 3A). Crustacean and bivalve densities were higher in peat than sand, and higher in both sand and peat than mudflats (Figures 3B and 3D). Worm densities

were highest in mudflats compared to sand and peat and were higher in peat than sand (Figure 3F). Snail densities were similarly highest in mudflats compared to sand and peat (Figure 3E) while other organisms were denser in mudflats than sand (Figure 3G).

Shorebird diet composition

We collected 60 total fecal samples from *C. alpina* (*n* = 21), *C. c. rufa* (*n* = 18), and *C. pusilla* (*n* = 21) on 18 mudflats from 14 May – 2 June, 2023 – 2024. We successfully amplified DNA in 98% (n = 59) of fecal samples using 18S and 97% (n = 58) using 23S markers. We obtained high-quality sequence reads in 57 samples by 18S (*C. alpina*, n = 19; *C. c. rufa*, n = 18; *C. pusilla*, n = 20) and 47 samples for 23S (*C. alpina*, n = 17; *C. c. rufa*, n = 14; *C. pusilla*, n = 16). The 18S dataset yielded an average of 4185 ± 454 (SE) sequence reads and 7 ± 0.2 (SE) unique ESVs per sample. In the 23S dataset we obtained an average of 780 ± 96 (SE) sequence reads and 7 ± 0.3 (SE) unique ESVs per sample from the 23S dataset. From 18S, we summarized 80 taxonomic categories from 157 ESVs, including 13 species, 15 genera, 17 families, 28 orders, and 7 classes (Table S3). From 23S, we summarized 29 taxonomic categories from 194 ESVs that included 2 species, 8 genera, 10 families, 5 orders, and 4 classes (Table S4).

Invertebrates in shorebird diets

We detected invertebrates in 100% of fecal samples using 18S rDNA markers (Figure S3; Table S5a-b). *C. alpina* mainly consumed crustaceans (78.9% FOO), particularly malacostracans (35.6% RRA and 73.7% FOO) such as amphipods and decapods (e.g., *Eriocheir spp*.). They also fed on bivalves (57.9% FOO) including *M. edulis* (16.1% RRA and 36.8% FOO) and Adapedonta clams (11.9% RRA and 36.8% FOO). *C. alpina* consumed worms from class

Polychaeta (57.9% FOO), primarily taxa representing order Phyllodocida (18.7% RRA and 42.1% FOO) such as *Alitta succinea* (clam worm). *C. alpina* additionally fed on snails (10.5% FOO), mainly belonging to order Caenogastropoda (5.7% RRA and 10.5% FOO), and other organisms (10.5% FOO), such as cnidarian *Diadumene leucolena* (ghost anemone; 1.3% RRA and 5.3% FOO), in smaller amounts (Figures 4A-B; Table S6a).

C. c. rufa diet was dominated by bivalves (83.3% FOO), mainly consisting of *M. edulis* (38.6% RRA and 66.7% FOO), although we also detected taxa from orders Arcida (e.g., family Noetiidae), Cardiida (e.g., family Tellinoidea), and Adapedonta (collectively 20.3% RRA). *C. c. rufa* also consumed crustaceans (38.9% FOO), primarily malacostracans (12.9% RRA and 33.3% FOO), including amphipods and decapods (e.g., *Eriocheir sinensis* and *Lepidopa spp*.). *C. c. rufa* fed on a diversity of worms (22.2% FOO), including polychaetes (2.1% RRA and 16.7% FOO; e.g., *A. succinea*), the nemertean *Cerebratulus lacteus* (milky ribbon worm; 1.5% RRA 5.6% FOO), and haplotaxid oligocheaetes (1.4% RRA and 5.6% FOO). Other organisms (11.1% FOO) consisting of teleost fish were also present in their diet (Figures 4C-D; Table S6b).

C. pusilla had the broadest diet of our study species. Crustaceans (65% FOO) comprised the largest part of their diet, consisting almost entirely of amphipods (37% RRA and 40% FOO) and ostracods (9.8% RRA and 10% FOO). *C. pusilla* were the only species to consume insects (30% FOO), primarily feeding on dipterans (12.4% RRA and 20% FOO). They also consumed polychaetes (6.2% RRA and 25% FOO), including species *Ninoe nigripes*, and sipunculids (4.4% RRA and 10% FOO). Bivalves (10% FOO), mainly consisting of *M. edulis* (4.2% RRA and 5% FOO), and snails (10% FOO; order Caenogastropoda) comprised a smaller percentage of their diet. *C. pusilla* also fed on other organisms (15% FOO) including myxosporean parasites (2.8% RRA and 5% FOO; Figures 4E-F; Table S6c).

Biofilm and algal components of diet

We detected biofilm in 49.1% of the fecal samples sequenced with 18S rDNA markers (n = 28; Figure S3; Table S5a-b) and 87.2% of samples sequenced with 23S rDNA markers (n = 41; Figure S4; Table S7a-b). By 18S, biofilm was consumed significantly by *C. c. rufa* (Figures 4C-D; Table S6b) and *C. pusilla* (Figures 4E-F; Tables S6c). Biofilm in the 18S diet of *C. c. rufa* consisted of dinoflagellates (10.9% RRA and 38.9% FOO), diatoms (4.9% RRA and 50% FOO), and microalgae (2.2% RRA and 55.6% FOO; Table S6b) while biofilm in the 18S diet of *C. pusilla* consisted mainly of diatoms (12% RRA and 50% FOO) and dinoflagellates (2.1% RRA and 25% FOO; Table S6c). By 23S, biofilm was consumed in significant amounts by all three focal species and was mainly comprised of diatoms with smaller amounts of microalgae (Figure 5; Table S8a-c). The abundance of biofilm was highest in *C. pusilla* diet (86.4% RRA and 100% FOO) and lowest *C. alpina* diet (71.6% RRA and 76.5% FOO). *C. pusilla* had the highest proportion of diatoms in their diet while *C. c. rufa* had the lowest (Figure 5; Table S8a-c).

Macroalgae occurred in 10.5% of the fecal samples by 18S (n = 6; Figure S3; Table S5a-b) and 29.8% of fecal samples by 23S (n = 14; Figure S4; Table S7a-b). By 18S, macroalgae was only present in significant amounts in the diet of *C. c. rufa* (Figure 4C-D; Table S6b). By 23S, macroalgae was present in all shorebird species' diets and was most abundant in the diet of *C. alpina* and was the least abundant in the diet of *C. pusilla* (Figure 5; Table S8a-c).

Prey selection

We found that 33% of observed consumption frequencies were inconsistent with the null model of no preferences and the degree of selectivity varied between shorebird species (Figure

S5; Table S9). The proportion of inconsistent consumption frequencies was highest in *C. c. rufa*, which consumed 60% of invertebrate diet bins more or less than expected based on the null model. Comparatively, 40% of observed consumption frequencies by *C. alpina* were inconsistent with predicted frequencies and *C. pusilla* exhibited no selection (0%). *C. alpina* and *C. c. rufa* consumed bivalves more frequently than expected (Figures 6A-B). *C. alpina* consumed worms less than expected (Figure 6A). *C. c. rufa* consumed crustaceans and worms less than expected (Figure 6B). *C. pusilla* consumed all invertebrates proportionate to their availability (Figure 6C).

DISCUSSION

This study is the first to simultaneously assess shorebird habitat use across substrates and in seaside lagoons and on barrier islands in Virginia, building on previous work that examined habitats separately (Besterman et al. 2020, Heller et al. 2022). Mudflats supported comparable numbers of shorebirds to the barrier island intertidal zone, suggesting that shorebirds congregate on mudflats when they are exposed. These findings, along with our results that shorebird species composition and abundance varied across substrates, are consistent with previous studies (Burger et al. 1997, Novcic 2016). Mudflats appear to be important foraging areas for *C. alpina* and *C. pusilla,* although *C. c. rufa* used mudflats more than expected based on prior research (Besterman and Pace 2021). These findings suggest that shorebird habitat use is variable and indicate that no single habitat meets the needs of all species. Thus, managing for a mosaic of intertidal habitats is essential for migratory shorebird conservation.

We successfully used fecal DNA metabarcoding to characterize the previously undescribed diets of *C. alpina*, *C. c. rufa*, and *C. pusilla* on mudflats in the Virginia barrier island system. Among our focal species, *C. pusilla* exhibited the broadest diet consistent with

studies in other parts of their migratory range (Gerwing et al. 2016). In the Bay of Fundy, *C. pusilla* have a versatile diet. While they primarily feed on amphipods and polychaetes (MacDonald et al. 2012), in some years ostracods were heavily consumed (Quinn and Hamilton 2012). *C. pusilla* are also known to opportunistically feed on insects, mollusks, fish, and cnidarians (Gerwing et al. 2016). Amphipods and polychaete worms were also important components of *C. alpina* diet, akin to findings from diet studies conducted in Europe (Martins et al. 2013). However, we found that mollusks were a much larger part of their diet, as has been observed in the Fraser River estuary along the U.S. Pacific Flyway (Mathot et al. 2010).

As expected for a known molluscivorous species (Dekinga and Piersma 1993), *C. c. rufa* foraging on mudflats primarily consumed bivalves. This aligns with findings from the only comparable fecal DNA metabarcoding study conducted in Virginia, which reported a high frequency of bivalves in the diet of *C. c. rufa* foraging on barrier island sand and peat substrates (Heller 2020). We also documented decapods in *C. c. rufa* diet, which is new for our study system but consistent with their known prey on South American wintering grounds (Fedrizzi and Carlos 2023). Additionally, *C. c. rufa* consumed a variety of worms including polychaetes, oligochaetes, and nemertean ribbon worms. While this also has not been previously recorded in Virginia, marine worms have been found in the stomachs of *C. c. rufa* in the Delaware Bay (Tsipoura and Burger 1999).

We detected biofilm in the diets of all three focal species, providing the first evidence that migratory shorebirds graze on biofilm in the Virginia barrier island system. While it is possible our results were the result of environmental contamination, biofilm grazing is an established behavior in *C. alpina* and *C. pusilla* around the world and the trophic position of small-bodied shorebirds as both primary and secondary consumers has been validated using

behavioral observations, stomach content analysis, and isotopic and DNA methodologies (Kuwae et al. 2008, Mathot et al. 2010, Gerwing et al. 2016, Hobson et al. 2022). Tongue bristles that allow for the gathering of paste-like food such as biofilm (Elner et al. 2005) have been documented in 21 shorebird species including *C. c. rufa* indicating that biofilm grazing is a widespread adaption among shorebirds (Kuwae et al. 2012). To our knowledge, ours is the first study to identify biofilm consumption in *C. c. rufa* using fecal DNA metabarcoding. However, the large quantities of sand and detritus found in the digestive tracts of *C. c. rufa* in earlier diet studies in the Delaware Bay (Tsipoura and Burger 1999) indicate biofilm consumption. Skimming behavior equated with biofilm grazing has been observed in *C. alpina* and *C. pusilla* in the Delaware Bay (Novcic 2016) along with our findings suggest that shorebirds have historically been utilizing biofilm during spring migration in the larger mid-Atlantic region.

Fecal DNA metabarcoding is a useful tool for detecting novel prey consumption (Gerwing et al. 2016). In our study, we found the invasive crustacean *E. sinensis* (Chinese mitten crab) in the diets of *C. alpina* and *C. c. rufa.* While shorebirds can sometimes exploit non-native invertebrates (Caldow et al. 2007), invasive species often reduce the availability of preferred, higher-quality prey. For example, the introduced *Carcinus maenas* (European green crab) reduced the availability of polychaetes, causing *C. alpina* to shift their foraging behavior and prey choice (Estelle and Grosholz 2012), which can result in reduced refueling efficiency and have larger impacts on migration strategies, breeding success, and annual survival (Anderson et al. 2021). Our results highlight how DNA-based tools offer unique opportunities to monitor biological invasions and could be used to assess the ecological impacts on shorebird diets and behavior.

As expected, *C. c. rufa* exhibited the most dietary specialization of our study species. We found that they preferentially consumed bivalves on mudflats at the expense of more abundantly available prey, consistent with findings on barrier islands in our study system (Cohen et al. 2010, Heller 2020). Our diet analysis suggests *C. c. rufa* consumed a wider range of bivalve taxa on mudflats than on barrier islands, where they primarily feed on Mytilida mussels and Venerida clams (Heller 2020). Optimal foraging theory predicts that individuals will exhibit greater selectivity when resources are more abundant (MacArthur and Pianka 1966), suggesting that barrier islands in Virginia offer more favorable foraging conditions for *C. c. rufa* than mudflats. *C. c. rufa* are efficient at tracking resources across the coastal landscape and typically forage in areas with the highest prey availability (Cohen et al. 2010, Heller et al. 2022), indicating that mudflats function as important foraging areas for this species. Overall, our findings show that *C. c. rufa* staging in Virginia exhibit dietary flexibility within the constraints of a specialized diet as they move throughout habitats within the coastal landscape.

We found that *C. alpina* similarly selected for bivalves on mudflats when foraging on mudflats, though to a lesser degree than *C. c. rufa*. This is surprising given that polychaetes are considered their preferred prey throughout their range (Iwamatsu et al. 2007). Prey selection in *C. alpina* is strongly linked to profitability (Martins et al. 2013), where the most profitable prey are those with the highest energetic intake per unit of handling time (Quaintenne et al. 2010). While soft-bodied prey such as worms and crustaceans are typically more profitable due to lower digestive costs (Zwarts et al. 1996), invertebrate populations exhibit high annual variability in response to changing environmental conditions (Cohen et al. 2010, Heller et al. 2022). It is possible that the bivalves available on mudflats during the years of our study had higher biomass-to-shell ratios than found in other locations and past studies, thereby increasing their

profitability. *M. edulis,* in particular*,* are energy-dense and can contain up to 10% more fat than polychaetes (Zwarts and Wanink 1993) which may explain the high rates of *M. edulis* consumption observed across focal species in our study. Further investigating prey choice in terms of biomass or prey size classes may provide additional insight into selective preferences of species such as *C. alpina* and *C. c. rufa* in the future (Cohen et al. 2010).

Migratory shorebird foraging ecology in the Virginia barrier island system is dynamic and diverse, underscoring the need to protect and restore a mosaic of intertidal habitats across the coastal landscape. Our findings highlight that mudflats are critical foraging areas for migratory shorebirds in Virginia, and any loss or degradation of these habitats would negatively impact populations. The dietary and behavioral plasticity evidenced by our study is encouraging for the resiliency of these populations staging in Virginia and shorebirds' ability to utilize biofilm may increase populations' stability in years of reduced availability of preferred prey (Kuwae et al. 2012). Ongoing management in Virginia should continue to encourage natural geomorphological processes to take place and avoid artificial shoreline stabilization, as it reduces foraging habitat quality and functionality both on and behind barrier islands (Murray et al. 2019).

DATA ARCHIVING STATEMENT

Data is available from the Virginia Coast Reserve's Environmental Data Initiative (https://doi.org/10.6073/pasta/6496141b889bc259810b95db46250a97, Lapenta and Karpanty 2024).

ACKNOWLEDGMENTS

We thank T. Brocato, L. Buckman, I. Burgos, W. Burgoyne, M. Bullerwell, L. Casteen, A. Cuba, L. Gehman, M. Graul, A. Hargis, D. Hoff, L. Hoffman, E. Kline, D. Leavitt, D. McBride, M. Nootbaar, K. Osworth, E. Rothenburger, C. Seewer, E. Staengl, W. Wei, and A. Zbesheski for assisting with data acquisition for this project. Additionally, we thank Jonah Ventures LLC for conducting the fecal DNA metabarcoding. We especially thank D. Fraser, J. Fraser, and S. Ritter (Virginia Tech Department of Fish and Wildlife Conservation), M. Payne (Seaside Ecotours LLC.), C. Baird, S. Hoffman, B. Doughty, T. Burkett, and D. Fauber (Virginia Coast Reserve Long-Term Ecological Research program's Coastal Research Center), A. Wilke, Z. Poulton, and M. Balitbit (The Nature Conservancy), S. Fate and E. Smith (Virginia Institute of Marine Science), K. Holcomb, K. Oliver, P. Denmon, and N. Walker (U. S. Fish and Wildlife Service), S. Miller, L. Levine, and M. Bonsteel (National Aeronautics and Space Administration), and partners at the Virginia Department of Conservation & Recreation, the Commonwealth of Virginia Marine Resources Commission, and the National Oceanic & Atmospheric Administration for logistical, intellectual, and permitting support throughout the project. We thank the NSF Virginia Coast Reserve Long-Term Ecological Research program (DEB-1832221 and DEB-2425178), the U.S. Fish and Wildlife Service, the Virginia Department of Wildlife Resources, the Virginia Society of Ornithology, and the Virginia Tech Department of Fish and Wildlife Conservation for funding this project. Any opinions, findings, conclusions, or recommendations expressed in this material are those of the authors and do not necessarily reflect the views of the National Science Foundation or any other funding partners.

LITERATURE CITED

Agusti, N., S. P. Shayler, J. D. Harwood, I. P. Vaughan, K. Sunderland, and W. O. C. Symondson. 2003. Collembola as alternative prey sustaining spiders in arable ecosystems: prey detection within predators using molecular markers. Molecular Ecology 12:3467–3475.

Anderson, A., C. Friis, C. Gratto-Trevor, C. Harris, O. Love, R. Morrison, S. Prosser, E. Nol, and P. Smith. 2021. Drought at a coastal wetland affects refuelling and migration strategies of shorebirds. Oecologia. https://doi.org/10.1007/s00442-021-05047-x.

Benson, D. A., I. Karsch-Mizrachi, D. J. Lipman, J. Ostell, and D. L. Wheeler. 2005. GenBank. Nucleic acids research 33:D34–D38.

Besterman, A. F. 2018. Bird observations on the tidal flats of the Virginia Coast Reserve, 2016-2018. Virginia Coast Reserve Long-Term Ecological Research Project Data Publication knb-lter-vcr.301.1.

Besterman, A. F., S. M. Karpanty, and M. L. Pace. 2020. Impact of exotic macroalga on shorebirds varies with foraging specialization and spatial scale. PLOS ONE 15:e0231337.

Besterman, A. F., K. J. McGlathery, M. A. Reidenbach, P. L. Wiberg, and M. L. Pace. 2021. Predicting benthic macroalgal abundance in shallow coastal lagoons from geomorphology and hydrologic flow patterns. Limnology and Oceanography 66:123–140.

Besterman, A. F., and M. L. Pace. 2021. Mudflat geomorphology determines invasive macroalgal effect on invertebrate prey and shorebird predators. Ecology 102.

Burger, J., L. Niles, and K. E. Clark. 1997. Importance of beach, mudflat and marsh habitats to migrant shorebirds on Delaware Bay. Biological Conservation 79:283–292.

Butler, R. W., N. C. Davidson, and R. G. Morrison. 2001. Global-scale shorebird distribution in relation to productivity of near-shore ocean waters. Waterbirds 224–232.

Caldow, R. W., R. A. Stillman, S. E. le V. dit Durell, A. D. West, S. McGrorty, J. D. Goss-Custard, P. J. Wood, and J. Humphreys. 2007. Benefits to shorebirds from invasion of a non-native shellfish. Proceedings of the Royal Society B: Biological Sciences 274:1449–1455.

Cannon, M., J. Hester, A. Shalkhauser, E. R. Chan, K. Logue, S. T. Small, and D. Serre. 2016. In silico assessment of primers for eDNA studies using PrimerTree and application to characterize the biodiversity surrounding the Cuyahoga River. Scientific reports 6:22908.

Clavel, J., R. Julliard, and V. Devictor. 2011. Worldwide decline of specialist species: toward a global functional homogenization? Frontiers in Ecology and the Environment 9:222–228.

Cohen, J. B., S. M. Karpanty, J. D. Fraser, and B. R. Truitt. 2010. The effect of benthic prey abundance and size on red knot (Calidris canutus) distribution at an alternative migratory stopover site on the US Atlantic Coast. Journal of Ornithology 151:355–364.

Cohen, J. B., S. M. Karpanty, J. D. Fraser, B. D. Watts, and B. R. Truitt. 2009. Residence Probability and Population Size of Red Knots During Spring Stopover in the Mid-Atlantic Region of the United States. Journal of Wildlife Management 73:939–945.

Correia, E., J. P. Granadeiro, B. Santos, A. Regalla, V. A. Mata, and T. Catry. 2023. Trophic ecology of a migratory shorebird community at a globally important non-breeding site: combining DNA metabarcoding and conventional techniques. Marine Ecology Progress Series 705:127–144.

Deagle, B. E., A. C. Thomas, J. C. McInnes, L. J. Clarke, E. J. Vesterinen, E. L. Clare, T. R. Kartzinel, and J. P. Eveson. 2019. Counting with DNA in metabarcoding studies: How should we convert sequence reads to dietary data? Molecular Ecology 28:391–406.

Deagle, B. E., A. C. Thomas, A. K. Shaffer, A. W. Trites, and S. N. Jarman. 2013. Quantifying sequence proportions in a DNA-based diet study using Ion Torrent amplicon sequencing: Which counts count? Molecular Ecology Resources 13:620–633.

Dekinga, A., and T. Piersma. 1993. Reconstructing diet composition on the basis of faeces in a mollusc-eating wader, the knot Calidris canutus. Bird study 40:144–156.

Drake, L. E., J. P. Cuff, R. E. Young, A. Marchbank, E. A. Chadwick, and W. O. Symondson. 2022. An assessment of minimum sequence copy thresholds for identifying and reducing the prevalence of artefacts in dietary metabarcoding data. Methods in Ecology and Evolution 13:694–710.

Durell, S. E. a. L. V. D. 2000. Individual feeding specialisation in shorebirds: population consequences and conservation implications. Biological Reviews 75:503–518.

Edgar, R. C. 2016. UNOISE2: improved error-correction for Illumina 16S and ITS amplicon sequencing. BioRxiv 081257.

Edgar, R. C., and H. Flyvbjerg. 2015. Error filtering, pair assembly and error correction for next-generation sequencing reads. Bioinformatics 31:3476–3482.

Elner, R. W., P. G. Beninger, D. L. Jackson, and T. M. Potter. 2005. Evidence of a new feeding mode in western sandpiper (Calidris mauri) and dunlin (Calidris alpina) based on bill and tongue morphology and ultrastructure. Marine Biology 146:1223–1234.

Estelle, V., and E. D. Grosholz. 2012. Experimental test of the effects of a non-native invasive species on a wintering shorebird. Conservation biology 26:472–481.

Fedrizzi, C. E., and C. J. Carlos. 2023. Diet of Red Knots (Calidris canutus rufa) at Lagoa do Peixe National Park, Brazil. The Wilson Journal of Ornithology 135:546–553.

Galanti, L., D. Shasha, and K. C. Gunsalus. 2021. Pheniqs 2.0: accurate, high-performance Bayesian decoding and confidence estimation for combinatorial barcode indexing. BMC bioinformatics 22:1–16.

Gerwing, T. G., J.-H. Kim, D. J. Hamilton, M. A. Barbeau, and J. A. Addison. 2016. Diet reconstruction using next-generation sequencing increases the known ecosystem usage by a shorebird. The Auk 133:168–177.

González, P. M., T. Piersma, and Y. Verkuil. 1996. Food, Feeding, and Refuelling of Red Knots during Northward Migration at San Antonio Oeste, Rio Negro, Argentina (Alimentacion y Reabastecimiento de Playeros Rojizos Calidris canutus rufa Durante su migracion al Norte en San Antonio Oeste, Rio Negro, Argentina). Journal of Field Ornithology 575–591.

Grassle, J. F. 2000. The Ocean Biogeographic Information System (OBIS): an on-line, worldwide atlas for accessing, modeling and mapping marine biological data in a multidimensional geographic context. Oceanography 13:5–7.

Hamsher, S. E., K. M. Evans, D. G. Mann, A. Poulíčková, and G. W. Saunders. 2011. Barcoding diatoms: exploring alternatives to COI-5P. Protist 162:405–422.

Heller, E. L. 2020. Factors affecting Western Atlantic red knots (Calidris canutus rufa) and their prey during spring migration on Virginia's barrier islands. doctoral, Virginia Polytechnic Institute and State University, Blacksburg, VA, USA.

Heller, E. L., S. M. Karpanty, J. B. Cohen, D. H. Catlin, S. J. Ritter, B. R. Truitt, and J. D. Fraser. 2022. Factors that affect migratory Western Atlantic red knots (Calidris canutus

rufa) and their prey during spring staging on Virginia's barrier islands. V. H. R. Paiva, editor. PLOS ONE 17:e0270224.

Hicklin, P., and C. Gratto-Trevor. 2020. Semipalmated Sandpiper (Calidris pusilla), version 1.0. A. F. Poole, editor. Birds of the World. Cornell Lab of Ornithology, Ithaca, NY, USA.

Hobson, K. A., T. Kuwae, M. C. Drever, W. E. Easton, and R. W. Elner. 2022. Biofilm and invertebrate consumption by western sandpipers (Calidris mauri) and dunlin (Calidris alpina) during spring migratory stopover: insights from tissue and breath CO2 isotopic (δ 13C, δ 15N) analyses. Conservation Physiology 10:coac006.

Iwamatsu, S., A. Suzuki, and M. Sato. 2007. Nereidid polychaetes as the major diet of migratory shorebirds on the estuarine tidal flats at Fujimae-Higata in Japan. Zoological science 24:676–685.

Koleček, J., J. Reif, M. Šálek, J. Hanzelka, C. Sottas, and V. Kubelka. 2021. Global population trends in shorebirds: migratory behaviour makes species at risk. The Science of Nature 108:9.

Kuwae, T., P. G. Beninger, P. Decottignies, K. J. Mathot, D. R. Lund, and R. W. Elner. 2008. Biofilm grazing in a higher vertebrate: the western sandpiper (Calidris mauri). Ecology 89:599–606.

Kuwae, T., E. Miyoshi, S. Hosokawa, K. Ichimi, J. Hosoya, T. Amano, T. Moriya, M. Kondoh, R. C. Ydenberg, and R. W. Elner. 2012. Variable and complex food web structures revealed by exploring missing trophic links between birds and biofilm: Missing trophic links in food webs. Ecology Letters 15:347–356.

MacArthur, R. H., and E. R. Pianka. 1966. On optimal use of a patchy environment. The American Naturalist 100:603–609.

MacDonald, E., M. G. Ginn, and D. J. Hamilton. 2012. Variability in Foraging Behavior and Implications for Diet Breadth among Semipalmated Sandpipers Staging in the Upper Bay of Fundy. The Condor 114:135–144.

MacLean, S. F., and R. T. Holmes. 1971. Bill Lengths, Wintering Areas, and Taxonomy of North American Dunlins, Calidris alpina. The Auk 88:893–901.

Martin, M. 2011. Cutadapt removes adapter sequences from high-throughput sequencing reads. EMBnet. journal 17:10–12.

Martins, R. C., T. Catry, C. D. Santos, J. M. Palmeirim, and J. P. Granadeiro. 2013. Seasonal variations in the diet and foraging behaviour of dunlins Calidris alpina in a south European estuary: improved feeding conditions for northward migrants. PLoS One 8:e81174.

Mathot, K. J., D. R. Lund, and R. W. Elner. 2010. Sediment in Stomach Contents of Western Sandpipers and Dunlin Provide Evidence of Biofilm Feeding. Waterbirds 33:300–306.

McInnes, J., R. Alderman, B. Deagle, M. Lea, B. Raymond, and S. Jarman. 2017. Optimised scat collection protocols for dietary DNA metabarcoding in vertebrates. Methods Ecol Evol 8: 192–202.

Murray, N. J., S. R. Phinn, M. DeWitt, R. Ferrari, R. Johnston, M. B. Lyons, N. Clinton, D. Thau, and R. A. Fuller. 2019. The global distribution and trajectory of tidal flats. Nature 565:222–225.

Novcic, I. 2016. Niche dynamics of shorebirds in Delaware Bay: Foraging behavior, habitat choice and migration timing. Acta Oecologica 75:68–76.

Novcic, I., R. R. Veit, D. S. Mizrahi, and W. O. Symondson. 2016. Molecular analysis of amphipods in the diets of migrating shorebirds. Wader Study 123:195–201.

Oehm, J., A. Juen, K. Nagiller, S. Neuhauser, and M. Traugott. 2011. Molecular scatology: how to improve prey DNA detection success in avian faeces? Molecular ecology resources 11:620–628.

Pruesse, E., C. Quast, K. Knittel, B. M. Fuchs, W. Ludwig, J. Peplies, and F. O. Glöckner. 2007. SILVA: a comprehensive online resource for quality checked and aligned ribosomal RNA sequence data compatible with ARB. Nucleic acids research 35:7188–7196.

Quaintenne, G., J. A. Van Gils, P. Bocher, A. Dekinga, and T. Piersma. 2010. Diet selection in a molluscivore shorebird across Western Europe: does it show short-or long-term intake rate-maximization? Journal of Animal Ecology 79:53–62.

Quinn, J., and D. Hamilton. 2012. Variation in diet of Semipalmated Sandpipers (Calidris pusilla) during stopover in the upper Bay of Fundy, Canada. Canadian Journal of Zoology 90:1181–1190.

R Core Team. 2024. R: A Language and Environment for Statistical Computing. R Foundation for Statistical Computing, Vienna, Austria. <https://www.R-project.org/>.

Ramirez, K. S., J. W. Leff, A. Barberán, S. Thomas Bates, J. Betley, T. W. Crowther, E. F. Kelly, E. E. Oldfield, E. A. Shaw, C. Steenbock, M. A. Bradford, D. H. Wall, and N. Fierer. 2014. Biogeographic patterns in below-ground diversity in New York City's Central Park are similar to those observed globally. Proceedings of the Royal Society B: Biological Sciences 281.

Rognes, T., T. Flouri, B. Nichols, C. Quince, and F. Mahé. 2016. VSEARCH: a versatile open source tool for metagenomics. PeerJ 4:e2584.

Schnurr, P. J., M. C. Drever, R. W. Elner, J. Harper, and M. T. Arts. 2020. Peak abundance of fatty acids from intertidal biofilm in relation to the breeding migration of shorebirds. Frontiers in Marine Science 7:63.

Sherwood, A. R., and G. G. Presting. 2007. Universal primers amplify a 23S rDNA plastid marker in eukaryotic algae and cyanobacteria 1. Journal of phycology 43:605–608.

Smith, P. A., A. C. Smith, B. Andres, C. M. Francis, B. Harrington, C. Friis, R. I. G. Morrison, J. Paquet, B. Winn, and S. Brown. 2023. Accelerating declines of North America's shorebirds signal the need for urgent conservation action. Ornithological Applications 125:duad003.

Stenhouse, E. H., P. Bellamy, W. Kirby, I. P. Vaughan, L. E. Drake, A. Marchbank, T. Workman, W. O. Symondson, and P. Orozco-terWengel. 2023. Multi-marker DNA metabarcoding reveals spatial and sexual variation in the diet of a scarce woodland bird. Ecology and Evolution 13:e10089.

Studds, C. E., B. E. Kendall, N. J. Murray, H. B. Wilson, D. I. Rogers, R. S. Clemens, K. Gosbell, C. J. Hassell, R. Jessop, and D. S. Melville. 2017. Rapid population decline in migratory shorebirds relying on Yellow Sea tidal mudflats as stopover sites. Nature communications 8:14895.

Tomkovich, P. S. 1992. An analysis of the geographic variability in knots Calidris canutus based on museum skins. Wader Study Group 64 (suppl):17–23.

Tsipoura, N., and J. Burger. 1999. Shorebird Diet during Spring Migration Stopover on Delaware Bay. The Condor 101:635–644.

Vaughan, I. P., N. J. Gotelli, J. Memmott, C. E. Pearson, G. Woodward, and W. O. C. Symondson. 2018. econullnetr: An r package using null models to analyse the structure

of ecological networks and identify resource selection. Methods in Ecology and Evolution 9:728–733.

Virginia Department of Game and Inland Fisheries. 2015. Virginia's 2015 Wildlife Action Plan. Virginia Department of Game and Inland Fisheries, Henrico, VA, USA.

Walters, D., L. J. Moore, O. Duran Vinent, S. Fagherazzi, and G. Mariotti. 2014. Interactions between barrier islands and backbarrier marshes affect island system response to sea level rise: Insights from a coupled model: Barrier Islands and Backbarrier Marshes. Journal of Geophysical Research: Earth Surface 119:2013–2031.

Watts, B. D., and B. R. Truitt. 2015. Spring migration of red knots along the Virginia barrier island system: Virginia Red Knots. The Journal of Wildlife Management 79:288–295.

Wilke, A. L., B. D. Watts, B. R. Truitt, and R. Boettcher. 2005. Breeding Season Status of the American Oystercatcher in Virginia, USA. Waterbirds 28:308–315.

Zwarts, L., B. Ens, J. Goss-Custard, J. Hulscher, and S. le V. Dit Durell. 1996. Causes of variation in prey profitability and its consequences for the intake rate of the Oystercatcher Haematopus ostralegus. Ardea 84:229–268.

Zwarts, L., and J. H. Wanink. 1993. How the food supply harvestable by waders in the Wadden Sea depends on the variation in energy density, body weight, biomass, burying depth and behaviour of tidal-flat invertebrates. Netherlands Journal of Sea Research 31:441–476.

FIGURES

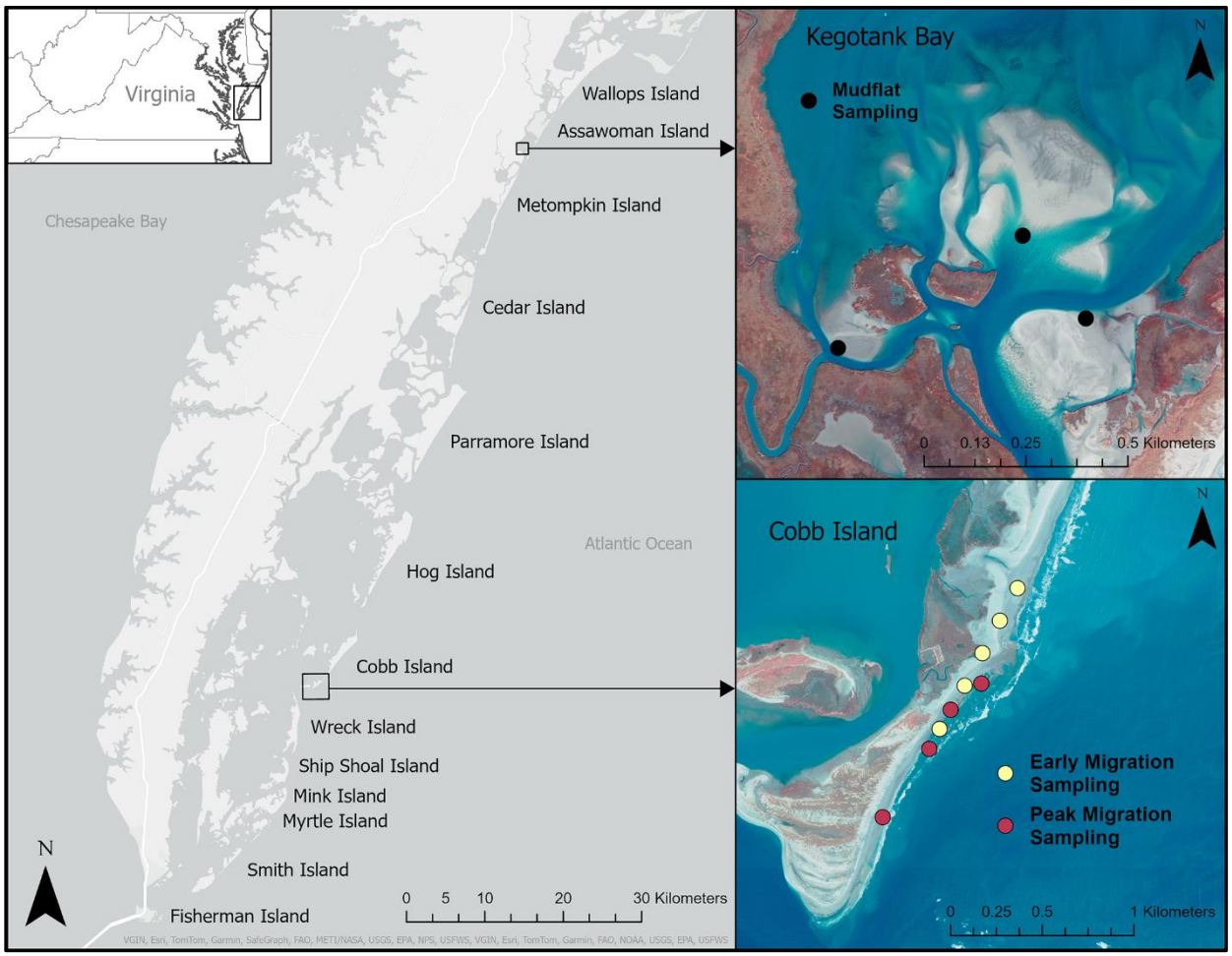

Figure 1. Study area within the Virginia barrier island system during spring migration (May 14 – June 2) 2023 – 2024, including 13 barrier islands (Wallops to Fisherman Island) and 58 mudflats distributed throughout the lagoon system. Inset maps provide examples of 2024 sampling points on mudflats (top) and barrier islands (bottom). Yellow indicates barrier island sampling points collected during the early migration period (May 14 – 20) and red during the peak migration period (May 21 – 28). Mudflats were sampled throughout the spring migration window (May 14 – June 2).

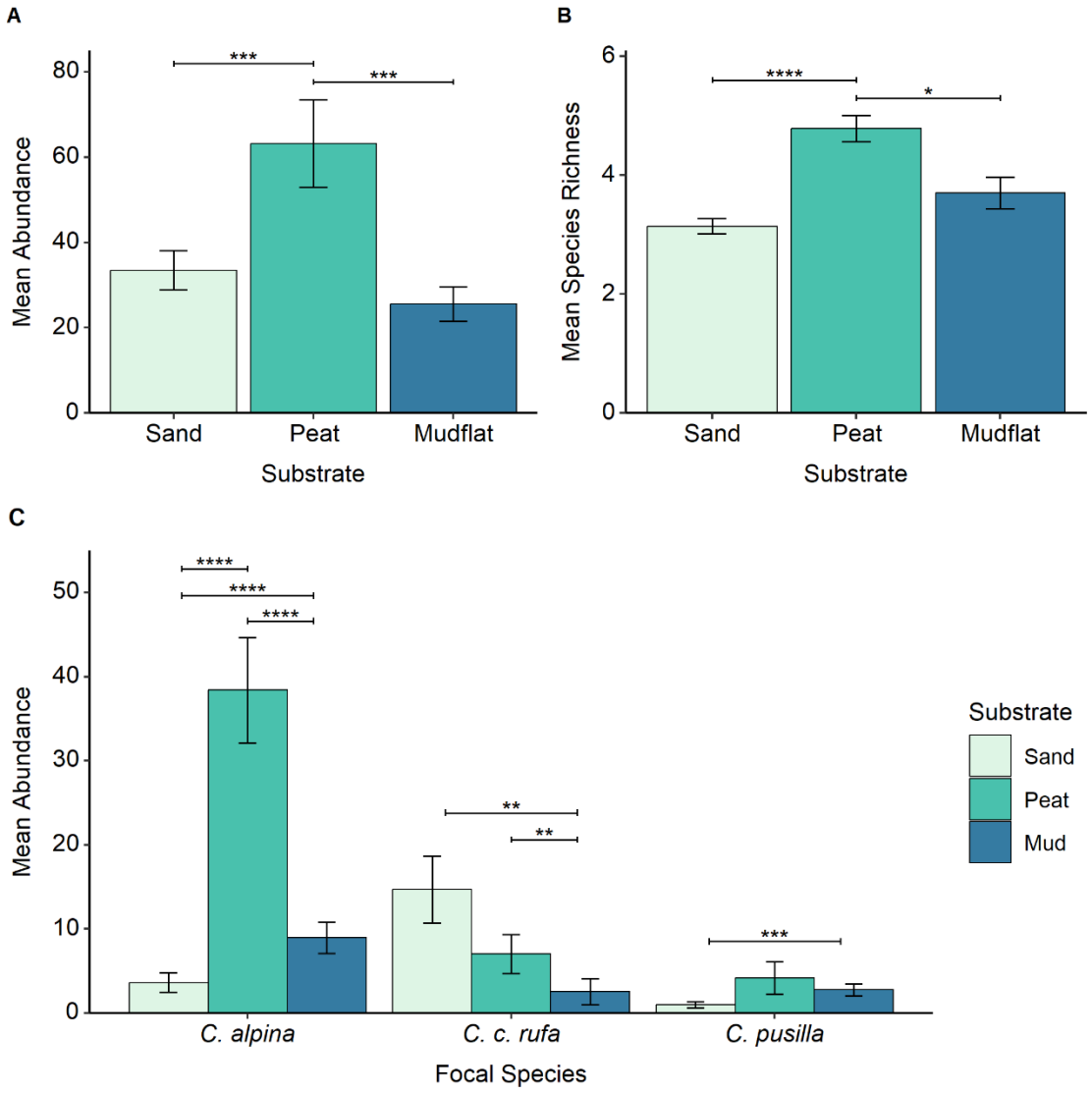

Figure 2. Shorebird habitat use across sand, peat, and mudflat substrates during spring migration May 14 – June 2, 2023 – 2024 in the Virginia barrier island system including (A) mean abundance (birds/point) of all shorebirds (B) mean species richness (species/point), and (C) mean abundances (birds/point) of *Calidris alpina* (dunlin), *Calidris canutus rufa* (red knot), and *Calidris pusilla* (semipalmated sandpiper). Error bars represent standard error (SE). Asterisks indicate significant differences based on pairwise Wilcoxon rank sum tests with Bonferroni correction: $P < 0.05$ (*), $P < 0.01$ (**), $P < 0.001$ (***), $P < 0.0001$ (****). Note: y-axis scales differ between graphs.

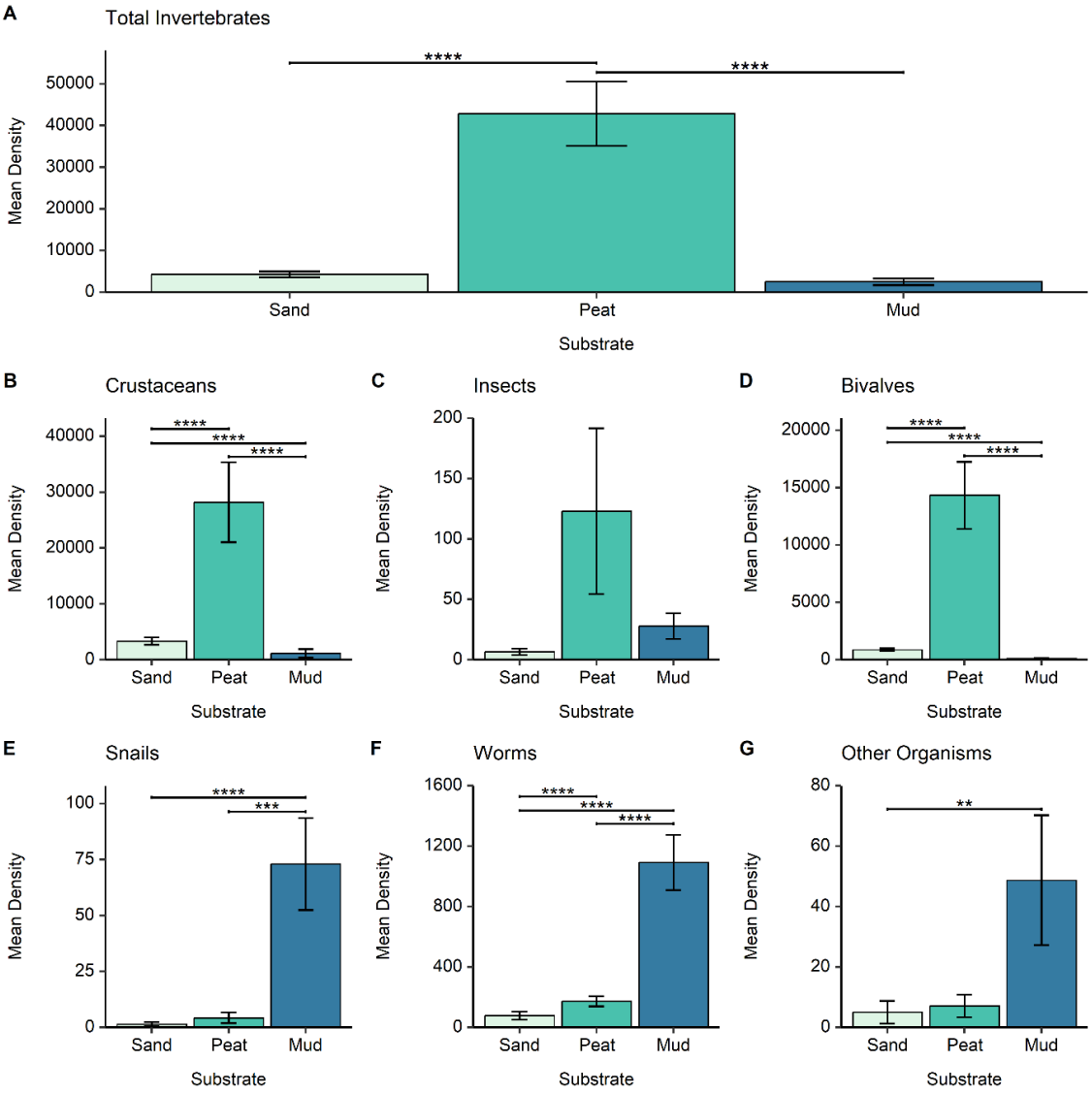

Figure 3. Mean density (organisms/m^2) of (A) all invertebrates, (B) crustaceans, (C) insects, (D) bivalves, (E) snails, (F) worms, and (G) other organisms captured in core samples collected on sand, peat, and mudflat substrates during spring migration (May 14 – June 2) 2023 – 2024 in the Virginia barrier island system. Error bars represent standard error (SE). Asterisks indicate significant differences based on pairwise Wilcoxon rank sum tests with Bonferroni correction: $P < 0.05$ (*), $P < 0.01$ (**), $P < 0.001$ (***), $P < 0.0001$ (****). Note: y-axis scales differ between graphs.

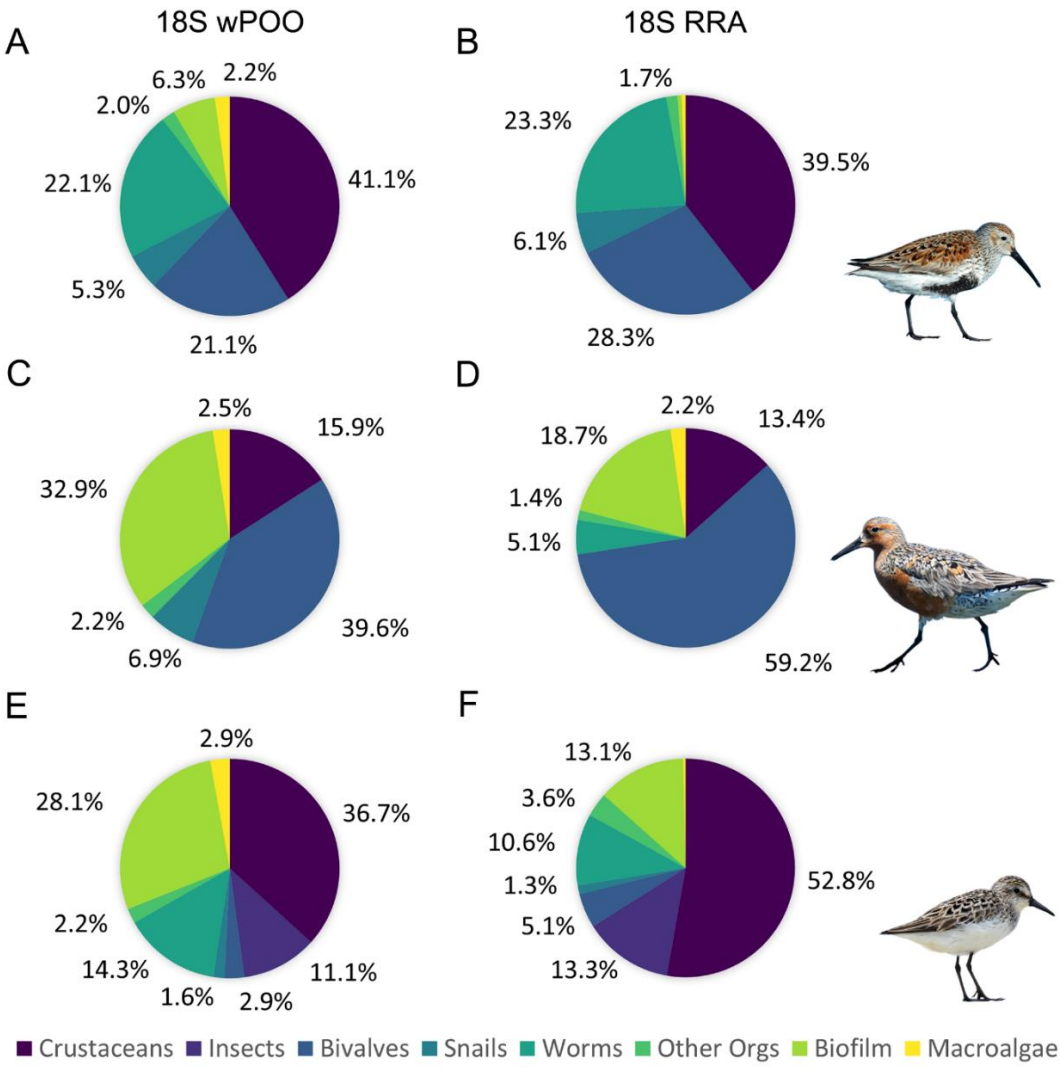

Figure 4. Diet composition of (A, B) *Calidris alpina* (dunlin), (C, D) *Calidris canutus rufa* (red knot), and (E, F) *Calidris pusilla* (semipalmated sandpiper) determined using 18S rDNA markers on fecal samples collected on mudflats during spring migration (May 14 – June 2) 2023 – 2024 in the Virginia barrier island system. We summarized 80 taxonomic categories from 157 ESVs and grouped into coarse diet bins. Weighted percent occurrence (wPOO; left panel) and relative read abundance (RRA; right panel) of diet bins are indicated by color blocks. Biofilm includes diatoms, microalgae, and dinoflagellates. Only diet bins with wPOO or RRA > 1% are shown (see Table S6a-c for details).

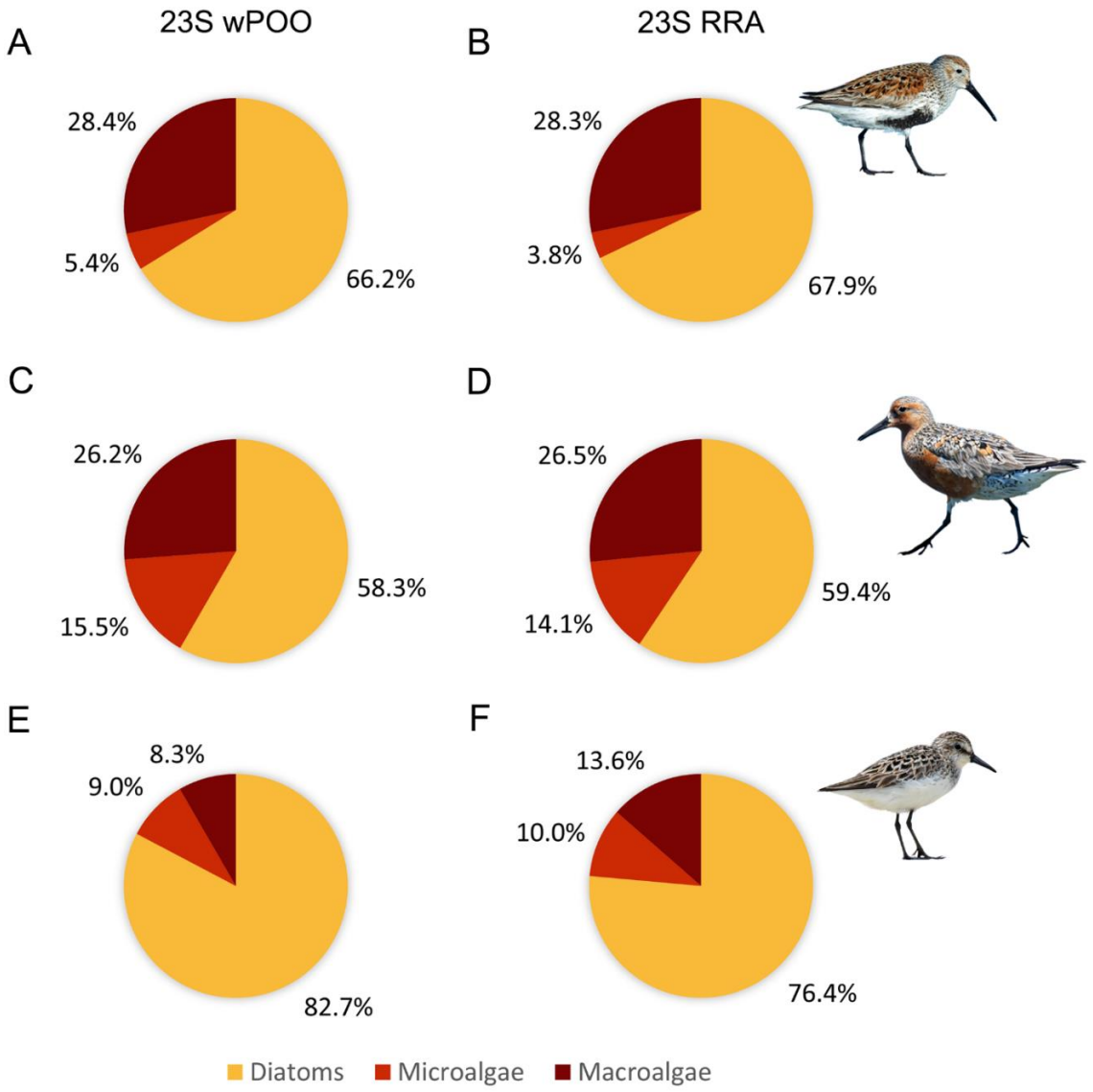

Figure 5. Diet composition of (A, B) *Calidris alpina* (dunlin), (C, D) *Calidris canutus rufa* (red knot), and (E, F) *Calidris pusilla* (semipalmated sandpiper) determined using 23S rDNA markers on fecal samples collected on mudflats during spring migration (May 14 – June 2) 2023 – 2024 in the Virginia barrier island system. We summarized 29 taxonomic categories from 194 ESVs and grouped into coarse diet bins. Weighted percent occurrence (wPOO; left panel) and relative read abundance (RRA; right panel) of diet bins are indicated by color blocks. Only diet bins with wPOO or RRA > 1% are shown (see Table S8a-c for details).

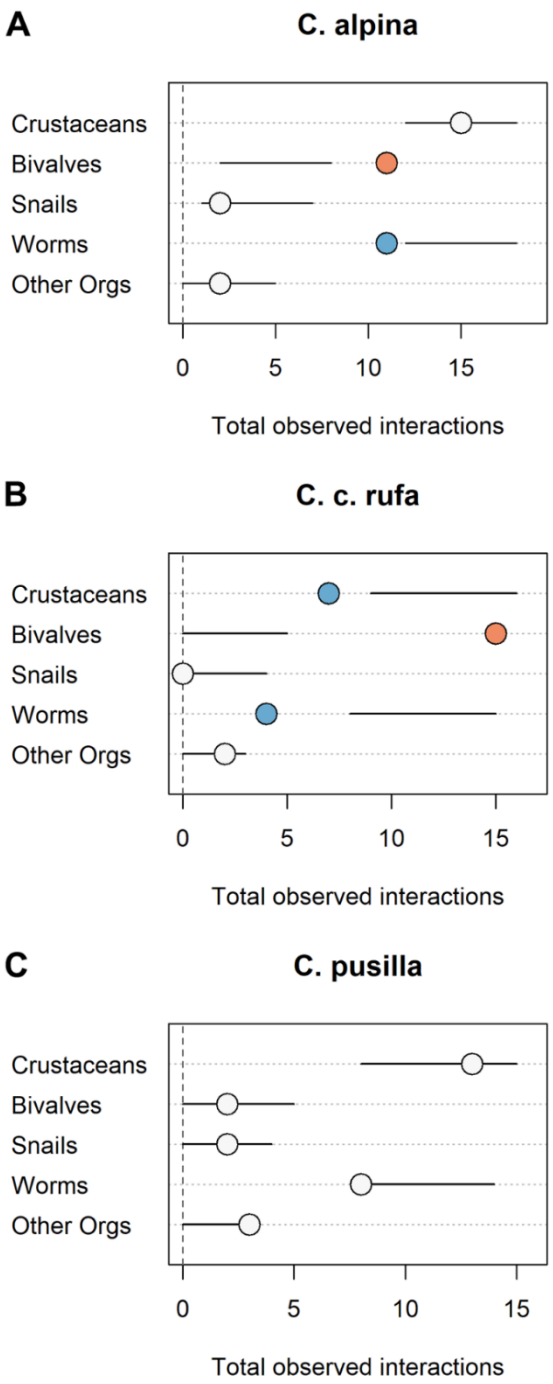

Figure 6. Preference plots illustrating selection of invertebrate prey by (A) *Calidris alpina* (dunlin), (B) *Calidris canutus rufa* (red knot), and (C) *Calidris pusilla* (semipalmated sandpiper) during spring migration (May 14 – June 2) 2023 – 2024 in the Virginia barrier island system. Plots compare observed consumption frequencies (dots) to 95% confidence intervals (bars) illustrating expected consumption frequencies based on the null model. Orange dots denote consumption frequencies stronger than expected (preference), blue dots weaker than expected (avoidance), and white dots consistent with the null model (no selection).

CHAPTER 3

Geomorphic and Climate Drivers Shape Bottom-Up Controls on Spring Staging Red Knots (*Calidris canutus rufa*) in the Virginia Barrier Island System

ABSTRACT

Global climate change is reshaping coastal ecosystems, with uncertain consequences for migratory shorebirds like the federally threatened red knot (*Calidris canutus rufa*). Understanding how sea-level rise and increasing climate variability affect red knot foraging ecology is critical for informing future conservation and ecosystem management at coastal staging sites. We integrated long-term biological, geomorphological, and climatological data to explore the direct and indirect pathways influencing red knots and their prey at intertidal foraging sites during spring migration (May 21 – 28, 2009–2023) in the Virginia barrier island system. Using piecewise structural equation modeling (SEM), we tested hypothesized causal networks linking 1) red knot presence and abundance and 2) invertebrate prey densities to habitat features, barrier island morphology, and geomorphic and climate drivers of ecosystem change. We also evaluated trends in key morphometric features of barrier islands from 2007–2023. Red knots were indirectly influenced by geomorphic and climate drivers through bottom-up effects on invertebrate community structure, mediated by island morphology. Narrower islands had reduced invertebrate density and richness, which indirectly resulted in lower red knot occurrence. Invertebrate responses were taxon-specific: shoreline change directly increased blue mussels but indirectly reduced coquina clams and crustaceans by narrowing islands. Half the islands significantly narrowed in island width, beach width, or both, although system-wide means remained relatively stable. Nonetheless, accelerating climate-driven change increases the likelihood of rapid ecosystem shifts. Our findings suggest that such changes may alter foraging

conditions for migratory shorebirds during migration, with broader implications for population resilience.

KEYWORDS

red knot, climate change, structural equation modeling, coastal ecosystems, migration

INTRODUCTION

Anthropogenic climate change poses a rapidly evolving threat to global biodiversity, particularly at the terrestrial-marine interface, where sea-level rise is placing mounting stress on coastal ecosystems (IPCC 2023). A warming climate also amplifies the frequency and intensity of extreme events, such as storms and marine heatwaves, pushing conditions beyond the historical range of variability (Sweet et al. 2022). When these climate drivers operate simultaneously, they can overwhelm natural disturbance-recovery processes, inducing shifts in ecosystem structure and function, referred to as state changes (Harris et al. 2018). Gaining insight into how these climate drivers alter fundamental ecosystem properties could promote effective biodiversity conservation.

Migratory animals are particularly vulnerable to climate change due to their complex ecological requirements (Robinson et al. 2009). Highly mobile migrants, such as birds, encounter diverse climatic conditions throughout their annual cycle, and increased variability in storms and large-scale climate processes can affect survival and breeding success (Clements et al. 2022). Among migratory birds, shorebirds have experienced significant population declines over the past half-century (Rosenberg et al. 2019, Smith et al. 2023), with climate change identified as a contributing factor (Zurell et al. 2018, Koleček et al. 2021). Species whose migration routes

include bottlenecks, areas where large portions of the population concentrate within a limited geographic region, are especially vulnerable (Iwamura et al. 2013).

The Western Atlantic red knot (*Calidris canutus rufa*), hereafter referred to as red knot, is a long-distance migrant breeding in the central Canadian Arctic and wintering as far south as Tierra del Fuego (Niles et al. 2010, Lyons et al. 2018). Red knots are listed as federally threatened in the United States (U.S.) following dramatic declines that reduced the Tierra del Fuego wintering population by ~80% (Atkinson et al. 2007, Smith et al. 2023). Historically widespread along the U.S. Atlantic coast during spring migration (Morrison et al. 1980), a significant portion of the remaining population now stages primarily in the Delaware Bay and Virginia barrier island system in the mid-Atlantic region (Cohen et al. 2009, Lyons et al. 2018). Red knots are dietary specialists (Cohen et al. 2010, Heller 2020, Lapenta et al. *in prep*), relying on sensitive coastal habitats during the non-breeding season (Niles et al. 2010), making them extremely vulnerable to climate change (Galbraith et al. 2014). Clarifying these relationships is vital to inform conservation efforts aimed at safeguarding this threatened species amid ongoing rapid environmental change.

Virginia's barrier islands are largely undeveloped, offering a unique opportunity to study red knots at a key staging site where natural processes operate with minimal human disturbance (Hein et al. 2021). These barrier islands are highly dynamic, responding to sea level rise through landward retreat, or island migration, over backbarrier marsh platforms (Mariotti 2021). This behavior maintains island elevation and preserve peat banks, previously buried marsh sections that become re-exposed along the ocean-facing shoreline as islands migrate towards land (Watts and Truitt 2015). Red knots disproportionately forage on exposed peat banks in Virginia, feeding on dense populations of blue mussels (*Mytilus edulis*) and small crustaceans such as amphipods

and copepods (Heller 2020). Additionally, other bivalves like coquina clams (*Donax variabilis*) serve as key prey for red knots throughout much of the sandy intertidal zone (Cohen et al. 2010, Heller et al. 2022).

Long-term research in the Virginia barrier island system has documented increasing trends in storm intensity, average daily water temperature, and the frequency of marine heat waves (Dominguez et al. 2024, Tassone and Pace 2024). Concurrently, Virginia is experiencing one of the highest rates of sea-level rise along the U.S. Atlantic coast (Sweet et al. 2022), which interacts with storm events and larger atmospheric oscillations to drive changes in barrier island behavior and morphology (Fenster and Dominguez 2022). The effects of storm disturbances on invertebrate populations are highly variable, depending on site-specific factors such as island and beach morphology, disturbance frequency, and co-occurring stressors like extreme water temperatures (Harris et al. 2011, Liénart et al. 2021). Because shorebird responses to significant shifts in prey communities may not be immediately apparent (Zhang et al. 2018), studying invertebrate populations in addition to shorebirds remains critical.

Virginia's barrier islands are projected to experience accelerating rates of change by 2100 (Mariotti and Hein 2022, UVA 2022), with uncertain consequences for red knots. Between 1984 and 2016, there was a 19% loss in barrier island area, primarily due to significant narrowing along the backbarrier transition zone between low marsh and upland habitats (Zinnert et al. 2019). Additionally, most islands in the chain are sediment-starved (Robbins et al. 2022), which can exacerbate island narrowing from the ocean-side in response to overwash disturbance. Reduced beach width may negatively affect red knots, as research suggests that migratory shorebird habitat use increases with wider beaches and foraging areas (Murchison et al. 2016). Furthermore, beach morphology strongly influences invertebrate community structure (Harris et

al. 2011). Consequently, alterations in beach morphology could disrupt prey communities, posing risks to red knot foraging and population resilience.

Anticipating how red knots will respond to environmental changes in the Virginia barrier island system first requires understanding the complex network of relationships linking red knots to long-term changes in beach morphology and climate variables. In this study, we combined long-term data on red knot and invertebrate prey demographics with geomorphological and climate data to explore direct and indirect causal pathways affecting red knots and their primary prey along the ocean-facing intertidal zone during spring migration. We applied piecewise structural equation modeling (SEM) to test a hypothesized network of relationships (Figure 1) developed from prior research in this system. These relationships included interactions among red knots, invertebrate prey populations, habitat features (e.g., intertidal substrate and tidal phase; Cohen et al. 2010, Heller et al. 2022), barrier island morphology (e.g., island width, beach width, island length, and inlet distance), shoreline change-rates (Mariotti and Hein 2022), island migration behavior (Robbins et al. 2022), storm frequency and intensity (e.g., storminess; Fenster and Dominguez 2022, Dominguez et al. 2024), and average daily water temperature (Heller et al. 2022). We also hypothesized that global climate oscillations, such as the North Atlantic Oscillation (NAO), influence local processes including storminess, water temperature (Hurrell 1995), and potentially shorebird migration patterns (Tonelli et al. 2024). Through this integrated approach, we aim to enhance understanding of the multifaceted climate and environmental drivers shaping red knot staging habitats, thereby informing adaptive management strategies to address the conservation challenges of unprecedented global climate change.

METHODS

Study area

The Virginia barrier island system is a dynamic coastal system located along the seaward margin of the Eastern Shore of Virginia. It comprises 14 barrier islands separated by tidal inlets, extending approximately 100 km from Assateague Island in the north to Fisherman Island in the south (Figure 2). The shallow lagoon behind these islands includes a mosaic of open bays, tidal creeks, mudflats, oyster reefs, and salt marshes (Robbins et al. 2022). Within the chain, 12 islands remain undeveloped and with no history of artificial stabilization or beach nourishment (Elko et al. 2021). Approximately 55,000 ha of barrier islands, backbarrier marshes, creeks, and tidal flats are protected by The Nature Conservancy (Hein et al. 2021) and the remaining areas are mostly owned and managed by a mixture of the following federal and state agencies: the U.S. Fish and Wildlife Service, the Virginia Marine Resources Commission, the Virginia Department of Conservation and Recreation, and the Virginia Department of Wildlife Resources (Watts and Truitt 2015). Wallops Island, home of the Wallops Flight Facility, is owned and managed by the National Aeronautics and Space Administration.

The system is transgressive, migrating landward at an average rate of approximately 4.8 m yr^{-1} from 1980 to 2017, a 45% increase since the post-industrial period (Mariotti and Hein 2022). Island behavior is controlled by longshore sand-transport fluxes, which vary considerably due to differences in inlet and shoreface dynamics as well as inter-island sand exchange processes (Robbins et al. 2022). Since the 1800s, the system has experienced a net sand volume loss of approximately 3.4% (Robbins et al. 2022). The system is subject to frequent tropical and extratropical storms, including nor'easters, averaging 14 storm events annually, with typical beach recovery times of roughly four years (Dominguez et al. 2024). Storm-driven beach erosion is most severe during the winter months (Fenster and Dominguez 2022).

Approximately 90% of the shoreline of the barrier islands consists of sandy intertidal habitat interspersed with peat banks (Watts and Truitt 2015, Heller et al. 2022). Previous research has found that crustaceans dominate invertebrate communities across both sand and peat substrates (Lapenta et al. *in prep*). Coquina clams are common in sand while blue mussels are densely concentrated in peat banks (Heller et al. 2022). Other prey present in barrier island sand and peat substrates in minimal numbers include angel wing clams (*Cyrtopleura costata*), Atlantic horseshoe crab eggs (*Limulus polyphemus*), polychaete worms, and various other miscellaneous prey in both substrates (Cohen et al. 2010, Lapenta et al. *in prep*).

Field methods and model variable descriptions

Shorebird, invertebrate, and habitat variables

We studied red knots and their invertebrate prey along the ocean-facing intertidal zone of 12 barrier islands from Wallops Island to Fisherman Island (Figure 2), between 21–28 May, 2009–2023 (excluding 2020 due to the global COVID-19 pandemic), coinciding with peak red knot abundance in the Virginia barrier island system (Cohen et al. 2009). Each year, we generated 100 unique random sampling points, separated a minimum of 200 m apart, in the ocean intertidal zone across the sampled islands. All random sampling point generation was completed using ArcGIS Software (ESRI, Redlands, California, USA, 2022) using the most recent United States Department of Agriculture Farm Service Agency's National Agriculture Imagery Program (NAIP) orthophotography imagery (Figure 2; Table S1; USDA 2023). At each point, we counted all non-flying birds within a 100 m radius semicircle from the water's edge and recorded habitat characteristics including substrate type (i.e., sand or peat) and tidal stage (i.e., high, falling, low, and rising).

Immediately following bird counts, we collected a core sample in the littoral zone (i.e., area between high and low tide lines) where substrate was saturated, avoiding waves, using PVC pipe (10 cm diameter x 3.5 cm depth; volume = 275 cm^3) cut to a red knot's bill length (Tomkovich 1992), to represent accessible prey. We collected cores at each point regardless of bird presence. We froze cores upon returning from the field until processing. We sorted cores for invertebrates using a series of sieves ranging in mesh sizes (4 - 0.25 mm) and a dissecting microscope. Invertebrates were grouped into crustaceans, coquina clams, blue mussels, and miscellaneous prey (e.g., insect larvae, crab eggs, snails, worms, and other clams; Heller et al. 2022). We report invertebrate density as organisms/m^2 to match prior studies (Cohen et al. 2010, Heller et al. 2022) and define invertebrate richness as the number of unique prey groups per sample.

Barrier island morphometrics

We measured barrier island morphometric variables using publicly available four-band (i.e., three true color and one near-infrared) multispectral aerial imagery from NAIP (USDA 2023) and the Virginia Department of Emergency Management's Virginia Geographic Information Network (VGIN 2023). NAIP imagery resolution ranged from 1 m (2008–2016) to 0.60 m (2018–2023), while the VGIN imagery was 0.30 m for all years (2007, 2013, 2017). Imagery acquisition dates varied across years and islands (Table S1).

We measured island length as shoreline length along the visible high tide line of each barrier for each year of available imagery (Robbins et al. 2022). We measured island width perpendicularly from the high tide line to the backbarrier, defined as the visible land-to-marsh, lagoon, or tidal flat transition (Figure 2). We included interior wetlands, while backbarrier marsh

was excluded (Robbins et al. 2022). We measured beach width perpendicularly from the high tide line to the first visible transition between dry sand and other land cover types (e.g., vegetation, marsh, lagoon, or tidal flat). We did not distinguish between the beach and dunes due to a lack of repeated samples of elevation data across islands and years.

We recorded island width and beach width every 100 m, including island end points, to capture variability in barrier island morphology. Because Myrtle and Mink Islands fluctuate between being conjoined and separated, we consider them to be one island in this analysis. Assawoman was conjoined with Wallops Islands throughout the study, so we delineated the boundary between these islands based on property ownership determined from a VGIN parcel map. We extracted width measurements from the two nearest cross-island transects closest to each year of random points that were then averaged. We then calculated distance to nearest inlet for each random point using the Near tool in ArcGIS Pro (version 3.0).

Climate drivers

To evaluate how storms influence shorebirds and invertebrate prey, both directly and via changes in island morphology, we quantified storminess using the cumulative storm impact index (CSII) developed by Fenster and Dominguez (2022), which accounts for both individual storm intensity and cumulative effects of successive storms. Because the collection dates for aerial imagery used to quantify barrier island morphometric values were variable but occurred more frequently in spring than fall (Table S1), and biological data were collected in spring, we summed the CSII of storm events occurring between January and May to capture the influence of winter and spring storms on barrier island morphometrics and biological variables. We retrieved hourly water level and monthly datums for Wachapreague, VA (Station 8631044; NOAA 2025)

as this centrally located station was assumed to represent storm conditions across the Virginia barrier island system (Robbins et al. 2022). We then identified and quantified storm events using the Storm Erosion Potential Index (SEPI; Zhang et al. 2001) defined by: 1) storm surge that exceeded two standard deviations (> 2SD) of the average surge and 2) storm tide exceeding the annual average Mean High Water ($\overline{MHW}$) of a semi-diurnal tide (12 hours). We calculated CSII as the sum of the SEPI of a given storm and a weighted factor (δ= 0.3) of the previous storm's CSII (Fenster and Dominguez 2022). Both SEPI and CSII have the same units of measurement (square meters x hours; m^2hr), representing cumulative area and duration of storm impact. Given the buffering effect of the lagoon system to the mainland peninsula, our CSII values likely underestimate the direct exposure of storm impacts experienced by barrier islands.

To examine whether storm effects vary with large-scale climate patterns, we obtained the North Atlantic Oscillation (NAO) index from the National Weather Service's Climate Prediction Center (CPC 2025). The NAO index reflects sea-level pressure differences between the subtropical high and the subpolar low (Hurrell 1995) and is expressed as a standardized anomaly based on climatological averages. To represent the prevailing atmospheric state during the winter/spring period relevant to both storm activity and biological data collection, we averaged monthly NAO index values for each year between January and May (e.g., seasonal NAO).

To assess the direct influence of water temperature on invertebrates, we used 6-min interval water temperature data from the Wachapreague, VA tide station (NOAA 2025), averaged for each day of biological data collection (May 21-28, 2009 – 2023).

Geomorphological drivers

To evaluate the effect of geomorphic change on island morphology, we obtained shoreline change rates from Mariotti and Hein (2022), based on 28 years of shoreline data between 1855–2017, measured every 100 m and averaged per island. We extracted island migration behavior classifications from descriptions of mesoscale island behavior detailed in Robbins et al. (2022). We classified islands with dominant mesoscale migration behavior as migrational, except when rotational behavior was also present. These migrational islands included Assawoman, Metompkin, Cedar, Wreck, Myrtle/Mink, and Smith Islands.

Statistical methods

Piecewise structural equation modeling

All calculations and statistical tests were performed in the R statistical computing environment (R version 4.4.2; R Core Team 2024). We developed two structural equation models (SEMs) using the piecewiseSEM package (Lefcheck 2016) to identify direct and indirect causal pathways influencing red knots and their prey at foraging sites on barrier island beaches during spring migration. To ensure consistency across models, we excluded any observations with missing data. Because storminess could not be calculated for 2007 and 2008 due to missing water level data from the Wachapreague station, we limited the analysis to 10 years of data from 2009–2023. The final dataset included n = 1,077 observations, with a mean of 108 observations per year (± 19.2 SD).

Relationships between variables in our SEMs are represented as unidirectional paths. Piecewise SEM uses local estimation, enabling flexibility in fitting distributions (Lefcheck 2016). Goodness-of-fit for SEMs is assessed using Shipley's test of directed separation, which evaluates the assumption that all variables are conditionally independent (Shipley 2009). The

hypothesized causal network is considered consistent with the data when there is weak support for the sum of the conditional independence claims, or Fisher's C statistic.

Prior to analysis, we converted island behavior, substrate, and tide to binary variables. Tide levels were simplified from four categories (high, rising, low, falling) to two (rising and falling). Historic tide charts were extracted from the NOAA Tides and Currents database (NOAA 2025). Because tide timing varies north-south across the system, predicted tides from multiple stations were used: Gargathy Neck (Station 8630637) for Assawoman and Metompkin Island, Wachapreague (Station 8631044) for Cedar through Hog Island, Oyster Harbor (Station 8631591) for Cobb through Ship Shoal Island, and Smith Island Coast Guard Station (Station 8631874) for Myrtle/Mink through Fisherman Island. Falling tide was defined as the period following the diurnal predicted high tide, and rising tide as the period following the diurnal predicted low tide.

We log-transformed island width and square-root transformed beach width (which contained zero values) to approximate normality. We then standardized all continuous variables by centering at the mean and dividing by 2 SD (Gelman 2008) to account for scale differences. Each SEM was composed of individual component models that contained all hypothesized relationships (Figure 1). All component models were fit using the glmmTMB package (Brooks et al. 2017). We included year and island as random effects in each component model to account for spatial and temporal variability in our data, except in models where inclusion of year produced singular fit warnings (variance ~ 0). In those cases (i.e., island width and crustacean component models), year was excluded as a random effect. We checked model assumptions via Q-Q plots and residual diagnostics using the 'DHARMa' package (Hartig and Hartig 2017). We assessed multicollinearity with correlation plots ('corrplot'; Wei et al. 2017) and evaluated global model performance with the 'performance' package (Lüdecke et al. 2021).

We fit continuous response variables to Gaussian distributions with identity links, while abundance and density variables were fit to negative binomial distributions with log links (Table 1). Component models for invertebrate density in the red knot SEM and crustaceans, coquina clams, and miscellaneous prey in the invertebrate SEM exhibited excess zeros and were fit with zero-inflated negative binomial distributions. These models include a zero-inflated component estimating the probability of extra zeros and a conditional (count) component estimating abundance, including zeros, conditional on the zero-inflated process (Yau et al. 2003). We used an information-theoretic approach to compare eight *a priori* zero-inflation models (Table S2) using AICcmodavg (Mazerolle 2023), ranked them by second-order AIC (AIC_c), and used ΔAIC_c and Akaike weights (ω_i) to assess support (Johnson and Omland 2004). The best-supported zero-inflation component ($\Delta AIC_c \leq 2$) was included in the final SEM models (Burnham and Anderson 2004). Our invertebrate richness response variable was underdispersed and violated assumptions of Poisson and negative binomial distributions, thus, we fit this component model using a Generalized Poisson, which includes an extra variance component (Consul and Famoye 1992).

In the red knot SEM, we specified correlated error terms to exclude causal relationships between red knot presence and abundance, invertebrate richness and density, and island width and beach width from the test of directed separation. In the invertebrate SEM, we included correlated error terms between all invertebrate variables. We identified missing paths via directed separation tests and expanded our network to include statistically significant ($p < 0.05$) paths if they were ecologically justified (Grace et al. 2012). We pruned non-significant paths using a stepwise procedure. We evaluated final model fit using Fisher's C test, where the hypothesized network was considered consistent with the data when $p > 0.05$.

We report both unstandardized (B) and standardized estimates (β), scaled by standard deviation, along with R^2 values for each component model in the red knot and invertebrate SEMs. We obtained standardized coefficients for negative binomial regressions using the observed empirical approach based on variance explained (R^2; Lefcheck 2016), and for logistic regressions using the latent-linear approach (Grace et al. 2018). In the red knot SEM, we were unable to calculate standardized coefficients for the Generalized Poisson distribution in the piecewise package but report those for all other component models.

Assessing morphometric change

Given that island morphometric features (i.e., island and beach width) directly influenced invertebrate prey density, and indirectly influenced red knot presence and abundance, we assessed trends in these variables. To quantify and compare morphometric change across islands between 2007 and 2023, we developed a composite capturing the magnitude of change in multiple variables. We first averaged island and beach width measurements per island for each year to account for spatial variability in transect sampling across imagery years. We then calculated the percent change between 2007 and 2023. To summarize overall morphometric change, we calculated the absolute percent change for each variable per island and summed them to generate a total morphometric change score:

$$\text{Total Change Score}_i = \sum_{j=1}^{3} |\Delta_j| \quad (1)$$

Where $|\Delta_j|$ is the absolute change in morphometric variable *j* for island *i.*

We assessed directional change in individual morphometric variables from 2007–2023 using Kendall's rank correlation coefficient (τ). This non-parametric test was selected based on

results from Shapiro-Wilke normality tests indicating non-normal distributions (Table S3). Kendall's tau is robust to outliers and non-linear, making it well-suited to our data. We conducted separate Kendall's tau tests for each variable on both the island scale (individual test per island per variable) and the system-wide scale, where yearly averages of morphometric variables across all islands were used.

RESULTS

Piecewise structural equation models

Red knot SEM

Tests of directed separation supported the addition of paths not included in our initial hypothesized network linking 1) island width to substrate, 2) island width to invertebrate density, and 3) island width to invertebrate richness. Interactions between seasonal NAO and average daily water temperature were not supported and thus removed. Average daily water temperature and island migration were not significantly related to any response variables and were thus removed. The final model fit the data well (Fisher's C = 102.19, $p = 0.11$). We found no direct effects of climate or geomorphic drivers on red knot presence or abundance (Figure 3; Table 2). Instead, climate and geomorphic effects on red knot presence and abundance were indirect, mediated by cascading effects between barrier island morphometrics, invertebrate variables, and sympatric species abundance (Figure 3; Table 2).

The interaction between storminess and seasonal NAO was directly linked to beach width (B = -0.57, $p = 0.01$) and island width (B = -0.16, $p = 0.04$), such that the effect of storminess changed depending on the strength and directionality of the NAO. During negative NAO phases, increased storminess was associated with wider beaches and islands; in contrast, positive NAO

phases were associated with narrower beaches and islands (Figure 4). Shoreline change-rate (B = -0.34, $p = 0.007$) had a direct negative effect on island width, where increasing rates of shoreline change were related to narrower islands. Several morphometric variables had direct links to barrier island width and beach width. We found that increasing distance from inlets was associated with narrower island (B = -0.14, $p < 0.0001$) and beaches (B = -0.21, $p < 0.0001$). Total island length was positively related to island width (B = 0.31, $p = 0.007$). These climate and geomorphic variables were then indirectly linked to red knots through a positive effect of island width on invertebrate richness (B = 0.08, $p = 0.03$), a negative effect of beach width on invertebrate density (B = -0.26, $p = 0.004$), and a strong positive effect of island width on invertebrate density (B = 0.50, $p < 0.0001$), which in turn indirectly influenced red knots via sympatric species abundance (B = 0.00001, $p < 0.0001$). Inlet distance also had a direct positive effect on invertebrate density (B = 0.32, $p = 0.003$).

Habitat variables influenced red knots via multiple pathways. Intertidal peat substrate had direct positive effects on red knot presence (B = 1.11, $p = 0.0005$), sympatric species abundance (B = 0.40, $p = 0.01$), invertebrate density (B = 1.52, $p < 0.0001$), and invertebrate richness (B = 0.51, $p < 0.0001$) and indirectly affected red knot abundance via invertebrate richness. Substrate was negatively associated with island width (B = -0.21, $p < 0.0001$), such that peat substrate was associated with narrower islands. Tide indirectly influenced red knot presence and abundance via invertebrate richness (B = 0.16, $p < 0.0001$), which increased from rising to falling tide.

Invertebrate SEM

Directed separation tests led to the addition of links between 1) crustaceans and both island migration and island width, 2) coquina clams and both island migration and island width,

and 3) blue mussels and shoreline change-rate to our initial hypothesized network. Once again, our model did not support interactions between seasonal NAO and average daily water temperature, and tidal phase was found to be insignificant; thus, these variables were not in the final model. The final invertebrate SEM fit the data well (Fisher's C = 75.28, $p = 0.31$) and revealed that multiple climate and geomorphic drivers directly influenced invertebrate density (Figure 5; Table 2). Average daily water temperature ($\beta = 0.28$, $p = 0.002$) and shoreline change-rate ($\beta = 0.17$, $p = 0.005$) had direct positive effects on blue mussel density while island migration negatively influenced crustacean ($\beta = -0.08$, $p = 0.01$) and coquina clam ($\beta = -0.11$, $p = 0.02$) densities.

As in the red knot SEM, the storminess and seasonal NAO interaction was directly linked to both beach width ($\beta = -0.21$, $p = 0.01$) and island width ($\beta = -0.06$, $p = 0.04$; Figure 4), shoreline change-rate negatively affected island width ($\beta = -0.34$, $p = 0.007$), inlet distance negatively influenced island width ($\beta = -0.14$, $p < 0.0001$) and beach width ($\beta = -0.20$, $p < 0.0001$), and island length positively influenced island width ($\beta = 0.31$, $p = 0.007$). These variables were then indirectly linked to crustacean density via island width ($\beta = 0.04$, $p = 0.02$) and beach width ($\beta = -0.04$, $p = 0.003$), and coquina clam density via island width ($\beta = 0.07$, $p = 0.004$). Inlet distance also had a direct positive effect on crustacean density ($\beta = 0.04$, $p = 0.0009$).

Intertidal substrate had strong effects on invertebrates and barrier island morphometrics. Substrate transitioning from sand to peat had direct positive effects on crustacean ($\beta = 0.12$, $p < 0.0001$), blue mussel ($\beta = 0.21$, $p < 0.0001$), and miscellaneous prey densities ($\beta = 0.06$, $p = 0.0003$), and a negative effect on coquina clams ($\beta = -0.08$, $p = 0.0006$). Substrate also indirectly

influenced crustacean and coquina clam densities via a direct negative effect on island width (β = -0.11, $p < 0.0001$). Islands were narrower when the intertidal shoreline was comprised of peat.

Morphometric Change

From 2007–2023, island width averaged 0.33 ± 0.28 km (mean ± SD) across all islands and years, with individual island means ranging from 0.09–0.65 km (Table S4). Beach width was similarly variable, averaging 0.11 ± 0.09 km, with island-specific means ranging from 0.06–0.16 km. We observed an 11% decrease in average island width and a 42% decrease in average beach width across the study system from 2007–2023 (Table 3). Kendall's tau correlation analyses suggested weak negative trends in mean island and beach widths system-wide, though the results were not statistically significant.

On the barrier island scale, we observed a decrease in average island width in 73% (n = 8) of the islands and a decrease in average beach width in 91% (n = 10) of the islands between 2007 and 2023 (Table 3). Ship Shoal Island exhibited the most geomorphological change between 2007 – 2023, while Smith Island changed the least (Table 3). We detected consistent directional trends in the combined geomorphic features of 55% (n = 6) of the islands in our study area (Table 3; Figure 6). Parramore (τ = -0.48, p = 0.03), Hog (τ = -0.48, p = 0.03) and Cobb (τ = -0.67, p = 0.003) Islands moderately narrowed in island width, while Ship Shoal Island moderately narrowed by beach width (τ = -0.52, p = 0.02). Cedar and Wreck Islands narrowed in both island and beach widths (Cedar island width: τ = -0.52, p = 0.02; Cedar beach width: τ = -0.52, p = 0.02; Wreck island width: τ = -0.58, p = 0.01; Wreck beach width: τ = -0.73, p = 0.001).

DISCUSSION

Our results provided a novel, system-level perspective on how long- and short-term drivers influence imperiled migratory shorebirds at an internationally significant staging site. Red knots foraging in the ocean-facing intertidal zone during spring migration were positively influenced by invertebrate prey and peat substrate, consistent with previous studies in the Virginia barrier island system (Cohen et al. 2010, Watts and Truitt 2015, Heller et al. 2022). Invertebrate richness emerged as a strong predictor of red knot presence and abundance. In contrast, invertebrate density influenced red knots indirectly by increasing the abundance of other shorebird species, whose presence in turn attracted red knots. This social factor had the strongest effect on red knot presence, echoing findings by Folmer and Piersma (2012), who reported that social aggregation outweighed prey availability and other environmental predictors in the Dutch Wadden Sea. They also found that combined direct and indirect effects better explained shorebird foraging patterns than any single direct influence, mirroring our findings. Overall, our results suggest that red knots respond primarily to changes in local foraging conditions rather than directly to island geomorphology or broader climate patterns. However, we found that geomorphic and climate drivers indirectly shaped foraging conditions by altering island morphology and invertebrate community structure, creating a bottom-up pathway linking ecosystem change to migratory shorebird populations.

Invertebrate responses to geomorphic and climate drivers were taxon-specific, likely reflecting species' substrate affinities and life history traits. Blue mussels, which attach to solid substrates like peat (Rzepecki et al. 1992), were positively associated with shoreline change-rate, suggesting that accelerated shoreline retreat exposes more peat along marsh-backed islands, thereby expanding suitable habitat for blue mussels. Conversely, coquina clams, which are

mobile burrowers dependent on sandy substrates (Ellers 1995), were negatively associated with island migration behavior, as were crustaceans. Although crustaceans occur in both sand and peat substrates (Heller et al. 2022, Lapenta et al. *in prep*), most of our data represent sand, which constitutes the majority of the intertidal zone. This suggests the observed decline in crustacean density on migrating islands is likely linked to migration-driven changes in sandy intertidal habitats. Frequent overwash associated with island migration (Wolner et al. 2013) may perpetuate suboptimal conditions for coquina clams and sand-burrowing crustaceans, which are sensitive to changes in sediment characteristics and beach morphology (Manning et al. 2014, Peterson et al. 2014).

Average daily water temperature was the only climate variable directly linked to invertebrate density, with a positive effect on blue mussels. This contrasts with studies showing long-term warming reduced mussel abundance (Liénart et al. 2021), although Heller et al. (2022) reported the same positive relationship in the Virginia barrier island system. In both cases, water temperature was measured in spring, when conditions likely remained below thermal tolerance thresholds and correspond with seasonal increases in food availability (Liénart et al. 2021). However, warmer winter conditions have been linked to reduced spring mussel recruitment and body size (Waldeck and Larsson 2013, Liénart et al. 2021), and repeated daily exposure to elevated temperatures lowers blue mussels' thermal tolerance over time (Seuront et al. 2019). Therefore, future warming and the increased frequency of marine heatwaves predicted for the Virginia barrier island system (Tassone and Pace 2024) likely pose a long-term threat to blue mussel populations, and by extension, to red knots, despite the short-term positive relationship observed here.

Consistent with our hypothesis, storminess modulated by the NAO was a dominant driver of beach width, which in turn influenced invertebrate density. During positive NAO phases, stronger-than-average winds shift storm tracks northward, increasing storm activity along the U.S. Atlantic coast (Hurrell 1995). Under these conditions, overwash events are more likely to be erosional rather than depositional, often causing lasting changes to beach morphology and increasing the likelihood of island breaching (Nienhuis and Lorenzo-Trueba 2019). Such breaching may negatively impact invertebrates, particularly crustaceans, whose density decreased near inlets where hydrodynamic conditions are more extreme. Our model suggests storm-driven changes in beach width indirectly affect crustacean density, though the effect varied. Notably, calmer conditions (negative NAO) were associated with wider beaches but lower crustacean densities, whereas stormier conditions (positive NAO) corresponded to narrower beaches and higher crustacean densities, highlighting shoreline invertebrates' sensitivity to climate-modulated beach dynamics.

In contrast, shoreline change-rate was a key indirect driver of invertebrate community structure through its influence on island width. Accelerated shoreline retreat reduced coquina clam and crustacean densities and decreased overall invertebrate richness. While storms affect island morphology on shorter timescales, chronic shoreline retreat driven by storm surge and sea-level rise can lead to long-term island narrowing, as shown by Fenster and Dominguez (2022). Even under calm conditions when islands widen, the effect of shoreline change on island width was stronger than that of storminess. This suggests that long-term shoreline retreat may be more disruptive to invertebrate communities in the Virginia barrier island system than episodic storm disturbance. Together, these findings reveal how interacting climate drivers reshape invertebrate

communities and reduce coastal ecosystem resilience, with cascading consequences for migratory shorebirds.

Over half the barrier islands in our study experienced morphological changes in island width, beach width, or both between 2007 and 2023. Narrowing of island width was more common than beach narrowing, and was especially pronounced on Cedar, Parramore, and Hog Islands, consistent with previous geomorphic studies in the region (Zinnert et al. 2019, Robbins et al. 2022). Despite island-specific variability, the overall barrier island system from Assawoman to Fisherman Island remained relatively stable during this period, with erosion in some areas offset by accretion in others. This echoes long-term observations by Robbins et al. (2022), who found only a 3% reduction in island volume across the system between 1887 and 2017. However, climate projections suggest that future conditions may be far less stable. Sea-level rise and intensified storm regimes are expected to push Virginia's barrier islands into new states of continuous migration (Reeves et al. 2021), with island migration rates projected to increase by at least ~48% by 2100 (Mariotti and Hein 2022).

Our results suggest that accelerated island migration will reduce densities of coquina clam and crustacean, key prey for red knots (Heller 2020, Heller et al. 2022), while temporarily increasing blue mussel abundance through expanded peat exposure. In the short-term, red knots may adapt by shifting their habitat use among islands in response to changing prey distributions (Watts and Truitt 2015). However, this flexibility masks a more serious long-term risk. Island migration drives backbarrier marsh loss (Deaton et al. 2017), and sea-level rise may eventually erode marsh platforms, reducing peat banks and causing blue mussel populations to decline as a result. This risk is exacerbated by warming ocean temperatures, which have already caused a poleward range contraction of blue mussels, making Virginia the southern edge of their current

U.S. Atlantic coast distribution (Jones et al. 2010). The combined pressures of climate change may severely reduce this critical resource for red knots during spring migration under predicted future scenarios.

Although structural equation modeling (SEM) is a powerful tool for exploring complex cause–effect relationships in ecological systems, it is important to recognize its interpretive boundaries. SEM requires *a priori* specification of directional pathways, limiting its ability to capture unmeasured variables, emergent dynamics, or bidirectional feedbacks (Grace et al. 2012, Lefcheck 2016). In dynamic coastal systems like the Virginia barrier island system, nonlinear and spatially and temporally variable feedbacks among geomorphic features, vegetation, and sediment transport processes shape barrier responses to sea-level rise and storms (Wolner et al. 2013, Zinnert et al. 2019, Reeves et al. 2021, Robbins et al. 2022). Many of these processes operate with time-lagged effects (Raff et al. 2018, Nienhuis and Lorenzo-Trueba 2019, Mariotti and Hein 2022). While our SEM approach revealed key linkages among climate drivers, geomorphology, invertebrate communities, and red knots, many feedbacks remain beyond the scope of a single modeling framework. Future work should integrate complementary approaches to better capture system behavior.

Continued long-term monitoring of prey and red knot populations is essential for improving understanding of their responses to increasing climate variability (Harris et al. 2018). While our model incorporated a robust 10-year dataset spanning 2009–2023, assessing climate change impacts often requires multi-decadal time series (Dominguez et al. 2024). Many geomorphic and climate drivers, such as sea-level rise, operate over timescales that exceed most ecological studies (Robbins et al. 2022). Long-term data are crucial for detecting tipping points and delayed ecological responses to change (Harris et al. 2018). Importantly, the bottom-up

effects we identified extend beyond red knots to sympatric shorebird species. Therefore, while this study focused on red knots, the vulnerabilities observed have implications for the broader shorebird community in Virginia and across the U.S. Atlantic flyway, especially in developed coastal areas where climate impacts tend to be more severe. Hardened structures and artificial stabilization accelerate erosion, causing more frequent and severe disruptions to invertebrate prey communities with prolonged recovery periods (Harris et al. 2011). Maintaining natural geomorphic processes will be critical for promoting long-term ecosystem resilience and supporting migratory shorebird population recovery in the face of accelerating climate change.

ACKNOWLEDGEMENTS

We thank L. Anderson, T. Brocato, L. Buckman, I. Burgos, W. Burgoyne, L. Casteen, M. Graul, J. Green, D. Hoff, T. Humbert, E. Kline, D. McBride, R. Meyers, M. Nootbaar, E. Rothenburger, A. Zbesheski, and all previous technicians who have assisted with field and laboratory data acquisition over the durations of this project. We especially thank D. Fraser and S. Ritter (Virginia Tech Department of Fish and Wildlife Conservation), C. Baird, S. Hoffman, B. Doughty, T. Burkett, and D. Fauber (Virginia Coast Reserve Long-Term Ecological Research program's Coastal Research Center), A. Wilke, Z. Poulton, and M. Balitbit (The Nature Conservancy), K. Holcomb, K. Oliver, P. Denmon, and N. Walker (U. S. Fish and Wildlife Service), and partners at the Virginia Department of Conservation & Recreation, the Commonwealth of Virginia Marine Resources Commission, and the National Oceanic & Atmospheric Administration for logistical, intellectual, and permitting support throughout the project. We thank the National Science Foundation's Virginia Coast Reserve Long-Term Ecological Research program (DEB-1832221 and DEB-2425178) and the Virginia Tech

Department of Fish and Wildlife Conservation for funding this project. Any opinions, findings, conclusions, or recommendations expressed in this material are those of the authors and do not necessarily reflect the views of the National Science Foundation or any other funding partners.

LITERATURE CITED

Atkinson, P. W., U. Thetford, N. A. Clark, U. Thethford, C. Espoz, P. M. Gonzalez, F. Inalafquen, D. E. Hernandez, and M. K. Peck. 2007. Status of the Red Knot (Calidris canutus rufa) in the Western Hemisphere. Studies in Avian Biology 1–185.

Brooks, M. E., K. Kristensen, K. J. Van Benthem, A. Magnusson, C. W. Berg, A. Nielsen, H. J. Skaug, M. Maechler, and B. M. Bolker. 2017. Modeling zero-inflated count data with glmmTMB. BioRxiv 132753.

Burnham, K. P., and D. R. Anderson. 2004. Multimodel inference: understanding AIC and BIC in model selection. Sociological methods & research 33:261–304.

Clements, S. J., J. P. Loghry, B. M. Ballard, and M. D. Weegman. 2022. Carry-over effects of weather and decision-making on nest success of a migratory shorebird. Ecology and Evolution 12:e9581.

Climate Prediction Center (CPC). 2025. North Atlantic Oscillation (NAO). Climate & Weather Linkage. <https://www.cpc.ncep.noaa.gov/products/precip/CWlink/pna/nao.shtml>. Accessed 7 Aug 2025.

Cohen, J. B., S. M. Karpanty, J. D. Fraser, and B. R. Truitt. 2010. The effect of benthic prey abundance and size on red knot (Calidris canutus) distribution at an alternative migratory stopover site on the US Atlantic Coast. Journal of Ornithology 151:355–364.

Cohen, J. B., S. M. Karpanty, J. D. Fraser, B. D. Watts, and B. R. Truitt. 2009. Residence Probability and Population Size of Red Knots During Spring Stopover in the Mid-Atlantic Region of the United States. Journal of Wildlife Management 73:939–945.

Consul, P., and F. Famoye. 1992. Generalized Poisson regression model. Communications in Statistics-Theory and Methods 21:89–109.

Deaton, C. D., C. J. Hein, and M. L. Kirwan. 2017. Barrier island migration dominates ecogeomorphic feedbacks and drives salt marsh loss along the Virginia Atlantic Coast, USA. Geology 45:123–126.

Dominguez, R., M. Fenster, and J. McManus. 2024. Storm surge frequency, magnitude, and cumulative storm beach impact along the US east coast. EGUsphere 2024:1–31.

Elko, N., T. R. Briggs, L. Benedet, Q. Robertson, G. Thomson, B. M. Webb, and K. Garvey. 2021. A century of US beach nourishment. Ocean & Coastal Management 199:105406.

Ellers, O. 1995. Behavioral Control of Swash-Riding in the Clam Donax variabilis. The Biological Bulletin 189:120–127.

ESRI. 2022. ArcGIS Pro 3.0. Environmental Systems Research Institute, Redlands, CA, USA.

Fenster, M., and R. Dominguez. 2022. Quantifying coastal storm impacts using a new cumulative storm impact index (CSII) model: Application along the Virginia coast, USA. Journal of Geophysical Research: Earth Surface 127:e2022JF006641.

Folmer, E. O., and T. Piersma. 2012. The contributions of resource availability and social forces to foraging distributions: a spatial lag modelling approach. Animal Behaviour 84:1371–1380.

Galbraith, H., D. W. DesRochers, S. Brown, and J. M. Reed. 2014. Predicting Vulnerabilities of North American Shorebirds to Climate Change. G. Ballard, editor. PLoS ONE 9:e108899.

Gelman, A. 2008. Scaling regression inputs by dividing by two standard deviations. Statistics in medicine 27:2865–2873.

Grace, J. B., D. R. Schoolmaster, G. R. Guntenspergen, A. M. Little, B. R. Mitchell, K. M. Miller, and E. W. Schweiger. 2012. Guidelines for a graph-theoretic implementation of structural equation modeling. Ecosphere 3:art73.

Grace, J. B., D. J. Johnson, J. S. Lefcheck, and J. E. Byrnes. 2018. Quantifying relative importance: computing standardized effects in models with binary outcomes. Ecosphere 9:e02283.

Harris, L., R. Nel, M. Smale, and D. Schoeman. 2011. Swashed away? Storm impacts on sandy beach macrofaunal communities. Estuarine, Coastal and Shelf Science 94:210–221.

Harris, R. M., L. J. Beaumont, T. R. Vance, C. R. Tozer, T. A. Remenyi, S. E. Perkins-Kirkpatrick, P. J. Mitchell, A. Nicotra, S. McGregor, and N. Andrew. 2018. Biological responses to the press and pulse of climate trends and extreme events. Nature climate change 8:579–587.

Hartig, F., and M. F. Hartig. 2017. Package 'dharma.' R package 531:532.

Hein, C. J., M. S. Fenster, K. B. Gedan, J. R. Tabar, E. A. Hein, and T. DeMunda. 2021. Leveraging the interdependencies between barrier islands and backbarrier saltmarshes to enhance resilience to sea-level rise. Frontiers in Marine Science 8:721904.

Heller, E. L. 2020. Factors affecting Western Atlantic red knots (Calidris canutus rufa) and their prey during spring migration on Virginia's barrier islands. doctoral, Virginia Polytechnic Institute and State University, Blacksburg, VA, USA.

Heller, E. L., S. M. Karpanty, J. B. Cohen, D. H. Catlin, S. J. Ritter, B. R. Truitt, and J. D. Fraser. 2022. Factors that affect migratory Western Atlantic red knots (Calidris canutus rufa) and their prey during spring staging on Virginia's barrier islands. V. H. R. Paiva, editor. PLOS ONE 17:e0270224.

Hurrell, J. W. 1995. Decadal trends in the North Atlantic Oscillation: Regional temperatures and precipitation. Science 269:676–679.

IPCC. 2023. Climate Change 2023: Synthesis Report. Contribution of Working Groups I, II and III to the Sixth Assessment Report of the Intergovernmental Panel on Climate Change. Intergovernmental Panel on Climate Change, Geneva, Switzerland.

Iwamura, T., H. P. Possingham, I. Chadès, C. Minton, N. J. Murray, D. I. Rogers, E. A. Treml, and R. A. Fuller. 2013. Migratory connectivity magnifies the consequences of habitat loss from sea-level rise for shorebird populations. Proceedings of the Royal Society B: Biological Sciences 280:20130325.

Johnson, J. B., and K. S. Omland. 2004. Model selection in ecology and evolution. Trends in ecology & evolution 19:101–108.

Jones, S. J., F. P. Lima, and D. S. Wethey. 2010. Rising environmental temperatures and biogeography: poleward range contraction of the blue mussel, Mytilus edulis L., in the western Atlantic: Mytilus edulis poleward range contraction. Journal of Biogeography 37:2243–2259.

Koleček, J., J. Reif, M. Šálek, J. Hanzelka, C. Sottas, and V. Kubelka. 2021. Global population trends in shorebirds: migratory behaviour makes species at risk. The Science of Nature 108:9.

Leatherman, S. P., T. E. Rice, and V. Goldsmith. 1982. Virginia Barrier Island Configuration: A Reappraisal. Science 215:285–287.

Lefcheck, J. S. 2016. piecewiseSEM: Piecewise structural equation modelling in r for ecology, evolution, and systematics. Methods in Ecology and Evolution 7:573–579.

Liénart, C., A. Garbaras, S. Qvarfordt, A. Ö. Sysoev, H. Höglander, J. Walve, E. Schagerström, J. Eklöf, and A. M. Karlson. 2021. Long-term changes in trophic ecology of blue mussels in a rapidly changing ecosystem. Limnology and Oceanography 66:694–710.

Lüdecke, D., M. S. Ben-Shachar, I. Patil, P. Waggoner, and D. Makowski. 2021. performance: An R package for assessment, comparison and testing of statistical models. Journal of open source software 6.

Lyons, J. E., B. Winn, T. Keyes, and K. S. Kalasz. 2018. Post-breeding migration and connectivity of red knots in the Western Atlantic. The Journal of Wildlife Management 82:383–396.

Manning, L. M., C. H. Peterson, and M. J. Bishop. 2014. Dominant macrobenthic populations experience sustained impacts from annual disposal of fine sediments on sandy beaches. Marine Ecology Progress Series 508:1–15.

Mariotti, G. 2021. Self-organization of coastal barrier systems during the Holocene. Journal of Geophysical Research: Earth Surface 126:e2020JF005867.

Mariotti, G., and C. J. Hein. 2022. Lag in response of coastal barrier-island retreat to sea-level rise. Nature Geoscience 15:633–638.

Mazerolle, M. 2023. AICcmodavg: model selection and multimodel inference based on (Q) AIC (c). R package version 2.3-2. 2023.

Morrison, R., B. Harrington, and L. Leddy. 1980. Migration routes and stopover areas of North American Red Knot Calidris canutus wintering in South America. Wader Study Group Bulletin 28:28.

Murchison, C. R., Y. Zharikov, and E. Nol. 2016. Human Activity and Habitat Characteristics Influence Shorebird Habitat Use and Behavior at a Vancouver Island Migratory Stopover Site. Environmental Management 58:386–398.

National Oceanic and Atmospheric Administration (NOAA). 2025. NOAA Tides and Currents. NOAA Tides & Currents. <https://tidesandcurrents.noaa.gov/>. Accessed 7 Aug 2025.

Nienhuis, J. H., and J. Lorenzo-Trueba. 2019. Can barrier islands survive sea-level rise? Quantifying the relative role of tidal inlets and overwash deposition. Geophysical research letters 46:14613–14621.

Niles, L. J., J. Burger, R. R. Porter, A. D. Dey, C. D. T. Minton, P. M. Gonzalez, A. J. Baker, J. W. Fox, and C. Gordon. 2010. First results using light level geolocators to track Red Knots in the Western Hemisphere show rapid and long intercontinental flights and new details of migration pathways. 8.

Peterson, C. H., M. J. Bishop, L. M. D'Anna, and G. A. Johnson. 2014. Multi-year persistence of beach habitat degradation from nourishment using coarse shelly sediments. Science of the Total Environment 487:481–492.

R Core Team. 2024. R: A Language and Environment for Statistical Computing. R Foundation for Statistical Computing, Vienna, Austria. <https://www.R-project.org/>.

Raff, J. L., J. L. Shawler, D. J. Ciarletta, E. A. Hein, J. Lorenzo-Trueba, and C. J. Hein. 2018. Insights into barrier-island stability derived from transgressive/regressive state changes of Parramore Island, Virginia. Marine Geology 403:1–19.

Reeves, I. R. B., L. J. Moore, A. B. Murray, K. A. Anarde, and E. B. Goldstein. 2021. Dune Dynamics Drive Discontinuous Barrier Retreat. Geophysical Research Letters 48.

Robbins, M. G., J. L. Shawler, and C. J. Hein. 2022. Contribution of longshore sand exchanges to mesoscale barrier-island behavior: Insights from the Virginia Barrier Islands, US East Coast. Geomorphology 403:108163.

Robinson, R. A., H. Q. Crick, J. A. Learmonth, I. M. Maclean, C. D. Thomas, F. Bairlein, M. C. Forchhammer, C. M. Francis, J. A. Gill, and B. J. Godley. 2009. Travelling through a warming world: climate change and migratory species. Endangered species research 7:87–99.

Rosenberg, K. V., A. M. Dokter, P. J. Blancher, J. R. Sauer, A. C. Smith, P. A. Smith, J. C. Stanton, A. Panjabi, L. Helft, M. Parr, and P. P. Marra. 2019. Decline of the North American avifauna. Science 366:120–124.

Rzepecki, L. M., K. M. Hansen, and J. H. Waite. 1992. Characterization of a cystine-rich polyphenolic protein family from the blue mussel Mytilus edulis L. The Biological Bulletin 183:123–137.

Seuront, L., K. R. Nicastro, G. I. Zardi, and E. Goberville. 2019. Decreased thermal tolerance under recurrent heat stress conditions explains summer mass mortality of the blue mussel Mytilus edulis. Scientific Reports 9:17498.

Shipley, B. 2009. Confirmatory path analysis in a generalized multilevel context. Ecology 90:363–368.

Smith, P. A., A. C. Smith, B. Andres, C. M. Francis, B. Harrington, C. Friis, R. I. G. Morrison, J. Paquet, B. Winn, and S. Brown. 2023. Accelerating declines of North America's shorebirds signal the need for urgent conservation action. Ornithological Applications 125:duad003.

Sweet, W. V., B. D. Hamlington, R. E. Kopp, C. P. Weaver, P. L. Barnard, D. Bekaert, W. Brooks, M. Craghan, G. Dusek, T. Frederikse, G. Garner, A. S. Genz, J. P. Krasting, E. Larour, D. Marcy, J. J. Marra, J. Obeysekera, M. Osler, M. Pendleton, D. Roman, L. Schmied, W. Veatch, K. D. White, and C. Zuzak. 2022. Global and Regional Sea Level Rise Scenarios for the United States: Updated Mean Projections and Extreme Water Level Probabilities Along U.S. Coastlines. Technical Report, National Oceanic and Atmospheric Administration.

Tassone, S. J., and M. L. Pace. 2024. Increased frequency of sediment heatwaves in a Virginia seagrass meadow. Estuaries and Coasts 47:656–669.

Tomkovich, P. S. 1992. An analysis of the geographic variability in knots Calidris canutus based on museum skins. Wader Study Group 64 (suppl):17–23.

Tonelli, B. A., C. Youngflesh, T. Cox, M. H. Neate-Clegg, E. B. Cohen, and M. W. Tingley. 2024. Spatial nonstationarity in phenological responses of Nearctic birds to climate variability. Ecology Letters 27:e14526.

U.S. Department of Agriculture (USDA). 2023. Imagery Catalogs | Farm Production and Conservation Business Center. Geospatial Services. <https://www.fpacbc.usda.gov/geospatial-services/customer-services/imagery-catalogs>. Accessed 7 Aug 2025.

UVA. 2022. Virginia Coast Reserve LTER Annual Report. University of Virginia, Charlottesville, VA, USA.

Virginia Geographic Information Network's (VGIN). 2023. Orthoimagery. Orthoimagery. <https://vgin.vdem.virginia.gov/pages/orthoimagery>. Accessed 7 Aug 2025.

Waldeck, P., and K. Larsson. 2013. Effects of winter water temperature on mass loss in Baltic blue mussels: Implications for foraging sea ducks. Journal of Experimental Marine Biology and Ecology 444:24–30.

Watts, B. D., and B. R. Truitt. 2015. Spring migration of red knots along the Virginia barrier islands: Virginia Red Knots. The Journal of Wildlife Management 79:288–295.

Wei, T., V. Simko, M. Levy, Y. Xie, Y. Jin, and J. Zemla. 2017. Package 'corrplot.' Statistician 56:e24.

Wolner, C. W. V., L. J. Moore, D. R. Young, S. T. Brantley, S. N. Bissett, and R. A. McBride. 2013. Ecomorphodynamic feedbacks and barrier island response to disturbance: Insights from the Virginia Barrier Islands, Mid-Atlantic Bight, USA. Geomorphology 199:115–128.

Yau, K. K., K. Wang, and A. H. Lee. 2003. Zero-inflated negative binomial mixed regression modeling of over-dispersed count data with extra zeros. Biometrical Journal: journal of mathematical methods in biosciences 45:437–452.

Zhang, K., B. C. Douglas, and S. P. Leatherman. 2001. Beach erosion potential for severe nor'easters. Journal of Coastal Research 309–321.

Zhang, S.-D., Z. Ma, C.-Y. Choi, H.-B. Peng, Q.-Q. Bai, W.-L. Liu, K. Tan, D. S. Melville, P. He, Y.-C. Chan, J. A. Van Gils, and T. Piersma. 2018. Persistent use of a shorebird staging site in the Yellow Sea despite severe declines in food resources implies a lack of alternatives. Bird Conservation International 28:534–548.

Zinnert, J. C., S. M. Via, B. P. Nettleton, P. A. Tuley, L. J. Moore, and J. A. Stallins. 2019. Connectivity in coastal systems: Barrier island vegetation influences upland migration in a changing climate. Global Change Biology 25:2419–2430.

Zurell, D., C. Graham, L. Gallien, W. Thuiller, and N. Zimmermann. 2018. Long-distance migratory birds threatened by multiple independent risks from global change. Nat Clim Chang 8: 992–996.

TABLES

Table 1. Distributions used to fit component models in piecewise structural equation models (SEMs) investigating direct and indirect drivers of red knot (*Calridris canutus rufa*) and invertebrate prey dynamics in the Virginia barrier island system during spring migration (May 21 – 28, 2009 – 2023). Continuous response variables were modeled with Gaussian distribution (identity-link), while count data were modeled with negative binomial distributions (log link). Zero-inflated negative binomial models accounted for excess zeros in invertebrate density components of the red knot SEM and in crustacean, coquina clam (*Donax variabilis*), and miscellaneous prey density responses (see Table S2). Invertebrate richness, exhibiting underdispersed, was modeled with a Generalized Poisson distribution (log link). Red knot presence was modeled with a binomial distribution (logit link).

Response	***Predictors***	***Distribution (link function)***
Red Knot SEM		
Beach width	~ island length + shoreline change-rate + island migration + distance to inlet + storminess x NAO	Gaussian (identity-link)
Island width	~ island length + shoreline change-rate + island migration + distance to inlet + storminess x NAO	Gaussian (identity-link)
Invertebrate richness	~ water temp + substrate + tide + beach width + distance to inlet + storminess x NAO	Generalized Poisson (log-link)

Invertebrate density	~ water temp + substrate + tide + beach width + distance to inlet + storminess x NAO	Zero-inflated negative binomial (log-link)
Sympatric abundance	~ invertebrate richness + invertebrate abundance + substrate + tide + beach width + island width + NAO	Negative binomial (log-link)
Red knot abundance	~ sympatric abundance + invertebrate richness + invertebrate abundance + substrate + tide + beach width + island width + NAO	Negative binomial (log-link)
Red knot presence	~ sympatric abundance + invertebrate richness + invertebrate abundance + substrate + tide + beach width + island width	Binomial (logit-link)
Invertebrate SEM		
Beach width	~ island length + shoreline change-rate + island migration + distance to inlet + storminess x NAO	Gaussian (identity-link)
Island width	~ island length + shoreline change-rate + island migration + distance to inlet + storminess x NAO	Gaussian (identity-link)
Crustacean density	~ water temp + substrate + tide + beach width + distance to inlet + storminess x NAO	Zero-inflated negative binomial (log-link)
Coquina clam density	~ water temp + substrate + tide + beach width + distance to inlet + storminess x NAO	Zero-inflated negative binomial (log-link)

Blue mussel density	~ water temp + substrate + tide + beach width + distance to inlet + storminess x NAO	Negative binomial (log-link)
Miscellaneous prey density	~ water temp + substrate + tide + beach width + distance to inlet + storminess x NAO	Zero-inflated negative binomial (log-link)

Table 2. Unstandardized estimates (B), standardized coefficients (β), standard error (SE), and p-values (*p*) from piecewise structural equation models (SEM; Figure 3) investigating the direct and indirect effects of habitat, climate, and geomorphic drivers on red knot (*Calidris canutus rufa*) presence, abundance, and invertebrate prey densities, in the Virginia barrier island system during spring migration (May 21 – 28, 2009–2023). R^2_M = marginal (fixed effects); R^2_C = conditional (fixed + random efftects).

Response **Predictor**	**Unstandardized Estimate (B)**	**Standardized Coefficient (β)**	**Standard Error (SE)**	***p***
RED KNOT SEM				
Red Knot Presence			***R^2_M = 0.13; R^2_C = 0.31***	
Sympatric abundance	0.01	0.25	0.001	< 0.0001
Invertebrate richness	0.32	0.17	0.08	0.0001
Substrate	1.11	0.13	0.32	0.0005
Red Knot Abundance			***R^2_M = 0.14; R^2_C = 0.52***	
Sympatric abundance	0.01	0.06	0.003	0.005
Invertebrate richness	0.56	0.07	0.16	0.0005
Sympatric Species Abundance			***R^2_M = 0.04; R^2_C = 0.39***	
Invertebrate density	0.00001	0.07	0	< 0.0001
Substrate	0.40	0.03	0.16	0.01
Invertebrate Richness			***R^2_M = 0.02; R^2_C = 0.06***	
Substrate	0.51	*	0.05	< 0.0001
Tide	0.16	*	0.03	< 0.0001

Island width	0.08	*	0.04	0.03
Invertebrate Density			***$R^2_M = 0.29$; $R^2_C = 1.00$***	
Substrate	1.52	0.15	0.17	< 0.0001
Beach width	-0.26	-0.05	0.09	0.004
Island width	0.50	0.09	0.11	< 0.0001
Distance to inlet	0.32	0.06	0.11	0.003
Island Width			***$R^2_M = 0.20$; $R^2_C = 0.46$***	
Substrate	-0.21	-0.11	0.05	< 0.0001
Island length	0.30	0.31	0.11	0.007
Shoreline change rate	-0.34	-0.34	0.13	0.007
Distance to inlet	-0.14	-0.14	0.02	< 0.0001
Storminess	0.04	0.04	0.03	0.1
NAO	0.10	0.10	0.03	0.0003
Storminess x NAO	-0.16	-0.06	0.08	0.04
Beach Width			***$R^2_M = 0.06$; $R^2_C = 0.25$***	
Distance to inlet	-0.21	-0.20	0.03	< 0.0001
Storminess	0.15	0.15	0.07	0.04
NAO	0.16	0.16	0.07	0.03
Storminess x NAO	-0.57	-0.21	0.23	0.01
INVERTEBRATE SEM				
Crustacean Density			***$R^2_M = 0.76$; $R^2_C = 1.00$***	
Substrate	1.55	0.12	0.18	< 0.0001
Beach width	-0.28	-0.04	0.09	0.003

Island width	0.29	0.04	0.12	0.02
Distance to inlet	0.30	0.04	0.09	0.0009
Island migration	-0.56	-0.08	0.22	0.01
Coquina Clam Density			***$R^2_M = 0.55$; $R^2_C = 1.00$***	
Substrate	-1.01	-0.08	0.29	0.0006
Island width	0.44	0.07	0.15	0.004
Island migration	-0.73	-0.11	0.32	0.02
Blue Mussel Density			***$R^2_M = 0.49$; $R^2_C = 0.96$***	
Substrate	14.80	0.21	2.56	< 0.0001
Water temperature	10.05	0.28	3.30	0.002
Shoreline change rate	6.36	0.17	2.25	0.005
Miscellaneous Prey Density			***$R^2_M = 0.03$; $R^2_C = 1.00$***	
Substrate	0.84	0.06	0.23	0.0003
Island Width			***$R^2_M = 0.20$; $R^2_C = 0.46$***	
Substrate	-0.21	-0.11	0.05	< 0.0001
Island length	0.30	0.31	0.11	0.007
Shoreline change rate	-0.34	-0.34	0.13	0.007
Distance to inlet	-0.14	-0.14	0.02	< 0.0001
Storminess	0.04	0.04	0.03	0.1
NAO	0.10	0.10	0.03	0.0003
Storminess x NAO	-0.16	-0.06	0.08	0.04
Beach Width			***$R^2_M = 0.06$; $R^2_C = 0.25$***	
Distance to inlet	-0.21	-0.20	0.03	< 0.0001

Storminess	0.15	0.15	0.07	0.04
NAO	0.16	0.16	0.07	0.03
Storminess x NAO	-0.57	-0.21	0.23	0.01

Table 3. Mean (± SD) island and beach width for individual barrier islands and the overall study system from Assawoman to Fisherman Island for 2007 and 2023. Kendall's tau (τ) and p-values indicate the direction and significance of temporal trends. Percent change represents the relative difference between 2007 and 2023, and total change provides a relative index of morphometric change across all measured features. Statistical significance was set at $p < 0.05$.

	2007	**2023**	**τ**	***p***	**% Change**	**Total Change**
Assawoman						1.62
Mean Island Width ± SD	0.19 ± 0.09	0.21 ± 0.07	0.42	0.06	6%	
Mean Beach Width ± SD	0.16 ± 0.1	0.1 ± 0.04	-0.27	0.24	-35%	
Metompkin						0.74
Mean Island Width ± SD	0.22 ± 0.11	0.2 ± 0.1	0.18	0.45	-7%	
Mean Beach Width ± SD	0.15 ± 0.05	0.11 ± 0.06	0.09	0.73	-25%	
Cedar						1.13
Mean Island Width ± SD	0.24 ± 0.16	0.18 ± 0.13	-0.52	0.02	-25%	
Mean Beach Width ± SD	0.19 ± 0.12	0.09 ± 0.1	-0.52	0.02	-53%	
Parramore						1.15
Mean Island Width ± SD	0.45 ± 0.32	0.36 ± 0.27	-0.48	0.03	-20%	
Mean Beach Width ± SD	0.1 ± 0.07	0.05 ± 0.07	-0.21	0.37	-49%	
Hog						0.84
Mean Island Width ± SD	0.65 ± 0.4	0.58 ± 0.2	-0.48	0.03	-11%	
Mean Beach Width ± SD	0.08 ± 0.07	0.07 ± 0.1	-0.15	0.54	-18%	

Cobb					1.72
Mean Island Width ± SD	0.25 ± 0.12	0.16 ± 0.17	-0.67	0.003	-34%
Mean Beach Width ± SD	0.09 ± 0.07	0.09 ± 0.09	0.24	0.30	9%
Wreck					2.07
Mean Island Width ± SD	0.32 ± 0.24	0.26 ± 0.13	-0.58	0.01	-21%
Mean Beach Width ± SD	0.17 ± 0.09	0.05 ± 0.05	-0.73	0.001	-72%
Ship Shoal					4.04
Mean Island Width ± SD	0.26 ± 0.13	0.33 ± 0.16	0.39	0.09	26%
Mean Beach Width ± SD	0.22 ± 0.15	0.05 ± 0.05	-0.52	0.02	-75%
Myrtle/Mink					1.14
Mean Island Width ± SD	0.11 ± 0.06	0.09 ± 0.05	0.21	0.37	-16%
Mean Beach Width ± SD	0.1 ± 0.05	0.05 ± 0.04	0.09	0.73	-45%
Smith					0.21
Mean Island Width ± SD	0.22 ± 0.19	0.17 ± 0.15	-0.30	0.19	-22%
Mean Beach Width ± SD	0.06 ± 0.04	0.04 ± 0.03	-0.06	0.84	-27%
Fisherman					1.82
Mean Island Width ± SD	0.66 ± 0.27	0.67 ± 0.34	0.21	0.37	2%
Mean Beach Width ± SD	0.14 ± 0.09	0.08 ± 0.05	-0.21	0.37	-44%
Whole System					
Mean Island Width ± SD	0.34 ± 0.29	0.3 ± 0.25	-0.24	0.30	-11%
Mean Beach Width ± SD	0.12 ± 0.09	0.07 ± 0.07	-0.36	0.11	-42%

FIGURES

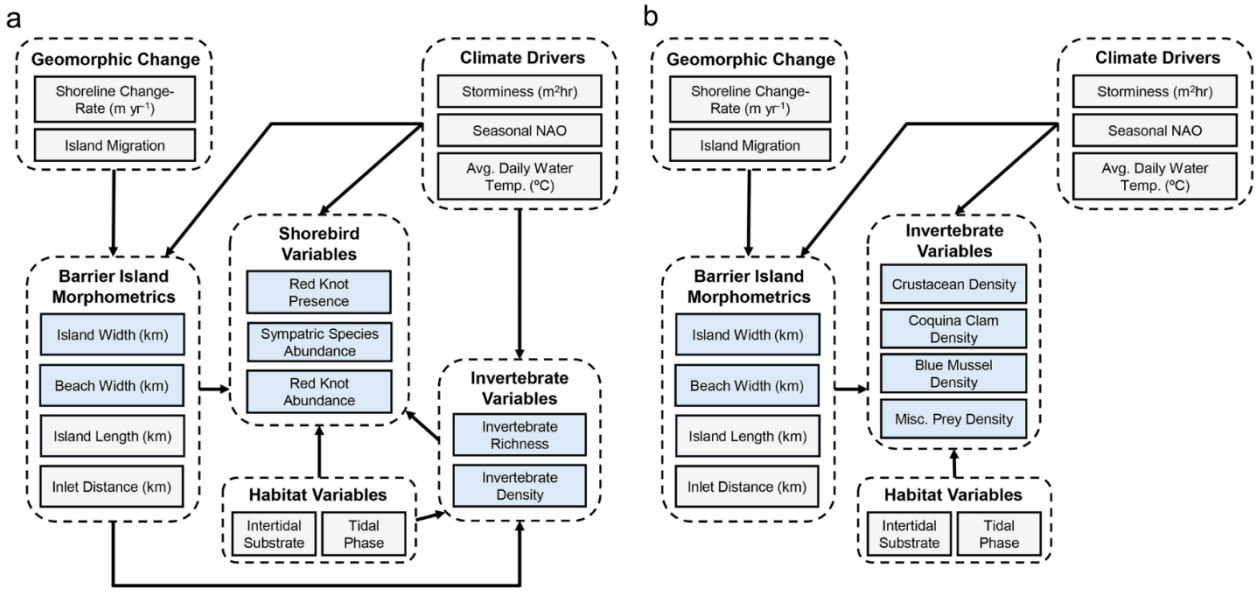

Figure 1. Conceptual diagram of hypothesized relationships influencing (a) red knot (*Calidris canutus rufa*) presence and abundance and (b) densities of crustaceans, coquina clams (*Donax variabilis*), blue mussels (*Mytilus edulis*), and miscellaneous prey, tested using piecewise structural equation modeling (SEM). Networks were informed by prior research on shorebird foraging ecology, geomorphology, and climate divers in the Virginia barrier island system. Units of measurement for continuous variables are shown in parentheses. Dashed lines indicate variable groupings. Blue boxes indicate response variables in component models within the piecewise SEMs.

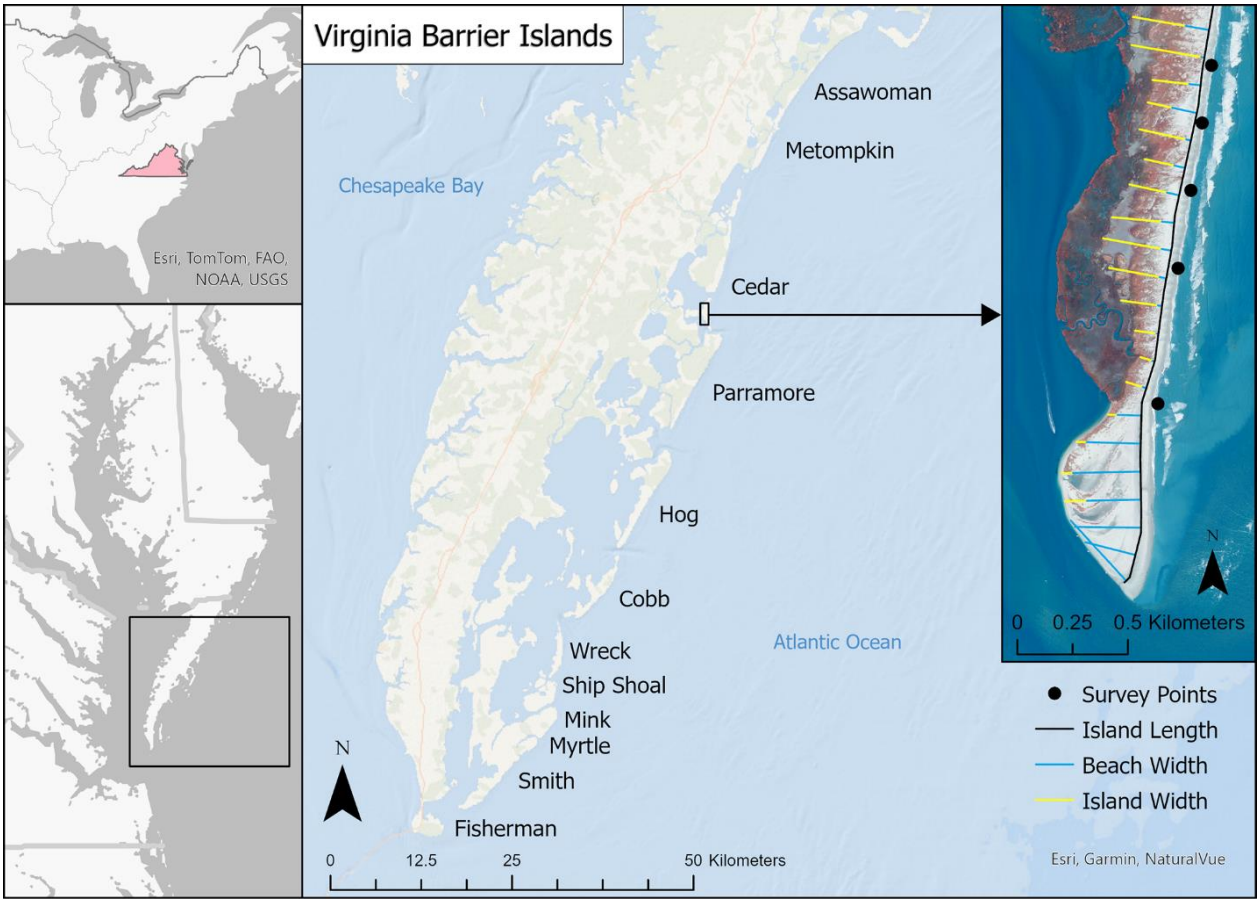

Figure 2. Study area within the Virginia barrier island system on the Eastern Shore of Virginia. Data on red knots (*Calidris canutus rufa*) and invertebrate prey were collected on 12 barrier islands during spring migration (May 21 – 28) from 2009–2023. the inset map (right) shows examples of random survey points (black dots) and island measurements (island width = yellow lines, beach width = blue lines, and island length = black line) used to assess morphometric change over time, based on 2023 aerial imagery from the U.S. Department of Agriculture's National Agriculture Imagery Program (NAIP).

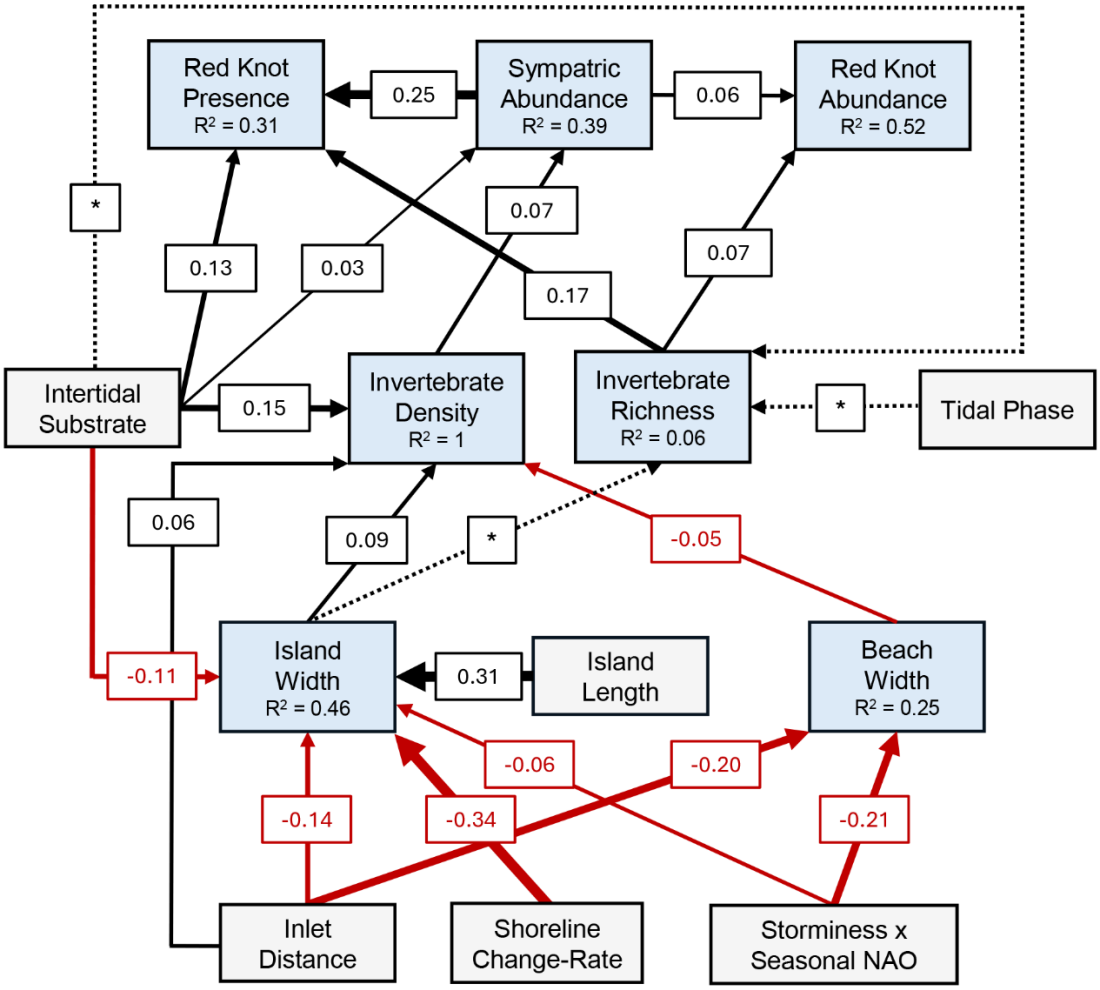

Figure 3. Final causal network for the red knot (*Calidris canutus rufa*) piecewise structural equation model showing significant paths ($p < 0.05$) influencing red knot presence and abundance during spring migration (May 21–28, 2009–2023) in the Virginia barrier island system. Black and red arrows denote positive and negative relationships, with widths scaled by standard coefficients in text boxes. Missing coefficients for the invertebrate richness component model are marked with * and dashed arrows. Blue boxes show response variables with conditional R^2 values. Correlated errors are omitted for clarity. The model includes an interaction between storminess and North Atlantic Oscillation (NAO).

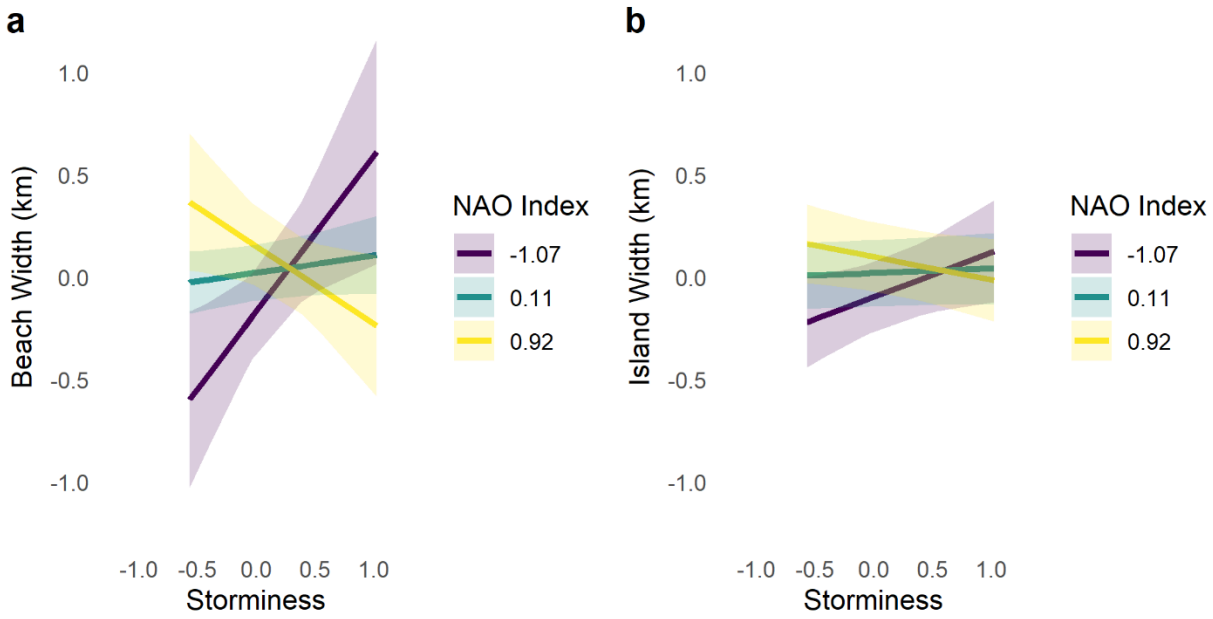

Figure 4. Interactive effects of storminess and the North Atlantic Oscillation (NAO) from final component models in piecewise structural equation models (SEM). Plots show the effects of storminess on (a) beach width and (b) island width across different NAO phases. Lines represent predicted marginal effects of storminess and NAO while holding other variables constant, with shaded areas showing 95% confidence intervals.

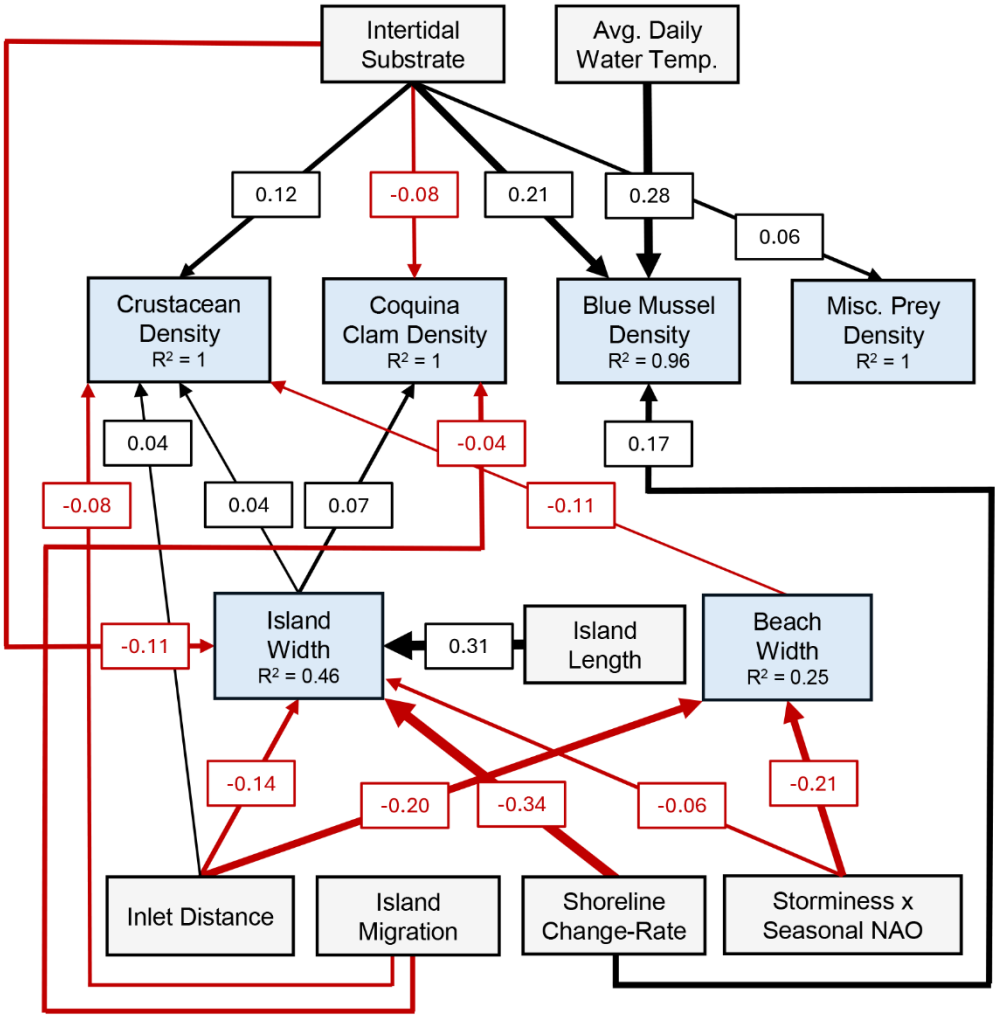

Figure 5. Final causal network for invertebrate piecewise structural equation model showing all significant paths ($p < 0.05$) influencing densities of crustaceans, coquina clams (*Donax variabilis*), blue mussels (*Mytilus edulis*), and miscellaneous (misc.) prey during spring migration (May 21 – 28, 2009 – 2023) in the Virginia barrier island system. Black and red arrows denote positive and negative relationships, with widths scaled by standard coefficients in text boxes. Blue boxes show response variables with conditional R^2 values. Correlated errors are omitted for clarity. The model includes an interaction between storminess and North Atlantic Oscillation (NAO).

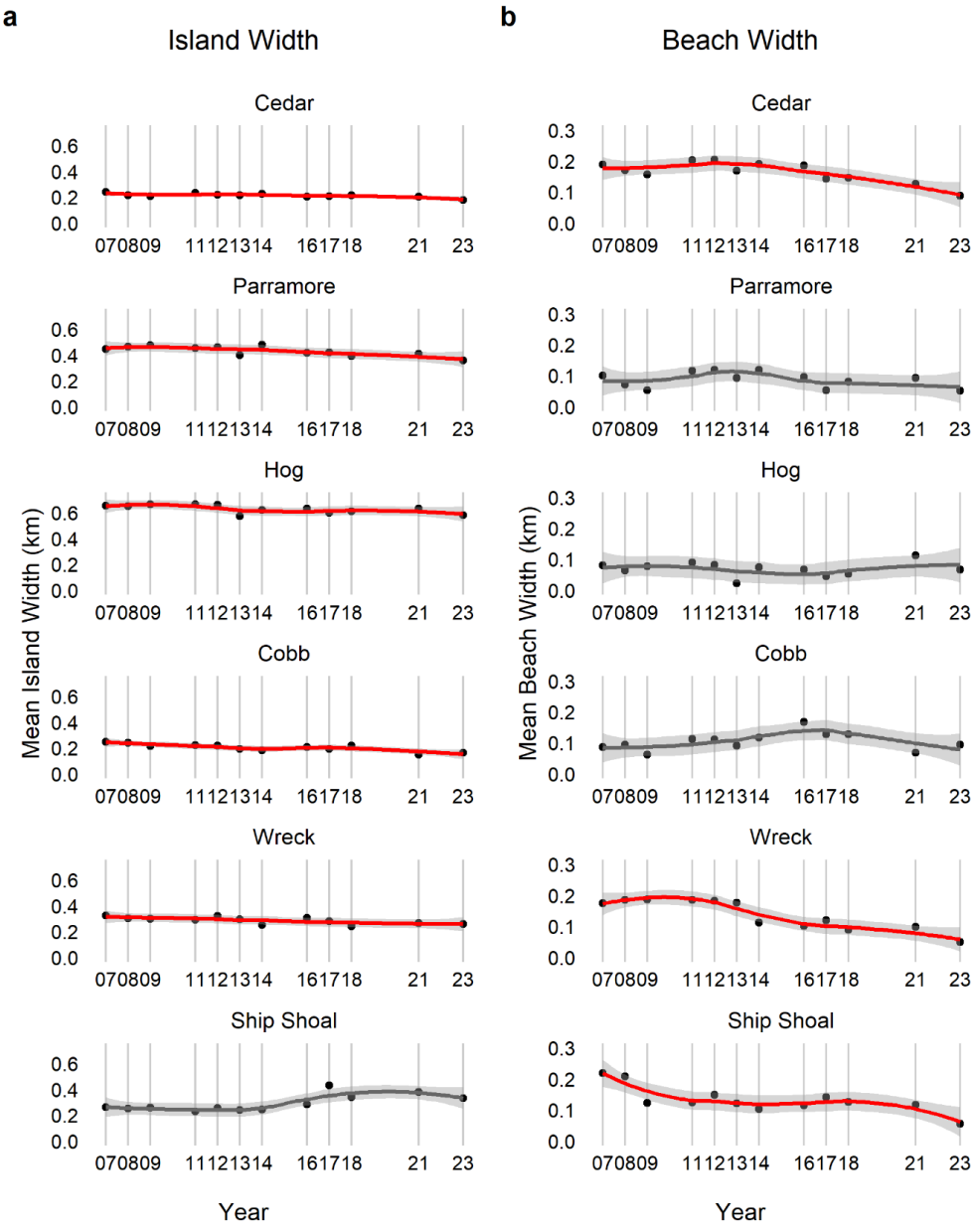

Figure 6. Trends in barrier island morphometrics from 2007–2023 for (a) mean island width (km) and (b) mean beach width (km) on barrier islands with significant morphometric change in the Virginia barrier island system. Shaded ribbons represent 95% confidence intervals from loess-smoothing lines. Red lines denote statistically significant trends based on Kendall's tau correlation analyses. Note the difference in scales between panels.

CHAPTER 4

Conclusions

NOVEL FINDINGS

My thesis advances our understanding of migratory shorebird ecology in the Virginia barrier island system, one of the few predominantly undeveloped coastal systems where climate is the primary driver of ecosystem change. First, I documented diverse habitat use and diet across the intertidal landscape by three focal migratory bird species red knots (*Calidris canutus rufa*), dunlin (*Calidris alpina*) and semipalmated sandpiper (*Calidris pusilla*) during northward spring migration. Second, I quantified how climate-driven geomorphic and environmental processes indirectly shape foraging conditions for red knots via bottom-up effects on preferred invertebrate prey. My work highlights the critical role of mudflats as foraging habitat for multiple species and reveal broader than expected behavioral and dietary flexibility in red knots. I provided the first DNA-based evidence of biofilm consumption by shorebirds in the mid-Atlantic, suggesting biofilm is an important spring migration resource for small-bodied shorebirds such as semipalmated sandpipers. My system-level analysis show that red knot foraging is influenced not only by prey and site-specific habitat features, but also by indirect effects of shoreline change, barrier island morphology, and storminess on prey communities. These bottom-up effects extend to other abundant foraging species on barrier islands, including dunlin, sanderling (*Calidris alba*), semipalmated sandpipers, and ruddy turnstones (*Arenaria interpres*). This is the first study to link climate and geomorphic dynamics to changes in invertebrate prey densities and shorebird occurrence in this system, contributing to our understanding of cascading effects of ecosystem state change in coastal environments.

MANAGEMENT IMPLICATIONS

My findings underscore the importance of conserving a mosaic of intertidal habitats, including mudflats, sand, and peat substrates, to support shorebird populations with diverse habitat and dietary requirements. Long-term resilience of red knots and other migratory species will require limiting artificial shoreline stabilization to maintain natural barrier island dynamics under accelerating sea-level rise and altered storm regimes. Future projections for the Virginia barrier island system are alarming, and my work could serve as a catalyst for finding change thresholds under changing climate conditions. For example, predicted accelerated island migration, a main driver of backbarrier marsh loss, will reduce marsh extent and contributes to diminished ecosystem resilience (Deaton et al. 2017, Mariotti and Hein 2022). In addition, expected rapid island narrowing increases the risk of island breaching (Nienhuis and Lorenzo-Trueba 2019), which further accelerates marsh loss. Hands-off conservation alone is insufficient to offset the habitat degradation from sea-level rise and coastal development, and human intervention is becoming increasingly necessary to maintain ecosystem function (Hobbs et al. 2011).

One promising proposal in the Virginia barrier island system involves an interdisciplinary, science-based engineering approach to develop a backbarrier marsh system on Cedar Island to enhance island resilience (Hein et al. 2021). While this may offer only a temporary buffer against long-term, pervasive climate change, our findings suggest it could benefit migratory shorebirds and their invertebrate prey by slowing the rate of shoreline retreat and island narrowing. Moreover, if successful, the creation and enhancement of backbarrier marshes could perpetuate and expand peat bank foraging habitat as the island will ultimately migrate over the marsh platform. The long-term persistence of peat banks would have positive

effects on both invertebrate communities, such as crustaceans and blue mussels, and the migratory shorebirds that depend on them.

Another complementary management approach could be the design and construction of intertidal flats to offset declining intertidal foraging area due to sea-level rise and storm-driven erosion. Although shorebirds often use human-created and -modified wetlands (e.g., agriculture, aquaculture, and reclamations sites), particularly in heavily developed coastal areas, the foraging value of these habitats varies widely (Jackson et al. 2020), and even conservation-focused engineered sites show mixed success in supporting diverse shorebird communities (Almeida et al. 2020, Wang et al. 2022). Drawing on decades of intervention projects in Japan, Kuwae et al. (2021) proposed a biofilm-centered approach to shorebird population recovery by designing intertidal flats that meet seven physical criteria to enhance foraging conditions. A biofilm-centered restoration approach was recommended as biofilm is a foundational component of estuarine ecosystems, contributing to photosynthetic activity, carbon sequestration, sediment stabilization, and provisioning for both invertebrates and shorebirds (Underwood and Kromkamp 1999, Saint-Béat et al. 2013, Serôdio et al. 2020). Thus, designing intertidal habitats to enhance biofilm abundance and quality offers a promising strategy to achieve both conservation and ecosystem service restoration goals. Furthermore, because the abundance of small-bodied sandpipers is closely linked to that of biofilm (Jiménez et al. 2015, Drever et al. 2024), their foraging behavior and abundance on intertidal flats can serve as effective ways to monitor restoration success (Kuwae et al. 2021). These adaptive strategies may be especially valuable in regions such as the Chesapeake Bay, where rapid wetland loss is reducing nesting and foraging habitat for waterbirds and heightening the risk of climate change impacts for surrounding coastal communities (Erwin et al. 2004, Rezaie et al. 2021).

FUTURE RESEARCH DIRECTIONS

I recommend that continued work in the Virginia barrier island system should investigate dietary flexibility across habitats and species. For example, we know little about the diets and prey selection patterns of the currently abundant dunlin and semipalmated sandpipers foraging on barrier island sand and peat substrates. Continued diet studies with larger sample sizes will improve confidence in prey use patterns, clarify interannual variability in prey choice, and shed light on how shorebirds respond to shifts in foraging conditions across the coastal landscape. Additionally, incorporating invertebrate biomass alongside abundance into selection models may provide a broader and more accurate picture of shorebird dietary preferences. Future work should also assess the degree of biofilm reliance during spring migration and examine how its abundance and quality vary with environmental conditions. Long-term monitoring or shorebirds, prey, and geomorphic conditions will be essential for detecting ecological responses to climate-driven changes and should be continued. Finally, future modeling efforts could extend our piecewise structural equation modeling approach using a Bayesian structural equation framework to predict changes in foraging habitat availability under accelerating climate change.

LITERATURE CITED

Almeida, B. A., E. Sebastián-González, L. dos Anjos, and A. J. Green. 2020. Comparing the diversity and composition of waterbird functional traits between natural, restored, and artificial wetlands. Freshwater Biology 65:2196–2210.

Deaton, C. D., C. J. Hein, and M. L. Kirwan. 2017. Barrier island migration dominates ecogeomorphic feedbacks and drives salt marsh loss along the Virginia Atlantic Coast, USA. Geology 45:123–126.

Drever, M. C., M. J. Mogle, T. J. Douglas, S. A. Flemming, D. J. Hamilton, J. D. Liefer, and R. W. Elner. 2024. Shorebird Abundance is Associated with Nutritional Quality of Intertidal Biofilm on the Fraser River Estuary. Estuaries and Coasts 47:519–534.

Erwin, R. M., G. M. Sanders, and D. J. Prosser. 2004. Changes in lagoonal marsh morphology at selected northeastern Atlantic coast sites of significance to migratory waterbirds. Wetlands 24:891–903.

Hein, C. J., M. S. Fenster, K. B. Gedan, J. R. Tabar, E. A. Hein, and T. DeMunda. 2021. Leveraging the interdependencies between barrier islands and backbarrier saltmarshes to enhance resilience to sea-level rise. Frontiers in Marine Science 8:721904.

Hobbs, R. J., L. M. Hallett, P. R. Ehrlich, and H. A. Mooney. 2011. Intervention ecology: applying ecological science in the twenty-first century. BioScience 61:442–450.

Jackson, M. V., C.-Y. Choi, T. Amano, S. M. Estrella, W. Lei, N. Moores, T. Mundkur, D. I. Rogers, and R. A. Fuller. 2020. Navigating coasts of concrete: Pervasive use of artificial habitats by shorebirds in the Asia-Pacific. Biological Conservation 247:108591.

Jiménez, A., R. W. Elner, C. Favaro, K. Rickards, and R. C. Ydenberg. 2015. Intertidal biofilm distribution underpins differential tide-following behavior of two sandpiper species

(Calidris mauri and Calidris alpina) during northward migration. Estuarine, Coastal and Shelf Science 155:8–16.

Kuwae, T., R. W. Elner, T. Amano, and M. C. Drever. 2021. Seven ecological and technical attributes for biofilm-based recovery of shorebird populations in intertidal flat ecosystems. Ecological Solutions and Evidence 2.

Mariotti, G., and C. J. Hein. 2022. Lag in response of coastal barrier-island retreat to sea-level rise. Nature Geoscience 15:633–638.

Nienhuis, J. H., and J. Lorenzo-Trueba. 2019. Can barrier islands survive sea-level rise? Quantifying the relative role of tidal inlets and overwash deposition. Geophysical research letters 46:14613–14621.

Rezaie, A. M., C. M. Ferreira, M. Walls, and Z. Chu. 2021. Quantifying the impacts of storm surge, sea level rise, and potential reduction and changes in wetlands in coastal areas of the Chesapeake Bay region. Natural Hazards Review 22:04021044.

Saint-Béat, B., C. Dupuy, P. Bocher, J. Chalumeau, M. De Crignis, C. Fontaine, K. Guizien, J. Lavaud, S. Lefebvre, and H. Montanié. 2013. Key features of intertidal food webs that support migratory shorebirds. PLoS One 8:e76739.

Serôdio, J., D. M. Paterson, V. Méléder, and W. Vyverman. 2020. Advances and challenges in microphytobenthos research: From cell biology to coastal ecosystem function. Frontiers in Marine Science 7:608729.

Underwood, G. J. C., and J. Kromkamp. 1999. Primary production by phytoplankton and microphytobenthos in estuaries. Estuaries 29:93.

Wang, X., X. Li, X. Ren, M. V. Jackson, R. A. Fuller, D. S. Melville, T. Amano, and Z. Ma. 2022. Effects of anthropogenic landscapes on population maintenance of waterbirds. Conservation Biology 36:e13808.

APPENDICES

Chapter 2:

Diet and Prey Selection of Migratory Shorebirds on Mudflats in the Virginia Barrier Island and Lagoon System using Fecal DNA Metabarcoding

APPENDIX S.1

For 18S rDNA libraries, each 25 µL PCR reaction was mixed according to the Promega PCR Master Mix specifications (Promega catalog # M5133, Madison, WI) which included 12.5ul Master Mix, 0.5 µl of each primer, 1.0 µl of gDNA, and 10.5 µl DNase/RNase-free H2O. DNA was PCR amplified using the following conditions: initial denaturation at 94 °C for 3 minutes, followed by 35 cycles of 45 seconds at 94 °C, 1 minute at 57 °C, and 90 s at 72 °C, and a final elongation at 72 °C for 10 minutes. For 23S rDNA libraries, each 40 µL PCR reaction was mixed according to the Promega PCR Master Mix specifications (Promega catalog # M5133, Madison, WI) which included 12.5ul Master Mix, 0.5 µM of each primer, 1.0 µl of gDNA, and 10.5 µl DNase/RNase-free H2O. DNA was PCR amplified using the following conditions: initial denaturation at 94 °C for 3 minutes, followed by 40 cycles of 30 seconds at 94 °C, 45 seconds at 55 °C, and 1 minute at 72 °C, and a final elongation at 72 °C for 10 minutes.

To determine amplicon size and PCR efficiency, each reaction was visually inspected using a 2% agarose gel with 5µl of each sample as input. Amplicons were then cleaned by incubating amplicons with Exo1/SAP for 30 minutes at 37C following by inactivation at 95C for 5 minutes and stored at -20C. A second round of PCR was performed to complete the sequencing library construct, appending the final Illumina sequencing adapters and integrating sample-specific, dual index sequences (2 x 10bp). The indexing PCR included Promega Master mix, 0.5

µM of each primer and 2 µl of template DNA (cleaned amplicon from the first PCR reaction) and consisted of an initial denaturation of 95 °C for 3 minutes followed by 8 cycles of 95 °C for 30 sec, 55 °C for 30 seconds and 72 °C for 30 seconds. Final indexed amplicons from each sample were cleaned and normalized using mag-bind normalization. A 15µl aliquot of PCR amplicon was purified and normalized using Cytiva SpeedBead magnetic carboxylate modified particles (#45152105050250). Samples were then pooled together by adding 5µl of each normalized sample to the pool. Sample library pools were sent for sequencing on an Illumina MiSeq (San Diego, CA) at the Texas A&M Agrilife Genomics and Bioinformatics Sequencing Core facility using the v2 500-cycle kit (cat# MS-102-2003). Necessary quality control measures were performed at the sequencing center prior to sequencing.

SUPPLEMENTARY TABLES

Table S1. Shapiro-Wilke normality test statistic (W) and p-value (*p*) for shorebird habitat use and invertebrate prey metrics on sand, peat, and mudflat substrates during spring migration (May 14 - June 2, 2023 – 2024) in the Virginia barrier island system. Statistical significance was set at $p < 0.05$.

Variable	W	*p*
Total shorebird abundance	0.52	< 0.001
Shorebird species richness	0.96	< 0.001
C. alpina abundance	0.43	< 0.001
C. c. rufa abundance	0.26	< 0.001
C. pusilla abundance	0.20	< 0.001
Total invertebrate density	0.35	< 0.001
Crustacean density	0.25	< 0.001
Insect density	0.10	< 0.001
Bivalve density	0.30	< 0.001
Snail density	0.21	< 0.001
Worm density	0.41	< 0.001
Other organism density	0.15	< 0.001

Table S2. Abundance and species richness of shorebirds (order Charadriiformes) observed on sand, peat, and mudflat substrates during spring migration (May 14 - June 2, 2023-2024) in the Virginia barrier island system. (****) Indicates species of critical, (***) very high, (**) high, and (*) moderate conservation need as designated in the 2015 Virginia Wildlife Action Plan. FT = Federally Threatened under U.S. Endangered Species Act.

Species (Common Name)	Substrate	Total Count	Mean (per point)	SE (per point)
Calidris canutus rufa (red knot) FT ****	Sand	2585	14.69	3.97
Calidris alba (sanderling) *	Sand	1801	10.23	1.55
Calidris alpina (dunlin) *	Sand	637	3.62	1.17
Haematopus palliatus (American oystercatcher) ***	Sand	248	1.41	0.15
Charadrius semipalmatus (semipalmated plover)	Sand	204	1.16	0.19
Calidris pusilla (semipalmated sandpiper)	Sand	172	0.98	0.38
Tringa semipalmata (willet)	Sand	123	0.70	0.090
Charadrius melodus (piping plover) FT **	Sand	40	0.23	0.044
Pluvialis squatarola (black-bellied plover)*	Sand	35	0.20	0.043
Arenaria interpres (ruddy turnstone)	Sand	30	0.17	0.059
peep[1]	Sand	14	0.080	0.080
Calidris minutilla (least sandpiper)	Sand	5	0.028	0.023
Charadrius vociferus (killdeer)	Sand	1	0.006	0.006
TOTAL	**SAND**	**5895**	**33.49**	**4.61**
Calidris alpina (dunlin) *	Peat	3416	38.38	6.23
Calidris canutus rufa (red knot) *FT* ****	Peat	626	7.03	2.28
Calidris alba (sanderling) *	Peat	433	4.87	0.64
Calidris pusilla (semipalmated sandpiper)	Peat	370	4.16	1.96
Arenaria interpres (ruddy turnstone)	Peat	360	4.04	0.80
Haematopus palliatus (American oystercatcher) ***	Peat	118	1.33	0.21
Pluvialis squatarola (black-bellied plover)*	Peat	100	1.12	0.16
Charadrius semipalmatus (semipalmated plover)	Peat	90	1.01	0.22
Tringa semipalmata (willet)	Peat	61	0.69	0.12
Charadrius melodus (piping plover) FT **	Peat	24	0.27	0.08
Limnodromus spp. (dowitcher *spp*.) *[2]	Peat	19	0.21	0.213
peep[1]	Peat	3	0.034	0.034
Calidris minutilla (least sandpiper)	Peat	2	0.022	0.016
Tringa melanoleuca (greater yellowlegs)	Peat	1	0.011	0.011
TOTAL	**PEAT**	**5623**	**63.18**	**10.26**

Calidris alpina (dunlin) *	Mud	608	8.94	1.86
Pluvialis squatarola (black-bellied plover)*	Mud	300	4.41	1.33
Calidris pusilla (semipalmated sandpiper)	Mud	188	2.76	0.73
Calidris canutus rufa (red knot) *FT* ****	Mud	173	2.54	1.55
Arenaria interpres (ruddy turnstone)	Mud	111	1.63	0.75
Charadrius semipalmatus (semipalmated plover)	Mud	106	1.56	0.45
Tringa semipalmata (willet)	Mud	76	1.12	0.36
Limnodromus spp. (dowitcher *spp.*) *[2]	Mud	49	0.72	0.22
Calidris alba (sanderling) *	Mud	40	0.59	0.19
Numenius phaeopus (whimbrel) *	Mud	39	0.57	0.16
Haematopus palliatus (American oystercatcher) ***	Mud	31	0.46	0.13
Limosa fedoa (marbled godwit)*	Mud	11	0.16	0.071
Tringa melanoleuca (greater yellowlegs)	Mud	2	0.029	0.021
Calidris minutilla (least sandpiper)	Mud	1	0.015	0.015
Actitis macularius (spotted sandpiper)	Mud	1	0.015	0.015
TOTAL	**MUD**	**1736**	**25.53**	**4.05**
OVERALL		**13254**	**39.61**	**3.81**

[1]Small-bodied shorebirds that could not be identified to species were lumped under "peep".

[2]Limnodromus *spp*. (dowitchers) could not be distinguished in the field, but individuals were presumed to be *Limnodromus griseus* (short-billed dowitcher) based on regional occurrence patterns (Takekawa and Warnock 2020).

Table S6a. Diet composition of *Calidris alpina* (dunlin) during spring migration (May 14 - June 2, 2023 – 2024) in the Virginia barrier island system, determined using 18S markers. Diet is summarized by frequency of occurrence (FOO), weighted percent of occurrence (wPOO), and relative read abundance (RRA). Values represent averages across all fecal samples for *C. alpina* and are expressed as percentages. Taxonomic categories are presented as Phylum_Class_Order_Family_*Genus_species. "***Overall"*** indicates taxonomic category summary.

18S - TAXONOMIC CATEGORY	FOO	wPOO	RRA
INVERTEBRATES	***100.0***	***91.5***	***98.5***
Crustaceans	***78.9***	***41.1***	***39.3***
Arthropoda_Copepoda (Overall)	**10.5**	**2.2**	**1.7**
Arthropoda_Copepoda	10.53	2.19	1.66
Arthropoda_Malacostraca (Overall)	**73.7**	**37.5**	**35.6**
Arthropoda_Malacostraca_Peracarida (Overall)	**63.2**	**27.9**	**24.6**
Arthropoda_Malacostraca_Peracarida	36.84	8.03	4.11
Arthropoda_Malacostraca_Peracarida_Amphipoda (Overall)	**57.9**	**19.9**	**20.5**
Arthropoda_Malacostraca_Peracarida_Amphipoda	57.89	19.87	20.54
Arthropoda_Malacostraca_Decapoda (Overall)	**21.1**	**9.6**	**11.0**
Arthropoda_Malacostraca_Decapoda	21.05	5.70	7.80
Arthropoda_Malacostraca_Decapoda_Varunidae_*Eriocheir*	10.53	3.95	3.18
Arthropoda_Thecostraca (Overall)	**5.3**	**1.3**	**2.1**
Arthropoda_Thecostraca_Rhizocephala (Overall)	**5.3**	**1.3**	**2.1**
Arthropoda_Theocostraca_Rhizocephala_Sacculinidae_ *Heterosaccus*	5.26	1.32	2.05
Bivalves	***57.9***	***21.1***	***28.2***
Mollusca_Bivalvia (Overall)	**57.9**	**21.1**	**28.2**
Mollusca_Bivalvia_Adapedonta (Overall)	**36.8**	**7.1**	**11.9**
Mollusca_Bivalvia_Adapedonta	36.84	7.15	11.86
Mollusca_Bivalvia_Cardiida (Overall)	**5.3**	**0.9**	**0.1**
Mollusca_Bivalvia_Cardiida_Tellinoidea	5.26	0.88	0.06
Mollusca_Bivalvia_Mytilida (Overall)	**36.8**	**10.9**	**16.1**
Mollusca_Bivalvia_Mytilida_Mytilidae_*Mytilus_edulis*	36.84	10.92	16.12
Mollusca_Bivalvia_Venerida (Overall)	**10.5**	**2.2**	**0.2**
Mollusca_Bivalvia_Venerida_Mactridae	5.26	0.88	0.07
Mollusca_Bivalvia_Venerida_Veneridae	5.26	1.32	0.09

Snails	***10.5***	***5.3***	***6.0***
Mollusca_Gastropoda (Overall)	**10.5**	**5.3**	**6.0**
Mollusca_Gastropoda_Caenogastropoda (Overall)	**10.5**	**3.5**	**5.7**
Mollusca_Gastropoda_Caenogastropoda	10.53	3.51	5.72
Mollusca_Gastropoda_Littorinimorpha (Overall)	**5.3**	**1.8**	**0.3**
Mollusca_Gastropoda_Littorinimorpha	5.26	1.75	0.31
Worms	***57.9***	***22.1***	***23.2***
Annelida_Polychaeta (Overall)	**57.9**	**22.1**	**23.2**
Annelida_Polychaeta_Eunicida (Overall)	**5.3**	**0.7**	**0.2**
Annelida_Polychaeta_Eunicida	5.26	0.66	0.22
Annelida_Polychaeta_Phyllodocida (Overall)	**42.1**	**11.8**	**18.7**
Annelida_Polychaeta_Phyllodocida	10.53	1.75	2.30
Annelida_Polychaeta_Phyllodocida_Nereididae_*Alitta_succinea*	31.58	9.43	16.08
Annelida_Polychaeta_Phyllodocida_Polynoidae_ *Lepidonotus_sublevis*	5.26	0.66	0.30
Annelida_Polychaeta_Scolecida (Overall)	**21.1**	**4.8**	**4.0**
Annelida_Polychaeta_Scolecida_Maldanidae_*Euclymene*	5.26	0.88	1.05
Annelida_Polychaeta_Scolecida_Orbiniidae_*Leitoscoloplos*	15.79	3.95	2.91
Annelida_Polychaeta_Terebellida (Overall)	**21.1**	**4.7**	**0.4**
Annelida_Polychaeta_Terebellida	15.79	2.98	0.31
Annelida_Polychaeta_Terebellida_Cirratulidae	5.26	1.75	0.07
Other Organisms	***10.5***	***2.0***	***1.7***
Chordata_Teleostei (Overall)	**5.3**	**0.7**	**0.4**
Chordata_Teleostei	5.26	0.66	0.41
Cnidaria_Anthozoa (Overall)	**5.3**	**1.3**	**1.3**
Cnidaria_Anthozoa_Actiniaria (Overall)	**5.3**	**1.3**	**1.3**
Cnidaria_Anthozoa_Actiniaria_Diadumenidae_ *Diadumene_leucolena*	5.26	1.32	1.26
BIOFILM	***15.8***	***6.3***	***0.9***
Diatoms	***10.5***	***3.5***	***0.6***
Bacillariophyta_Bacillariophyceae (Overall)	**5.3**	**1.8**	**0.5**
Bacillariophyta_Bacillariophyceae_Naviculales (Overall)	**5.3**	**1.8**	**0.5**
Bacillariophyta_Bacillariophyceae_Naviculales_ Pleurosigmataceae_*Pleurosigma*	5.26	1.75	0.46
Bacillariophyta_Coscinodiscophyceae (Overall)	**5.3**	**1.8**	**0.1**
Bacillariophyta_Coscinodiscophyceae_Thalassiosirales (Overall)	**5.3**	**1.8**	**0.1**
Bacillariophyta_Coscinodiscophyceae_Thalassiosirales_ Thalassiosiraceae_*Thalassiosira*	5.26	1.75	0.13
Dinoflagellates	***5.3***	***1.1***	***0.1***

Myzozoa_Dinophyceae (Overall)	**5.3**	**1.1**	**0.1**
Myzozoa_Dinophyceae_Peridiniales (Overall)	**5.3**	**1.1**	**0.1**
Myzozoa_Dinophyceae_Peridiniales_Peridiniaceae_ *Kryptoperidinium_foliaceum*	5.26	1.05	0.06
Microalgae	***5.3***	***1.8***	***0.3***
Chlorophyta_Trebouxiophyceae (Overall)	**5.3**	**1.8**	**0.3**
Chlorophyta_Trebouxiophyceae	5.26	1.75	0.27
MACROALGAE	***10.5***	***2.2***	***0.6***
Macroalgae	***10.5***	***2.2***	***0.6***
Rhodophyta_Florideophyceae (Overall)	**10.5**	**2.2**	**0.6**
Rhodophyta_Florideophyceae	5.26	0.88	0.10
Rhodophyta_Florideophyceae_Gracilariales (Overall)	**5.3**	**1.3**	**0.5**
Rhodophyta_Florideophyceae_Gracilariales_Gracilariaceae	5.26	1.32	0.49

Table S6b. Diet composition of *Calidris canutus rufa* (red knot) during spring migration (May 14 - June 2, 2023 – 2024) in the Virginia barrier island system, determined using 18S markers. Diet is summarized by frequency of occurrence (FOO), weighted percent of occurrence (wPOO), and relative read abundance (RRA). Values represent averages across all fecal samples for *C. c. rufa* and are expressed as percentages. Taxonomic categories are presented as Phylum_Class_Order_Family_*Genus_species. "***Overall"*** indicates taxonomic category summary.

18S - TAXONOMIC CATEGORY	FOO	wPOO	RRA
INVERTEBRATES	***100.0***	***64.6***	***79.1***
CRUSTACEANS	***38.9***	***15.9***	***13.4***
Arthropoda_Copepoda (Overall)	**11.1**	**1.6**	**0.5**
Arthropoda_Copepoda_Calanoida (Overall)	**5.6**	**0.9**	**0.5**
Arthropoda_Copepoda_Calanoida_Temoridae_*Temora_ longicornis*	5.56	0.93	0.47
Arthropoda_Copepoda_Harpacticoida (Overall)	**5.6**	**0.7**	**0.1**
Arthropoda_Copepoda_Harpacticoida	5.56	0.69	0.06
Arthropoda_Malacostraca (Overall)	**33.3**	**14.3**	**12.9**
Arthropoda_Malacostraca_Peracarida (Overall)	**22.2**	**7.5**	**5.6**
Arthropoda_Malacostraca_Peracarida_Amphipoda (Overall)	**27.8**	**6.4**	**5.0**
Arthropoda_Malacostraca_Amphipoda	22.22	5.00	4.86
Arthropoda_Malacostraca_Amphipoda_Ischyroceridae	5.56	1.39	0.10
Arthropoda_Malacostraca_Peracarida_Isopoda (Overall)	**5.6**	**1.1**	**0.6**
Arthropoda_Malacostraca_Isopoda	5.56	1.11	0.60
Arthropoda_Malacostraca_Decapoda (Overall)	**22.2**	**6.8**	**7.3**
Arthropoda_Malacostraca_Decapoda	11.11	2.65	2.85
Arthropoda_Malacostraca_Decapoda_Albuneidae_*Lepidopa*	5.56	1.11	1.53
Arthropoda_Malacostraca_Decapoda_Crangonoidea_ *Crangon crangon*	5.56	0.79	0.10
Arthropoda_Malacostraca_Decapoda_Varunidae_*Eriocheir*	5.56	1.11	1.75
Arthropoda_Malacostraca_Decapoda_Varunidae_ *Eriocheir sinensis*	5.56	1.11	1.08
BIVALVES	***83.3***	***39.6***	***59.2***
Mollusca_Bivalvia (Overall)	**83.3**	**39.6**	**59.2**
Mollusca_Bivalvia_Adapedonta (Overall)	**11.1**	**6.3**	**5.9**
Mollusca_Bivalvia_Adapedonta	11.11	6.25	5.87

Mollusca_Bivalvia_Arcida (Overall)	**33.3**	**11.0**	**8.1**
Mollusca_Bivalvia_Arcida	22.22	4.26	3.15
Mollusca_Bivalvia_Arcida_Noetiidae	33.33	6.76	5.00
Mollusca_Bivalvia_Cardiida (Overall)	**16.7**	**5.7**	**6.2**
Mollusca_Bivalvia_Cardiida	5.56	1.39	0.10
Mollusca_Bivalvia_Cardiida_Tellinoidea	16.67	4.35	6.15
Mollusca_Bivalvia_Mytilida (Overall)	**66.7**	**14.6**	**38.6**
Mollusca_Bivalvia_Mytilida_Mytilidae_*Mytilus_edulis*	66.67	14.58	38.57
Mollusca_Bivalvia_Nuculanoida (Overall)	**5.6**	**1.1**	**0.1**
Mollusca_Bivalvia_Nuculanoida	5.56	1.11	0.12
Mollusca_Bivalvia_Venerida (Overall)	**5.6**	**0.9**	**0.2**
Mollusca_Bivalvia_Venerida	5.56	0.93	0.23
WORMS	***22.2***	***6.9***	***5.1***
Annelida_Clitellata (Overall)	**5.6**	**0.8**	**1.4**
Annelida_Clitellata_Haplotaxida (Overall)	**5.6**	**0.8**	**1.4**
Annelida_Clitellata_Haplotaxida	5.56	0.79	1.41
Annelida_Polychaeta (Overall)	**16.7**	**5.0**	**2.1**
Annelida_Polychaeta_Phyllodocida (Overall)	**16.7**	**3.6**	**2.1**
Annelida_Polychaeta_Phyllodocida_Nereididae_*Alitta_succinea*	11.11	2.50	1.74
Annelida_Polychaeta_Phyllodocida_Phyllodocida_*Nephtys_hombergii*	5.56	1.11	0.35
Annelida_Polychaeta_Scolecida (Overall)	**5.6**	**1.4**	**0.1**
Annelida_Polychaeta_Scolecida_Orbiniidae_*Leitoscoloplos*	5.56	1.39	0.07
Nemertea_Pilidiophora (Overall)	**5.6**	**1.1**	**1.5**
Nemertea_Pilidiophora_Heteronemertea (Overall)	**5.6**	**1.1**	**1.5**
Nemertea_Pilidiophora_Heteronemertea_Lineidae_*Cerebratulus_lacteus*	5.56	1.11	1.51
OTHER ORGANISMS	***11.1***	***2.2***	***1.4***
Chordata_Teleostei (Overall)	**11.1**	**2.2**	**1.4**
Chordata_Teleostei	11.11	2.22	1.42
BIOFILM	***77.8***	***32.1***	***18.0***
Diatoms	***50.0***	***10.8***	***4.9***
Bacillariophyta_Bacillariophyceae (Overall)	**22.2**	**5.5**	**3.6**
Bacillariophyta_Bacillariophyceae	11.11	2.22	0.15
Bacillariophyta_Bacillariophyceae_Naviculales (Overall)	**5.6**	**1.4**	**1.4**
Bacillariophyta_Bacillariophyceae_Naviculales	5.56	1.39	1.45
Bacillariophyta_Bacillariophyceae_Coscinodiscales (Overall)	**5.6**	**1.9**	**2.0**
Bacillariophyta_Bacillariophyceae_Coscinodiscales_Heliopeltaceae_*Actinoptychus*	5.56	1.85	2.00
Bacillariophyta_Coscinodiscophyceae (Overall)	**27.8**	**5.4**	**1.3**

Bacillariophyta_Coscinodiscophyceae_Thalassiosirales (Overall)	**27.8**	**5.4**	**1.3**
Bacillariophyta_Coscinodiscophyceae_Thalassiosirales_ Thalassiosiraceae	11.11	1.72	0.17
Bacillariophyta_Coscinodiscophyceae_Thalassiosirales_ Thalassiosiraceae_*Thalassiosira*	22.22	3.66	1.13
Dinoflagellates	***38.9***	***9.1***	***10.9***
Myzozoa_Dinophyceae (Overall)	**38.9**	**9.1**	**10.9**
Myzozoa_Dinophyceae	5.56	0.69	0.07
Myzozoa_Dinophyceae_Peridiniales (Overall)	**27.8**	**6.6**	**10.8**
Myzozoa_Dinophyceae_Peridiniales_Heterocapsaceae_ Heterocapsa	5.56	1.85	0.86
Myzozoa_Dinophyceae_Peridiniales_Peridiniaceae_ *Kryptoperidinium foliaceum*	22.22	4.72	9.92
Myzozoa_Dinophyceae_Gymnodiniales (Overall)	**5.6**	**1.9**	**0.1**
Myzozoa_Dinophyceae_Gymnodiniales_Gymnodiniaceae	5.56	1.85	0.07
Microalgae	***55.6***	***12.1***	***2.2***
Chlorophyta_Trebouxiophyceae (Overall)	**55.6**	**12.1**	**2.2**
Chlorophyta_Trebouxiophyceae	55.56	11.30	2.05
Chlorophyta_Trebouxiophyceae_Chlorellales (Overall)	**5.6**	**0.8**	**0.1**
Chlorophyta_Trebouxiophyceae_Chlorellales_Chlorellaceae	5.56	0.79	0.10
Chlorophyta_Chlorophyceae (Overall)	**5.6**	**0.8**	**0.7**
Chlorophyta_Chlorophyceae	5.56	0.79	0.70
MACROALGAE	***11.1***	***2.5***	***2.2***
Macroalgae	***11.1***	***2.5***	***2.2***
Rhodophyta_Florideophyceae (Overall)	**11.1**	**2.5**	**2.2**
Rhodophyta_Florideophyceae_Gracilariales (Overall)	**5.6**	**1.1**	**1.9**
Rhodophyta_Florideophyceae_Gracilariales_Gracilariaceae	5.56	1.11	1.93
Rhodophyta_Florideophyceae_Ceramiales (Overall)	**5.6**	**1.4**	**0.3**
Rhodophyta_Florideophyceae_Ceramiales_Ceramiaceae	5.56	0.69	0.21
Rhodophyta_Florideophyceae_Ceramiales_Ceramiaceae_ *Ceramium*	5.56	0.69	0.10

Table S6c. Diet composition of *Calidris pusilla* (semipalmated sandpiper) during spring migration (May 14 - June 2, 2023 – 2024) in the Virginia barrier island system, determined using 18S markers. Diet is summarized by frequency of occurrence (FOO), weighted percent of occurrence (wPOO), and relative read abundance (RRA). Values represent averages across all fecal samples for *C. pusilla* and are expressed as percentages. Taxonomic categories are presented as Phylum_Class_Order_Family_*Genus_species. "***Overall"*** indicates taxonomic category summary.

18S - TAXONOMIC CATEGORY	FOO	wPOO	RRA
INVERTEBRATES	***100.0***	***69.0***	***86.6***
Crustaceans	***65.0***	***36.7***	***52.8***
Arthropoda_Copepoda (Overall)	**10.0**	**1.2**	**1.4**
Arthropoda_Copepoda	5.00	0.38	0.12
Arthropoda_Copepoda_Calanoida (Overall)	**10.0**	**0.8**	**1.3**
Arthropoda_Copepoda_Calanoida_Acartiidae_*Acartia_tonsa*	10.00	0.80	1.29
Arthropoda_Malacostraca (Overall)	**45.0**	**30.6**	**41.5**
Arthropoda_Malacostraca_Peracarida (Overall)	**45.0**	**30.6**	**41.5**
Arthropoda_Malacostraca_Peracarida	20.00	9.17	0.57
Arthropoda_Malacostraca_Peracarida_Amphipoda (Overall)	**40.0**	**20.8**	**37.0**
Arthropoda_Malacostraca_Peracarida_Amphipoda	40.00	20.83	37.04
Arthropoda_Malacostraca_Peracarida_Isopoda (Overall)	**5.0**	**0.6**	**3.9**
Arthropoda_Malacostraca_Peracarida_Isopoda	5.00	0.56	3.91
Arthropoda_Ostracoda (Overall)	**10.0**	**5.0**	**9.8**
Arthropoda_Ostracoda_Podocopida (Overall)	**10.0**	**5.0**	**9.8**
Arthropoda_Ostracoda_Podocopida	5.00	1.25	0.23
Arthropoda_Ostracoda_Podocopida_Cytheridae	10.00	3.75	9.61
Insects	***30.0***	***11.1***	***13.3***
Arthropoda_Insecta (Overall)	**30.0**	**11.1**	**13.3**
Arthropoda_Insecta_Coleoptera (Overall)	**5.0**	**0.8**	**0.1**
Arthropoda_Insecta_Coleoptera	5.00	0.83	0.07
Arthropoda_Insecta_Diptera (Overall)	**20.0**	**9.1**	**12.4**
Arthropoda_Insecta_Diptera	20.00	9.06	12.36
Arthropoda_Insecta_Thysanoptera (Overall)	**5.0**	**1.3**	**0.9**

Arthropoda_Insecta_Thysanoptera	5.00	1.25	0.86
Bivalves	***10.0***	***2.9***	***5.1***
Mollusca_Bivalvia (Overall)	**10.0**	**2.9**	**5.1**
Mollusca_Bivalvia_Mytilida (Overall)	**5.0**	**1.3**	**4.2**
Mollusca_Bivalvia_Mytilida_Mytilidae_*Mytilus_edulis*	5.00	1.25	4.24
Mollusca_Bivalvia_Venerida (Overall)	**5.0**	**1.7**	**0.9**
Mollusca_Bivalvia_Venerida	5.00	1.67	0.87
Snails	***10.0***	***1.6***	***1.3***
Mollusca_Gastropoda (Overall)	**10.0**	**1.6**	**1.3**
Mollusca_Gastropoda_Caenogastropoda (Overall)	**10.0**	**1.6**	**1.3**
Mollusca_Gastropoda_Caenogastropoda	10.00	1.63	1.29
Worms	***40.0***	***14.3***	***10.6***
Annelida_Polychaeta (Overall)	**35.0**	**12.3**	**6.2**
Annelida_Polychaeta_Eunicida (Overall)	**25.0**	**5.6**	**4.1**
Annelida_Polychaeta_Eunicida_Lumbrineridae_*Ninoe*	25.00	3.44	1.81
Annelida_Polychaeta_Eunicida_Lumbrineridae_*Ninoe_nigripes*	15.00	2.19	2.31
Annelida_Polychaeta_Phyllodocida (Overall)	**5.0**	**2.5**	**0.7**
Annelida_Polychaeta_Phyllodocida_Nereididae_*Alitta_succinea*	5.00	2.50	0.71
Annelida_Polychaeta_Scolecida (Overall)	**5.0**	**3.3**	**0.7**
Annelida_Polychaeta_Scolecida_Capitellidae_ Notomastus latericeus	5.00	1.67	0.53
Annelida_Polychaeta_Scolecida_Maldanidae_*Euclymene*	5.00	1.67	0.21
Annelida_Polychaeta_Spionida (Overall)	**10.0**	**0.8**	**0.7**
Annelida_Polychaeta_Spionida	10.00	0.80	0.67
Annelida_Sipuncula (Overall)	**10.0**	**2.1**	**4.4**
Annelida_Sipuncula_Sipuncula (Overall)	**10.0**	**2.1**	**4.4**
Annelida_Sipuncula_Sipuncula	10.00	2.08	4.35
Other Organisms	***15.0***	***2.2***	***3.6***
Cnidaria_Myxozoa (Overall)	**5.0**	**1.3**	**2.8**
Cnidaria_Myxozoa_Bivalvulida (Overall)	**5.0**	**1.3**	**2.8**
Cnidaria_Myxozoa_Bivalvulida	5.00	1.25	2.79
Porifera_Demospongiae (Overall)	**10.0**	**0.9**	**0.8**
Porifera_Demospongiae_Clionaida (Overall)	**10.0**	**0.9**	**0.8**
Porifera_Demospongiae_Clionaida_Clionaidae	10.00	0.94	0.77
BIOFILM	***55.0***	***28.7***	***14.5***
Diatoms	***50.0***	***20.2***	***12.0***
Bacillariophyta_Bacillariophyceae (Overall)	**35.0**	**14.2**	**7.7**
Bacillariophyta_Bacillariophyceae	12.50	3.65	2.53
Bacillariophyta_Bacillariophyceae_Bacillariales (Overall)	**10.0**	**1.4**	**0.2**

Bacillariophyta_Bacillariophyceae_Bacillariales	5.00	0.42	0.10
Bacillariophyta_Bacillariophyceae_Bacillariales_Bacillariaceae	5.00	1.00	0.09
Bacillariophyta_Bacillariophyceae_Naviculales (Overall)	**30.0**	**8.2**	**4.8**
Bacillariophyta_Bacillariophyceae_Naviculales	20.00	2.61	1.32
Bacillariophyta_Bacillariophyceae_Naviculales_Naviculaceae	15.00	3.92	1.96
Bacillariophyta_Bacillariophyceae_Naviculales_Naviculaceae_ *Navicula*	10.00	0.80	1.38
Bacillariophyta_Bacillariophyceae_Naviculales_Pleurosigmataceae	5.00	0.42	0.09
Bacillariophyta_Bacillariophyceae_Naviculales_Pleurosigmataceae *Pleurosigma*	5.00	0.42	0.07
Bacillariophyta_Bacillariophyceae_Thalassiophysales (Overall)	**5.0**	**1.0**	**0.1**
Bacillariophyta_Bacillariophyceae_Thalassiophysales_ Catenulaceae_*Amphora*	5.00	1.00	0.11
Bacillariophyta_Coscinodiscophyceae (Overall)	**35.0**	**5.9**	**4.4**
Bacillariophyta_Coscinodiscophyceae_Thalassiosirales (Overall)	**35.0**	**5.9**	**4.4**
Bacillariophyta_Coscinodiscophyceae_Thalassiosirales_ *Skeletonemataceae_Skeletonema*	5.00	0.38	0.64
Bacillariophyta_Coscinodiscophyceae_Thalassiosirales_ Thalassiosiraceae	10.00	1.67	0.99
Bacillariophyta_Coscinodiscophyceae_Thalassiosirales_ Thalassiosiraceae_*Thalassiosira*	20.00	3.89	2.74
Dinoflagellates	***25.0***	***6.2***	***2.1***
Myzozoa_Dinophyceae (Overall)	**25.0**	**6.2**	**2.1**
Myzozoa_Dinophyceae	5.00	1.25	0.15
Myzozoa_Dinophyceae_Gymnodiniales (Overall)	**5.0**	**0.8**	**0.1**
Myzozoa_Dinophyceae_Gymnodiniales	5.00	0.83	0.12
Myzozoa_Dinophyceae_Peridiniales (Overall)	**20.0**	**4.1**	**1.8**
Myzozoa_Dinophyceae_Peridiniales	5.00	0.38	0.18
Myzozoa_Dinophyceae_Peridiniales_Peridiniaceae_ *Kryptoperidinium_foliaceum*	15.00	3.75	1.62
Microalgae	***10.0***	***2.4***	***0.4***
Chlorophyta_Trebouxiophyceae (Overall)	**10.0**	**1.8**	**0.2**
Chlorophyta_Trebouxiophyceae	10.00	1.81	0.23
Cryptophyta_Cryptophyceae (Overall)	**5.0**	**0.6**	**0.1**
Cryptophyta_Cryptophyceae_Pyrenomonadales (Overall)	**5.0**	**0.6**	**0.1**
Cryptophyta_Cryptophyceae_Pyrenomonadales	5.00	0.56	0.15
MACROALGAE	***10.0***	***2.9***	***0.4***
Macroalgae	***10.0***	***2.9***	***0.4***
Chlorophyta_Ulvophyceae (Overall)	**10.0**	**2.9**	**0.4**
Chlorophyta_Ulvophyceae_Ulvales (Overall)	**10.0**	**2.9**	**0.4**

Chlorophyta_Ulvophyceae_Ulvales_Kornmanniaceae_ *Pseudendoclonium*	5.00	0.38	0.28
Chlorophyta_Ulvophyceae_Ulvales_Ulvaceae	5.00	2.50	0.07

Table S8a. Diet composition of *Calidris alpina* (dunlin) during spring migration (May 14 - June 2, 2023 – 2024) in the Virginia barrier island system, determined using 23S markers. Diet is summarized by frequency of occurrence (FOO), weighted percent of occurrence (wPOO), and relative read abundance (RRA). Values represent averages across all fecal samples for *C. alpina* and are expressed as percentages. Taxonomic categories are presented as Phylum_Class_Order_Family_*Genus_species. "***Overall"*** indicates taxonomic category summary.

23S - TAXONOMIC CATEGORY	FOO	wPOO	RRA
BIOFILM	***76.5***	***71.6***	***71.7***
Diatoms	***76.5***	***66.2***	***67.9***
Bacillariophyta_Bacillariophyceae (Overall)	**52.9**	**33.8**	**32.7**
Bacillariophyta_Bacillariophyceae	17.65	11.76	10.41
Bacillariophyta_Bacillariophyceae_Bacillariales	**5.9**	**2.0**	**0.9**
Bacillariophyta_Bacillariophyceae_Bacillariales_Bacillariaceae_*Tryblionella*	5.88	1.96	0.95
Bacillariophyta_Bacillariophyceae_Naviculales (Overall)	**35.3**	**20.1**	**21.3**
Bacillariophyta_Bacillariophyceae_Naviculales	17.65	9.31	11.12
Bacillariophyta_Bacillariophyceae_Naviculales_Naviculaceae	17.65	10.78	10.18
Bacillariophyta_Coscinodiscophyceae (Overall)	**41.2**	**32.4**	**35.3**
Bacillariophyta_Coscinodiscophyceae	41.18	32.35	35.25
Microalgae	***11.8***	***5.4***	***3.8***
Chlorophyta_Mamiellophyceae (Overall)	**11.8**	**5.4**	**3.8**
Chlorophyta_Mamiellophyceae_Mamiellales (Overall)	**11.8**	**5.4**	**3.8**
Chlorophyta_Mamiellophyceae_Mamiellales_Bathycoccaceae	5.88	1.96	0.63
Chlorophyta_Mamiellophyceae_Mamiellales_Bathycoccaceae_*Ostreococcus*	5.88	1.96	3.06
Chlorophyta_Mamiellophyceae_Mamiellales_Mamiellaceae	5.88	1.47	0.14
MACROALGAE	***35.3***	***28.4***	***28.3***
Macroalgae	***35.3***	***28.4***	***28.3***
Ochrophyta_Phaeophyceae (Overall)	**17.6**	**13.7**	**12.0**
Ochrophyta_Phaeophyceae_Ectocarpales (Overall)	**17.6**	**13.7**	**12.0**
Ochrophyta_Phaeophyceae_Ectocarpales_Ectocarpaceae_*Ectocarpus_siliculosus*	17.65	13.73	11.99
Rhodophyta_Florideophyceae (Overall)	**23.5**	**14.7**	**16.3**
Rhodophyta_Florideophyceae_Ceramiales (Overall)	**11.8**	**3.9**	**3.1**

Rhodophyta_Florideophyceae_Ceramiales	5.88	1.96	2.03
Rhodophyta_Florideophyceae_Ceramiales_Ceramiaceae	5.88	1.96	1.11
Rhodophyta_Florideophyceae_Gracilariales (Overall)	**11.8**	**4.9**	**7.2**
Rhodophyta_Florideophyceae_Gracilariales	5.88	1.47	0.16
Rhodophyta_Florideophyceae_Gracilariales_Gracilariaceae	11.76	3.43	7.09
Rhodophyta_Florideophyceae_Rhodymeniales (Overall)	**5.9**	**5.9**	**5.9**
Rhodophyta_Florideophyceae_Rhodymeniales_Lomentariaceae	5.88	5.88	5.88

Table S8b. Diet composition of *Calidris canutus rufa* (red knot) during spring migration (May 14 - June 2, 2023 – 2024) in the Virginia barrier island system, determined using 23S markers. Diet is summarized by frequency of occurrence (FOO), weighted percent of occurrence (wPOO), and relative read abundance (RRA). Values represent averages across all fecal samples for *C. c. rufa* and are expressed as percentages. Taxonomic categories are presented as Phylum_Class_Order_Family_*Genus_species. "***Overall"*** indicates taxonomic category summary.

23S - TAXONOMIC CATEGORY	FOO	wPOO	RRA
BIOFILM	***85.7***	***73.8***	***73.5***
Diatoms	***78.6***	***58.3***	***59.4***
Bacillariophyta_Bacillariophyceae (Overall)	**42.9**	**22.6**	**18.9**
Bacillariophyta_Bacillariophyceae	21.43	9.52	12.53
Bacillariophyta_Bacillariophyceae_Bacillariales	**14.3**	**6.0**	**0.9**
Bacillariophyta_Bacillariophyceae_Bacillariales_Bacillariaceae	14.29	5.95	0.91
Bacillariophyta_Bacillariophyceae_Naviculales (Overall)	**14.3**	**7.1**	**5.5**
Bacillariophyta_Bacillariophyceae_Naviculales	7.14	3.57	2.76
Bacillariophyta_Bacillariophyceae_Naviculales_Naviculaceae	7.14	3.57	2.74
Bacillariophyta_Coscinodiscophyceae (Overall)	**64.3**	**35.7**	**40.4**
Bacillariophyta_Coscinodiscophyceae	64.29	35.71	40.45
Microalgae	***21.4***	***15.5***	***14.1***
Chlorophyta_Trebouxiophyceae (Overall)	**7.1**	**4.8**	**2.5**
Chlorophyta_Trebouxiophyceae	7.14	2.38	0.67
Chlorophyta_Trebouxiophyceae_Chlorellales (Overall)	**7.1**	**2.4**	**1.9**
Chlorophyta_Trebouxiophyceae_Chlorellales_Chlorellaceae	7.14	2.38	1.86
Haptophyta_Coccolithophyceae (Overall)	**14.3**	**10.7**	**11.6**
Haptophyta_Coccolithophyceae_Prymnesiales (Overall)	**14.3**	**10.7**	**11.6**
Haptophyta_Coccolithophyceae_Prymnesiales_ Chrysochromulinaceae	14.29	10.71	11.55
MACROALGAE	***35.7***	***26.2***	***26.5***
Macroalgae	***35.7***	***26.2***	***26.5***
Chlorophyta_Ulvophyceae (Overall)	**7.1**	**3.6**	**6.5**
Chlorophyta_Ulvophyceae_Ulvales (Overall)	**7.1**	**3.6**	**6.5**
Chlorophyta_Ulvophyceae_Ulvales	7.14	3.57	6.51
Ochrophyta_Phaeophyceae (Overall)	**14.3**	**10.7**	**9.6**

Ochrophyta_Phaeophyceae_Ectocarpales (Overall)	**14.3**	**10.7**	**9.6**
Ochrophyta_Phaeophyceae_Ectocarpales	7.14	3.57	2.42
Ochrophyta_Phaeophyceae_Ectocarpales_Acinetosporaceae_ *Pylaiella_littoralis*	7.14	7.14	7.14
Rhodophyta_Florideophyceae (Overall)	**14.3**	**11.9**	**10.5**
Rhodophyta_Florideophyceae_Ceramiales (Overall)	**7.1**	**7.1**	**7.1**
Rhodophyta_Florideophyceae_Ceramiales_Ceramiaceae	7.14	7.14	7.14
Rhodophyta_Florideophyceae_Gracilariales (Overall)	**7.1**	**4.8**	**3.3**
Rhodophyta_Florideophyceae_Gracilariales	7.14	2.38	0.38
Rhodophyta_Florideophyceae_Gracilariales_Gracilariaceae	7.14	2.38	2.93

Table S8c. Diet composition of *Calidris pusilla* (semipalmated sandpiper) during spring migration (May 14 - June 2, 2023 – 2024) in the Virginia barrier island system, determined using 23S markers. Diet is summarized by frequency of occurrence (FOO), weighted percent of occurrence (wPOO), and relative read abundance (RRA). Values represent averages across all fecal samples for *C. pusilla* and are expressed as percentages. Taxonomic categories are presented as Phylum_Class_Order_Family_*Genus_species. "***Overall"*** indicates taxonomic category summary.

23S - TAXONOMIC CATEGORY	FOO	wPOO	RRA
BIOFILM	***100.0***	***91.7***	***86.4***
Diatoms	***93.8***	***82.7***	***76.4***
Bacillariophyta_Bacillariophyceae (Overall)	**75.0**	**52.7**	**45.2**
Bacillariophyta_Bacillariophyceae	12.50	3.65	2.53
Bacillariophyta_Bacillariophyceae_Bacillariales	**31.3**	**9.1**	**3.6**
Bacillariophyta_Bacillariophyceae_Bacillariales_Bacillariaceae	31.25	8.44	3.31
Bacillariophyta_Bacillariophyceae_Bacillariales_Bacillariaceae_ *Nitzschia*	6.25	0.63	0.29
Bacillariophyta_Bacillariophyceae_Naviculales (Overall)	**68.8**	**38.3**	**38.3**
Bacillariophyta_Bacillariophyceae_Naviculales	18.75	3.23	1.92
Bacillariophyta_Bacillariophyceae_Naviculales_Naviculaceae	68.75	31.35	30.46
Bacillariophyta_Bacillariophyceae_Naviculales_Naviculaceae_ *Navicula*	12.50	3.75	5.96
Bacillariophyta_Bacillariophyceae_Thalassiophysales (Overall)	**12.5**	**1.7**	**0.7**
Bacillariophyta_Bacillariophyceae_Thalassiophysales_ Catenulaceae_*Halamphora*	12.50	1.67	0.72
Bacillariophyta_Coscinodiscophyceae (Overall)	**50.0**	**30.0**	**31.2**
Bacillariophyta_Coscinodiscophyceae	50.00	27.71	30.17
Bacillariophyta_Coscinodiscophyceae_Thalassiosirales (Overall)	**12.5**	**2.3**	**1.0**
Bacillariophyta_Coscinodiscophyceae_Thalassiosirales_ Melosiraceae_*Melosira*	6.25	0.63	0.25
Bacillariophyta_Coscinodiscophyceae_Thalassiosirales_ Skeletonemataceae *Skeletonema*	12.50	1.67	0.77
Microalgae	***18.8***	***9.0***	***10.0***
Chlorophyta_Mamiellophyceae (Overall)	**6.3**	**6.3**	**6.3**
Chlorophyta_Mamiellophyceae_Mamiellales (Overall)	**6.3**	**6.3**	**6.3**
Chlorophyta_Mamiellophyceae_Mamiellales_Bathycoccaceae	6.25	3.13	0.18

Chlorophyta_Mamiellophyceae_Mamiellales_Bathycoccaceae_ *Ostreococcus*	6.25	3.13	6.07
Cryptophyta_Cryptophyceae (Overall)	**6.3**	**2.1**	**3.6**
Cryptophyta_Cryptophyceae	6.25	2.08	3.57
Haptophyta_Coccolithophyceae (Overall)	**6.3**	**0.6**	**0.2**
Haptophyta_Coccolithophyceae_Prymnesiales (Overall)	**6.3**	**0.6**	**0.2**
Haptophyta_Coccolithophyceae_Prymnesiales_ Chrysochromulinaceae_Chrysochromulina	6.25	0.63	0.22
MACROALGAE	***18.8***	***8.3***	***13.6***
Macroalgae	***18.8***	***8.3***	***13.6***
Rhodophyta_Florideophyceae (Overall)	**18.8**	**8.3**	**13.6**
Rhodophyta_Florideophyceae_Ceramiales (Overall)	**18.8**	**8.3**	**13.6**
Rhodophyta_Florideophyceae_Ceramiales_Ceramiaceae	6.25	3.13	6.01
Rhodophyta_Florideophyceae_Ceramiales_Rhodomelaceae	12.50	5.21	7.54

Table S9. Diet selectivity of *Calidris alpina* (dunlin), *Calidris canutus rufa* (red knot), and *Calidris pusilla* (semipalmated sandpiper) on mudflats during spring migration (May 14 - June 2, 2023 – 2024) in the Virginia barrier island system, determined using network null modeling. Observed shorebird (consumer) - invertebrate (resource) interaction strengths, derived from diet analysis (FOO), were compared to expected (null) frequencies generated by the null model with 95% confidence intervals. Results indicating "Stronger" than expected interactions represent preference; "Weaker" than expected indicate avoidance; and "ns" (Not Significant) indicates no selection. SES = standardized effect size for the interaction.

Consumer	Resource	Observed	Null	Lower.95.CL	Upper.95.CL	Test	SES
C. alpina	Bivalves	11	5.20	2	8	Stronger	3.52
C. alpina	Crustaceans	15	15.07	12	18	ns	-0.04
C. alpina	Other Orgs	2	2.39	0	5	ns	-0.29
C. alpina	Snails	2	3.51	1	7	ns	-1.00
C. alpina	Worms	11	14.84	12	18	Weaker	-2.60
C. c. rufa	Bivalves	15	1.91	0	5	Stronger	10.52
C. c. rufa	Crustaceans	7	12.19	9	16	Weaker	-2.94
C. c. rufa	Other Orgs	2	0.81	0	3	ns	1.38
C. c. rufa	Snails	0	1.23	0	4	ns	-1.18
C. c. rufa	Worms	4	11.86	8	15	Weaker	-4.40
C. pusilla	Bivalves	2	2.49	1	5	ns	-0.42
C. pusilla	Crustaceans	13	11.44	8	15	ns	0.91
C. pusilla	Other Orgs	3	1.20	0	3	ns	1.90
C. pusilla	Snails	2	1.75	0	4	ns	0.24
C. pusilla	Worms	8	11.12	8	14	ns	-1.82

LIST OF EXTERNAL SUPPLEMENTARY TABLES

Table S3. Taxonomies of diet items identified using 18S rDNA markers in shorebird fecal samples collected on mudflats during spring migration (May 14 - June 2, 2023 – 2024) in the Virginia barrier island system. A total of 80 taxonomic categories were summarized from 157 ESVs, including 13 species, 15 genera, 17 families, 28 orders, and 7 classes. We excluded 3,707 ESVs representing non-diet items, low taxonomic resolution groups (e.g., Eukaryota), and taxa lacking sufficient classification (e.g., missing class), including kingdoms Bacteria and Archaea, phyla Ascomycota, Basidiomycota, Nematozoa, Phragmoplastophyta, Peronosporomycetes, Zoopagomycota, Apicomplex, Protalveolata, Ciliophora, Mucoromycota, Cercozoa, Amoebozoa, MAST-12, Heterolobosea, Cryptomycota, Euglenozoa, Parabasalia, Platyhelminthes, Chytridiomycota, Discoba, Rotifera, Microsporidia, Xenacoelomorpha, Dictyostelia, Holozoa, Apusomonadidae, LKM15, Aphelidea, SAR, Bicosoecida, and Labyrinthulomycetes and class Aves. Additionally, 548 ESVs were removed during post-bioinformatics filtering by discarding samples with fewer than 100 reads, sequence reads representing < 1 % of total reads per sample, and sequence reads representing < 0.5% of total reads per ESV. Taxonomic assignment thresholds were as follows: ESVs with ≥ 99% match to a single were assigned species-level taxonomy; those with ≥ 98% match to species within the same genus were assigned genus-level; those with a ≥ 95% match to species or genus within the same family were assigned family-level; and remaining ESVs were assigned to order or class. All species-, genus-, and family- level assignments were cross-referenced with the Ocean Biodiversity Information System (OBIS) database to confirm regional occurrence. Finally, all taxa were grouped into diet bins:

crustaceans, insects, bivalves, snails, worms, other organisms, diatoms, dinoflagellates, microalgae (unicellular), and macroalgae (multicellular).

Table S4. Taxonomies of diet items identified using 23S rDNA marker in shorebird fecal samples collected on mudflats during spring migration (May 14 - June 2, 2023 – 2024) in the Virginia barrier island system. A total of 29 taxonomic categories were summarized from 194 ESVs, including 2 species, 8 genera, 10 families, 5 orders, and 4 classes. We excluded 441 ESVs representing non-diet items, low taxonomic resolution groups (e.g., Eukaryota), and taxa missing classification (e.g., missing class), including kingdom Bacteria and phyla Streptophyta and Apicomplexa. An additional 283 ESVs were removed during post-bioinformatics filtering by discarding samples with < 100 reads, sequence reads representing < 1 % of total reads per sample, and sequence reads representing < 0.5% of total reads per ESV. Taxonomic assignment thresholds were as follows: ESVs with ≥ 99% match to a single were assigned species-level taxonomy; those with ≥ 98% match to species within the same genus were assigned genus-level; those with a ≥ 95% match to species or genus within the same family were assigned family-level; and remaining ESVs were assigned to order or class. All species-, genus-, and family- level assignments were cross-referenced with the Ocean Biodiversity Information System (OBIS) database to confirm regional occurrence. Finally, taxa were grouped into diet bins: diatoms, microalgae (unicellular), and macroalgae (multicellular).

Table S5a. Weighted percentages of occurrence (wPOO) of diet items detected using 18S rDNA markers for individual fecal samples collected on mudflats during spring migration (May 14 - June 2, 2023 – 2024) in the Virginia barrier island system. Values are presented as percentages

(%). Abbreviations: C.alpina = *Calidris alpina* (dunlin), C.c.rufa = *Calidris canutus rufa* (red knot), and C.pusilla = *Calidris pusilla* (semipalmated sandpiper).

Table S5b. Relative read abundances (RRA) of diet items detected using 18S rDNA marker for individual fecal samples collected on mudflats during spring migration (May 14 - June 2, 2023 – 2024) in the Virginia barrier island system. Values are presented as percentages (%). Abbreviations: C.alpina = *Calidris alpina* (dunlin), C.c.rufa = *Calidris canutus rufa* (red knot), and C.pusilla = *Calidris pusilla* (semipalmated sandpiper).

Table S7a. Weighted percentages of occurrence (wPOO) of diet items detected using 23S rDNA marker for individual fecal samples collected on mudflats during spring migration (May 14 - June 2, 2023 – 2024) in the Virginia barrier island system. Values are presented as percentages (%). Abbreviations: C.alpina = *Calidris alpina* (dunlin), C.c.rufa = *Calidris canutus rufa* (red knot), and C.pusilla = *Calidris pusilla* (semipalmated sandpiper).

Table S7b. Relative read abundances (RRA) of diet items detected using 23S rDNA marker for individual fecal samples collected on mudflats during spring migration (May 14 - June 2, 2023 – 2024) in the Virginia barrier island system. Values are presented as percentages (%). Abbreviations: C.alpina = *Calidris alpina* (dunlin), C.c.rufa = *Calidris canutus rufa* (red knot), and C.pusilla = *Calidris pusilla* (semipalmated sandpiper).

SUPPLEMENTARY FIGURES

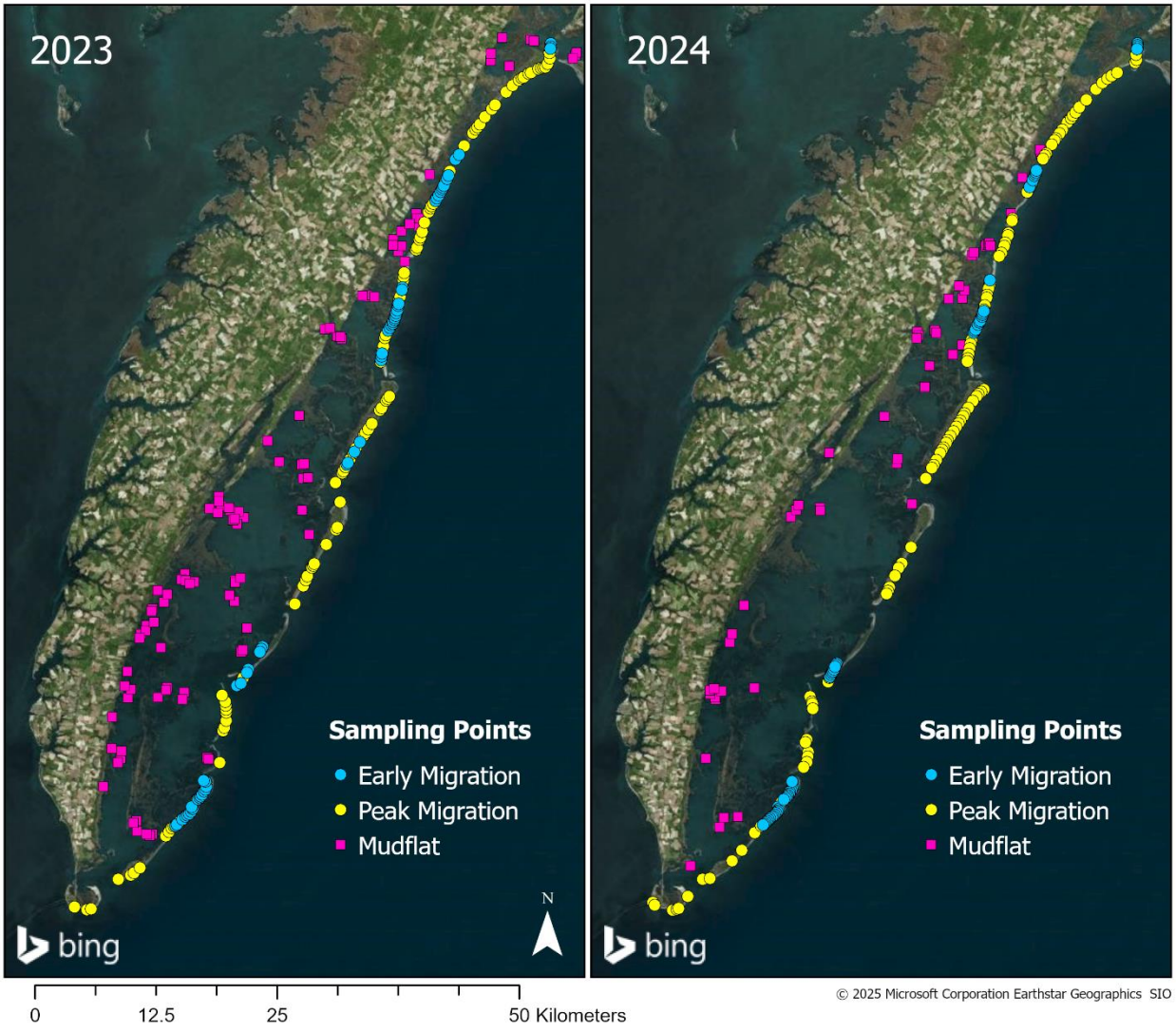

Figure S1. Locations of proposed random sampling points within our the Virginia barrier island system for the 2023 (left panel) and 2024 (right panel) field seasons. Each year, 60 random points were generated for early migration (May 14 - 20; blue dots) and 115 random points for peak migration (May 21 – 28; yellow dots). In 2023, 100 random mudflat sampling points (May 14 – June 2; pink squares) were generated to account for uncertainty in mudflat locations, while 50 mudflat points were generated in 2024.

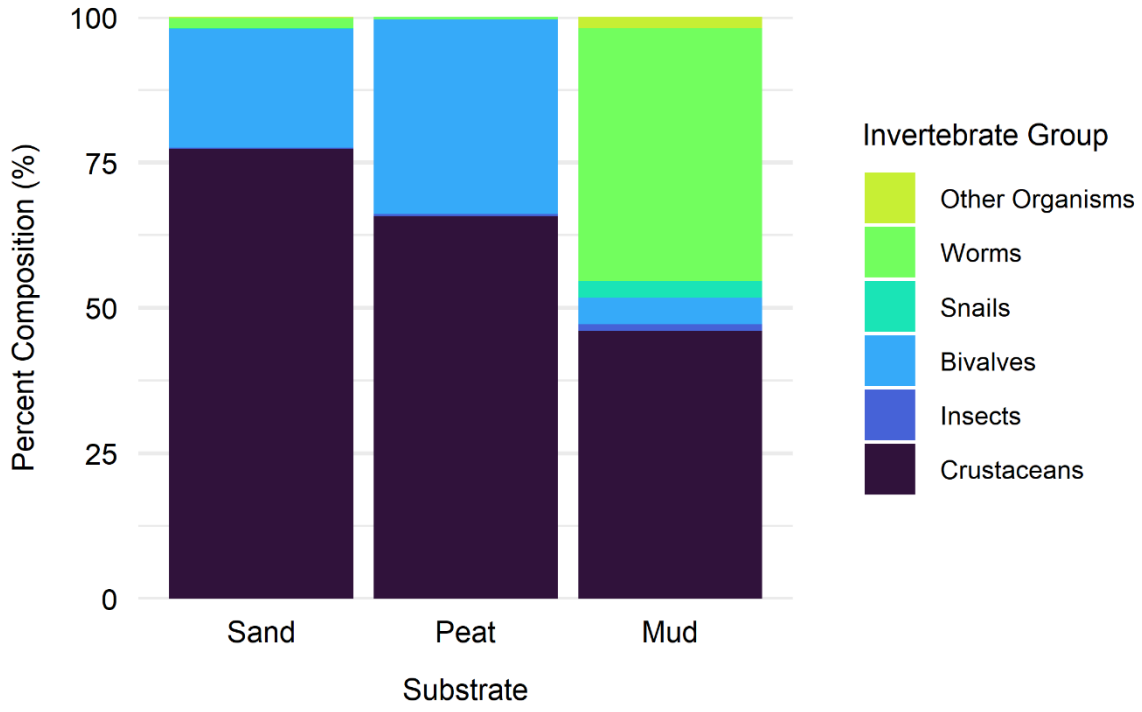

Figure S2. Invertebrate community composition (percentage of total) across sand, peat, and mudflat substrates during spring migration (May 14 – June 2, 2023 – 2024) in the Virginia barrier island system.

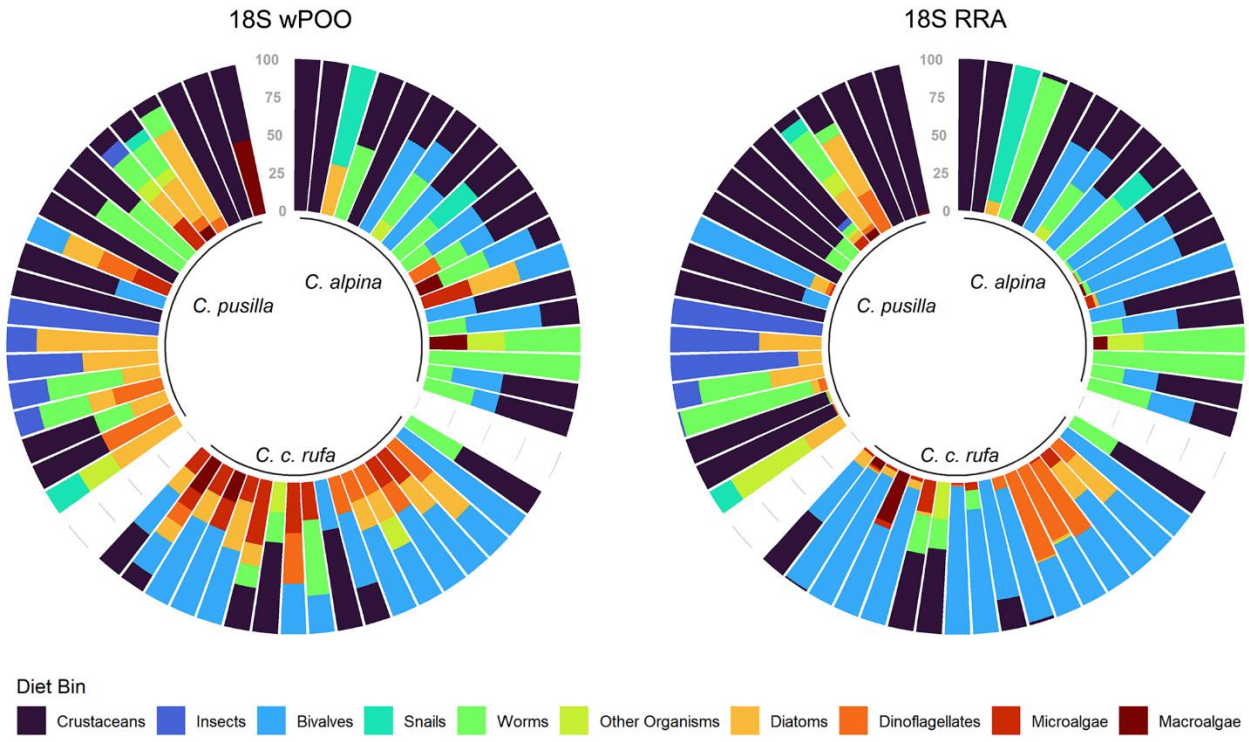

Figure S3. Proportions of diet bins in individual fecal samples detected using 18S rDNA markers. Samples were collected from *Calidris alpina* (dunlin, n = 19), *Calidris canutus rufa* (red knot, n = 18), and *Calidris pusilla* (semipalmated sandpiper, n = 20) on mudflats during spring migration (May 14 – June 2, 2023 – 2024) in the Virginia barrier island system. Colored blocks represent weighted percent occurrence (wPOO; left panel) and relative read abundance (RRA; right panel) of each diet bin. Bars correspond to individual fecal samples by species (see Table S6a-c for details).

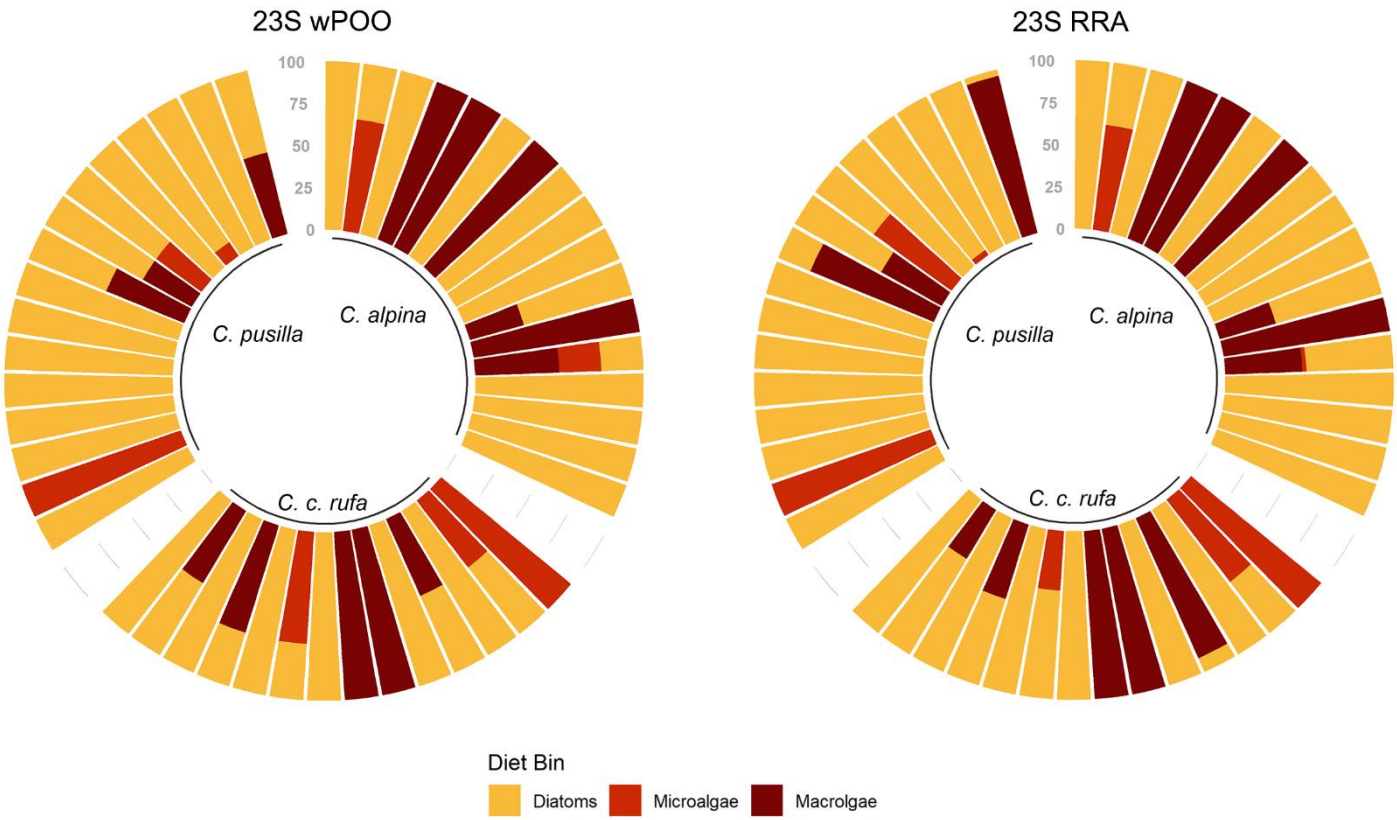

Figure S4. Proportions of diet bins in individual fecal samples detected using 23S rDNA markers. Samples were collected from *Calidris alpina* (dunlin, n = 17), *Calidris canutus rufa* (red knot, n = 14), and *Calidris pusilla* (semipalmated sandpiper, n = 16) on mudflats during spring migration (May 14 – June 2, 2023 – 2024) in the Virginia barrier island system. Colored blocks show weighted percent occurrence (wPOO; left panel) and relative read abundance (RRA; right panel) for each diet bin. Bars correspond to individual fecal samples by species (see Table S8a-b for details).

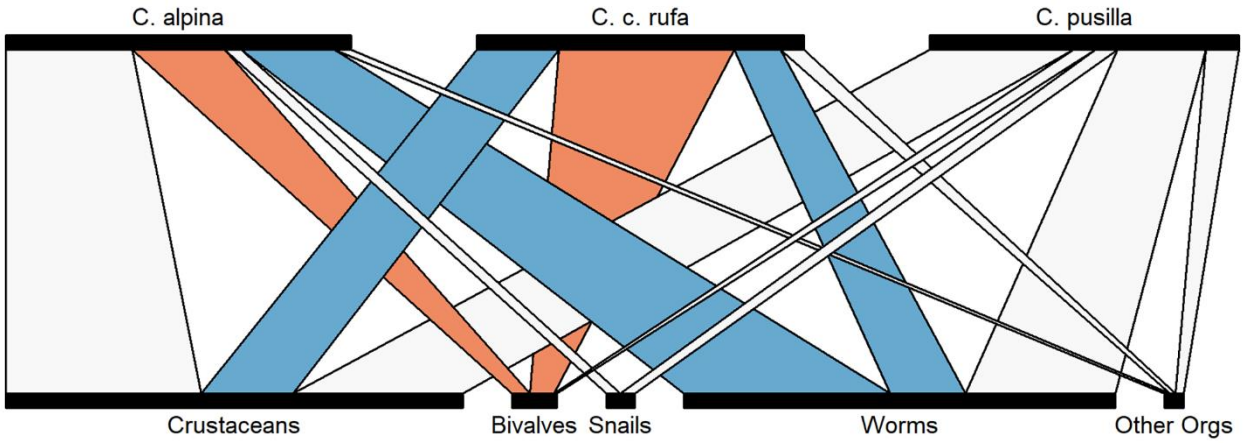

Figure S5. Bipartite network depecting trophic interactions between *Calidris alpina* (dunlin), *Calidris canutus rufa* (red knot), and *Calidris pusilla* (semipalmated sandpiper) and their invertebrate prey during spring migration (May 14 – June 2, 2023 – 2024) in the Virginia barrier island system. Links between the top (shorebirds) and bottom (invertebrates) bars represent observed consumption frequencies based on frequency of occurrence (FOO) relative to prey availability in core samples. Orange links indicate preference (stronger than expected consumption), blue links indicate avoidance (weaker than expected consumption), and white links represent no selection (consumption proportional to availability). Top bar widths correspond to the number of fecal samples per shorebird species; bottom bar widths correspond to mean invertebrate abundance in core samples.

Chapter 3:

Geomorphic and climate drivers shape bottom-up controls on spring staging red knots in the Virginia Barrier Islands.

APPENDIX S.2

SUPPLEMENTARY TABLES

Table S1 Summary of multispectral aerial imagery used to measure barrier island morphometrics in the Virginia barrier island system from 2007 – 2023. Imagery was acquired from the United States Department of Agriculture's Farm Services Agency's National Agriculture Imagery Program (NAIP) and from the Virginia Department of Emergency Management's Virginia Geographic Information Network (VGIN). The table includes imagery year, source (NAIP or VGIN), spatial resolution, spatial coverage of barrier islands, and imagery acquisition dates. Flight dates varied across islands in some years.

Year	Source	Resolution	Spatial Coverage	Flight Dates (mm/dd/yyyy)
2023	NAIP	0.6 m	Assawoman – Metompkin	10/09–11/04/2023
			Cedar – Parramore	10/28–11/04/2023
			Hog	10/09–10/28/2023
			Cobb – Fisherman	10/09/2023
2021	NAIP	0.6 m	Assawoman – Metompkin	10/17/2021
			Cedar – Hog	9/14–10/17/2021
			Cobb	10/17/2021

			Wreck – Ship Shoal	9/13–10/17/2021
			Myrtle/Mink – Fisherman	9/13/2021
2018	NAIP	0.6 m	Assawoman	11/10/2018
			Metompkin	11/04–11/10/2018
			Cedar	11/04/2018
			Parramore	10/31–11/04/2018
			Hog – Smith	10/31/2018
			Fisherman	8/27/2018
2017	VGIN	0.3 m	Assawoman – Fisherman	2/26/2017
2016	NAIP	1 m	Assawoman – Fisherman	6/26/2016
2014	NAIP	1 m	Assawoman – Fisherman	9/27/2014
2013	VGIN	0.3 m	Assawoman – Fisherman	Unknown dates
2012	NAIP	1 m	Assawoman – Fisherman	5/12/2012
2011	NAIP	1 m	Assawoman – Parramore	5/30/2011
			Hog – Cobb	5/30–6/02/2011
			Wreck – Fisherman	5/22/2011
2009	NAIP	1 m	Assawoman	6/01/2009
			Metompkin	6/01–7/14/2009
			Cedar	6/19–7/14/2009
			Parramore	6/30–7/14/2009
			Hog – Myrtle/Mink	6/30/2009
			Smith	6/30–8/09/2009

			Fisherman	8/9/2009
2008	NAIP	1 m	Assawoman - Cedar	5/25/2008
			Parramore	5/25–5/26/2008
			Hog – Fisherman	5/26/2008
2007	VGIN	0.3 m	Assawoman	2/28 – 03/06/2007
			Metompkin – Parramore	2/28/2007
			Hog – Cobb	2/24 – 2/28/2007
			Wreck – Myrtle/Mink	2/28/2007
			Smith	2/24 – 2/28/2007
			Fisherman	2/28/2007

Table S2. Model selection results for the zero-inflated component of models fit to zero-inflated negative binomial distributions in piecewise structural equation models (SEMs). An information theoretic approach was used to compare eight *a priori* hypotheses explaining excess zeros observed in densities of invertebrates, crustaceans, coquina clams, and miscellaneous prey. Models were compared using the second order second-order Akaike Information Criterion (AICc). Zero-inflation components with $\Delta AICc \leq 2$ were considered well supported and were included in final SEM (highlighted in bold).

Zero-inflated model component	k	ΔAIC_c	ω_i	LL
Invertebrate density component model				
tide	**6**	**0.00**	**0.58**	**-9716.49**
tide + substrate	7	2.00	0.21	-9716.48
storminess	6	2.94	0.13	-9717.96
null	5	5.30	0.04	-9720.15
substrate	6	7.02	0.02	-9720.00
water temp	6	7.05	0.02	-9720.02
beach width	5	162.59	0.00	-9798.80
beach width + distance to inlet	6	164.51	0.00	-9798.75
storminess + water temp	6	169.28	0.00	-9801.13
distance to inlet	5	170.86	0.00	-9802.93
Crustacean density component model				
beach width	**5**	**0.00**	**0.54**	**-8410.89**
beach width + distance to inlet	6	0.33	0.46	-8410.04
distance to inlet	5	11.65	0.00	-8416.72

tide	5	13.47	0.00	-8417.62
null	4	13.79	0.00	-8418.79
tide + substrate	6	14.84	0.00	-8417.30
water temp	5	15.01	0.00	-8418.40
substrate	5	15.47	0.00	-8418.62
storminess	5	15.49	0.00	-8418.63
storminess + water temp	6	16.71	0.00	-8418.24
Coquina clam density component model				
tide + substrate	**7**	**0.00**	**0.98**	**-5769.30**
substrate	6	8.06	0.02	-5774.34
tide	6	27.19	0.00	-5783.90
null	5	31.10	0.00	-5786.87
water temp	6	32.15	0.00	-5786.39
storminess	6	32.78	0.00	-5786.70
beach width + distance to inlet	6	40.34	0.00	-5790.48
beach width	5	42.14	0.00	-5792.39
distance to inlet	5	46.49	0.00	-5794.57
storminess + water temp	6	49.20	0.00	-5794.91
Miscellaneous prey component model				
tide + substrate	**7**	**0.00**	**0.71**	**-3780.48**
storminess	6	1.80	0.29	-3782.39
substrate	6	17.07	0.00	-3790.03
tide	6	25.60	0.00	-3794.30

null	5	49.65	0.00	-3807.33
water temp	6	51.43	0.00	-3807.21
storminess + water temp	6	201.51	0.00	-3882.25
beach width	5	239.27	0.00	-3902.14
beach width + distance to inlet	6	239.96	0.00	-3901.47
distance to inlet	5	249.34	0.00	-3907.18

Table S3. Results of Shapiro-Wilke normality tests for barrier island morphometric variables (2007 – 2023). Table includes Shapiro-Wilke test statistic (W) and statistical significance (*p*) of island and beach width measurements for Assawoman through Fisherman Islands in the Virginia barrier island system. Statistical significance is considered $p < 0.05$.

Island	Morphometric Variable	W	*p*	Distribution
Assawoman				
	Island Width	0.93	< 0.0001	Not normal
	Beach Width	0.97	< 0.0001	Not normal
Metompkin				
	Island Width	0.89	< 0.0001	Not normal
	Beach Width	0.95	< 0.0001	Not normal
Cedar				
	Island Width	0.85	< 0.0001	Not normal
	Beach Width	0.90	< 0.0001	Not normal
Parramore				
	Island Width	0.87	< 0.0001	Not normal
	Beach Width	0.92	< 0.0001	Not normal
Hog				
	Island Width	0.83	< 0.0001	Not normal
	Beach Width	0.74	< 0.0001	Not normal
Cobb				
	Island Width	0.94	< 0.0001	Not normal

	Beach Width	0.84	< 0.0001	Not normal
Wreck				
	Island Width	0.86	< 0.0001	Not normal
	Beach Width	0.95	< 0.0001	Not normal
Ship Shoal				
	Island Width	0.94	< 0.0001	Not normal
	Beach Width	0.86	< 0.0001	Not normal
Myrtle/Mink				
	Island Width	0.89	< 0.0001	Not normal
	Beach Width	0.95	< 0.0001	Not normal
Smith				
	Island Width	0.80	< 0.0001	Not normal
	Beach Width	0.97	< 0.0001	Not normal
Fisherman				
	Island Width	0.85	< 0.0001	Not normal
	Beach Width	0.87	< 0.0001	Not normal

LIST OF EXTERNAL SUPPLEMENTARY TABLES

Table S4. Mean island and beach width for individual barrier islands and the entire study system from Assawoman to Fisherman Island from 2007 – 2023. Values are presented means ± standard deviation (SD). Kendall's tau (τ) and associated p-values (*p*) indicate the direction and significance of temporal trends. Percent change reflects the relative difference between 2007 and 2023 values. Total change represents a relative index of morphometric change across all measured features. Statistical significance was defined as $p < 0.05$.

LITERATURE CITED

National Oceanic and Atmospheric Administration (NOAA). 2025. NOAA Tides and Currents. NOAA Tides & Currents. <https://tidesandcurrents.noaa.gov/>. Accessed 7 Aug 2025.